Electronic Supplementary Information (59 pages)

Low-oxidation state cobalt-magnesium complexes: ion-pairing and reactivity

John A. Kelly,[a] Johannes Gramüller,[b] Ruth M. Gschwind[b] and Robert Wolf[a]

[a]University of Regensburg, Institute of Inorganic Chemistry, 93040 Regensburg

[b]University of Regensburg, Institute of Organic Chemistry, 93040 Regensburg

Contents

1. Synthesis

All reactions and product manipulations were carried out in flame-dried glassware under an inert atmosphere of argon using standard Schlenk-line or glovebox techniques (maintained at <0.1 ppm H_2O and O_2). Solvents were purified, dried, and degassed with an MBraun SPS800 solvent purification system and then stored under argon over activated 3 Å molecular sieves or a potassium mirror in gas-tight ampules. NMR spectra were recorded on Bruker Avance 300 or 400 spectrometers at 300 K unless otherwise noted and internally referenced to residual solvent resonances (^{1}H NMR: [D^8]-THF: 1.72 ppm, C_6D_6: 7.16 ppm, $^{13}C\{^1H\}$ NMR: C_6D_6: 128.06 ppm,). Chemical shifts δ are given in ppm referring to external standards of tetramethylsilane (^{1}H, $^{13}C\{^1H\}$), 85% phosphorus acid (^{31}P and $^{31}P\{^1H\}$ spectra). C_6D_6 (99.6%) and d^8-THF (99.5 %) were stored over activated 3 Å molecular sieves. UV/vis spectra were recorded on an Ocean Optics Flame Spectrometer. Elemental analyses were determined by the analytical department of Regensburg University. ^{Ar}nacnacH[1], (^{Ar}nacnac)MgI(OEt_2),[1,2] $[K(THF)_{0.2}][Co(\eta^4\text{-}COD)_2]$[3] and *t*BuCP[4,5] were all prepared according to literature procedure. All other reagents were used as received.

(^{Mes}nacnac)MgCo(COD)$_2$ (1):

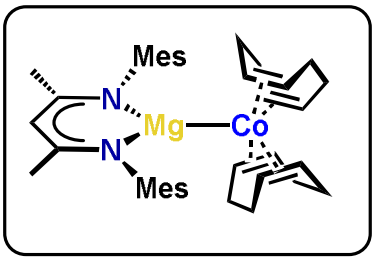

(^{Mes}nacnac)MgI(OEt_2) (3.0 g, 5.36 mmol) suspended in diethyl ether/toluene (1:1) was added dropwise to a stirred suspension of $[K(THF)_{0.2}][Co(\eta^4\text{-}COD)_2]$ (1.77 g, 5.36 mmol) in diethyl ether, cooled to –78 °C. Upon complete addition, the reaction was left to stir and slowly warm to ambient temperature overnight. All volatiles were removed *in vacuo* and the resulting residue extracted with toluene. This was then concentrated and stored at –20 °C to yield yellow crystals of (^{Mes}nacnac)MgCo(COD)$_2$ (2.0 g, 59%). UV/vis (toluene λ_{max} / nm, ε_{max} / L mol^{-1} cm^{-1}): 346 (27000). ^{1}H NMR (400 MHz, C_6D_6, 298 K): δ/ppm = 1.20 (br m, 6H, COD-*H*), 1.49 (br m, 4H, COD-*H*), 1.73 (s, 6H, NCC*H*$_3$), 1.93 (br m, 4H, COD-*H*), 2.09 (s, 6H, ^{para}Me-*H*), 2.29 (br s, 12H, ^{ortho}Me-*H*), 2.62 – 2.83 (br m, 6H, COD-*H*), 3.38 (br m, 2H, COD-*H*), 4.18 (br m, 2H, COD-*H*), 5.06 (s, 1H, (NC)$_2$C*H*), 6.77 (s, 4H, ^{meta}*H*); (400 MHz, d^8-THF, 298 K): 1.60 (s, 6H, NCC*H*$_3$), 1.85 (br m, 8H, COD-*H*), 2.14 (s, 12H, ^{ortho}Me-*H*), 2.16 (br m, 16H, COD-*H*), 2.24 (s, 6H, ^{para}Me-*H*), 5.07 (s, 1H, (NC)$_2$C*H*), 6.92 (s, 4H, ^{meta}*H*); $^{13}C\{^1H\}$ NMR (400 MHz, C_6D_6, 298K): δ/ppm = 19.1, 20.8, 24.3, 26.8, 29.6, 36.7, 39.7, 40.6, 76.1, 78.2, 80.5, 95.3, 131.9, 133.8, 145.9, 169.8. Elemental analysis calcd. For $C_{39}H_{53}N_2MgCo$ (Mw: 632.11 g mol^{-1}) C 73.99, H 8.44, N 4.42; found C 73.95, 7.84, 4.36.

(^{Dep}nacnac)MgCo(COD)$_2$ (2):

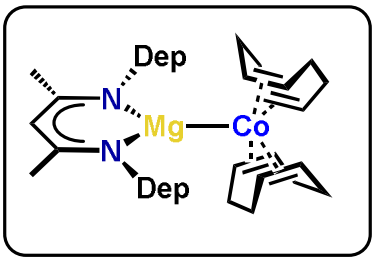

(^{Dep}nacnac)MgI(OEt$_2$) (4.0 g, 6.8 mmol) dissolved in diethyl ether/toluene (1:1) was added dropwise to a stirred suspension of [K(THF)$_{0.2}$][Co(η^4-COD)$_2$] (2.24 g, 6.8 mmol) in diethyl ether, cooled to –78 °C. Upon complete addition, the reaction was left to stir and slowly warm to ambient temperature overnight. All volatiles were removed *in vacuo* and the resulting residue extracted with toluene. Toluene was then removed *in vacuo* *n*-hexane was added causing precipitation of a yellow solid. This was isolated via filtration, washed with *n*-hexane and dried *in vacuo* to yield (^{Dep}nacnac)MgCo(COD)$_2$ as a yellow powder (3.96 g, 88%). X-ray quality crystals were grown from a concentrated toluene solution stored at 5 °C. UV/vis (toluene, λ_{max} / nm, ε_{max} / L mol^{-1} cm^{-1}): 350 (27000), (THF): 348 (27000). ^{1}H NMR (400 MHz, C_6D_6, 298 K): δ/ppm = 0.93 – 1.64 (br m, 10H, COD-*H*), 1.20 (t, 12H, CH_2CH_3), 1.74 (s, 6H, NCC*H*$_3$), 1.85 – 2.21 (br m, 4H, COD-*H*), 2.47 – 3.01 (br m, 14H, C*H*$_2$CH$_3$/COD-*H*), 3.39 (br m, 2H, COD-*H*), 4.16 (br m 2H, COD-*H*), 5.03 (s, 1H, (NC)$_2$C*H*), 7.05 (s, 6H, $^{meta/para}$Ar-*H*); (400 MHz, d^8-THF, 298 K): δ/ppm = 1.28 (t, 12H, CH_2CH_3), 1.66 (s, 6H, NCC*H*$_3$), 1.84 (br m, 8H, COD-*H*), 2.14 (br m, 16H, COD-*H*), 2.58 (m, 8H, C*H*$_2$CH$_3$), 5.10 (s, 1H, (NC)$_2$C*H*), 6.99 – 7.21 (m, 6H, $^{meta/para}$Ar-*H*); ^{13}C{^{1}H} NMR (400 MHz, C_6D_6, 298K): δ/ppm = 14.1, 24.1, 24.4, 26.2, 29.1, 36.2, 39.4, 40.0, 75.3, 77.7, 80.0, 94.8, 125.1, 137.3, 146.9, 169.4. Elemental analysis calcd. for $C_{41}H_{57}N_2MgCo$ (Mw: 661.16 g mol^{-1}) C 74.48, H 8.69, N 4.24; found C 73.95, 8.23, 4.15.

(^{Dipp}nacnac)MgCo(COD)$_2$ (3):

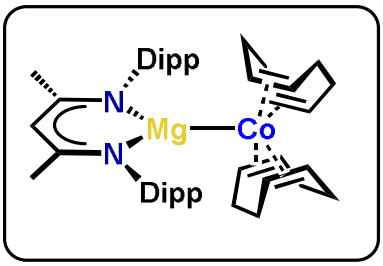

[K(THF)$_{0.2}$][Co(η^4-COD)$_2$] (0.51 g, 1.55 mmol) was suspended in toluene and heated to 75 °C overnight. Then all volatiles were removed *in vacuo* and the residue washed with toluene, suspended in diethyl ether and cooled to –78 °C. To this was added (^{Dipp}nacnac)MgI(OEt$_2$) (1.0 g, 1.55 mmol) suspended in diethyl ether/toluene (1:1) dropwise. Upon complete addition, the reaction was left to stir and slowly warm to ambient temperature overnight. All volatiles were removed *in vacuo* and the resulting residue extracted with toluene. This was left standing at 5 °C to allow any remaining cobalt particles to settle. This was then filtered, concentrated and stored at –20 °C to yield yellow crystals of (^{Dipp}nacnac)MgCo(COD)$_2$ (0.33 g, 30%). X-ray quality crystals were grown from a concentrated *n*-hexane solution. ^{1}H NMR (400 MHz, C_6D_6, 298 K): δ/ppm = 1.21 (d, 12H, CH(C*H*$_3$)$_2$), 1.28 (d, 12H, CH(C*H*$_3$)$_2$), 1.52 (br m, 4H, COD-*H*), 1.71 (s, 6H, NCC*H*$_3$), 1.97 (br m, 2H, COD-*H*), 2.15 – 3.03 (br m, 8H, COD-*H*/C*H*(CH$_3$)$_2$, 3.08 – 3.79 (br m, 6H, COD-*H*), 4.23 (br m, 2H, COD-*H*), 4.94 (s, 1H, (NC)$_2$C*H*), 7.12 (s, 6H, $^{meta/para}$Ar-*H*); ^{13}C{^{1}H} NMR (400 MHz, C_6D_6,

298K): δ/ppm = 25.3, 26.0, 29.3, it was not possible to observe COD carbons, 95.4, 126.0, 146.7, 170.7, it was not possible to observe the COD carbons. Elemental analysis calcd. for $C_{45}H_{65}N_2MgCo$ (Mw: 717.27 g mol^{-1}) C 75.35 H 9.13 N 3.91; found C 74.59 H 8.37 N 3.83 (Low C value attributed to the presence of minor amounts cobalt particles, formed during heating. Such was observed for $\{K(DME)_2\}\{Co(\eta_4\text{-}C_{14}H_{10})_2\}$).[5]

[(Depnacnac)Mg)(DMAP)$_3$][Co(COD)$_2$] (2·DMAP):

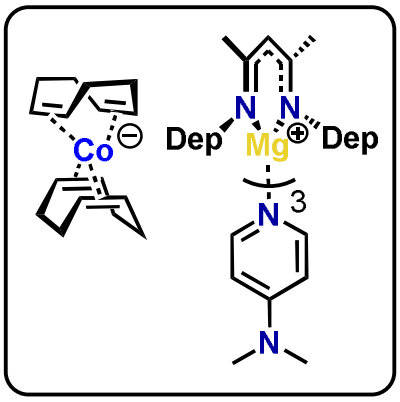

Toluene was added to a Schlenk flask containing (Depnacnac)MgCo(COD)$_2$ (**2**, 0.1 g, 0.15 mmol) and DMAP (0.055 g, 0.45 mmol) at ambient temperature and then stirred overnight. The reaction solution was then concentrated, filtered and on standing at ambient temperature an orange solid crystallised overnight. The solid was isolated via filtration, washed with *n*-hexane and dried *in vacuo* to yield [(Depnacnac)Mg(DMAP)$_3$][Co(COD)$_2$] as an orange solid (0.081 g, 52 %). UV/vis (toluene, λ_{max} / nm, ε_{max} / L mol^{-1} cm^{-1}): 347 (29000). ^{1}H NMR (400 MHz, C_6D_6, 298 K): δ/ppm = 1.04 (t, 12H, CH_2CH_3), 1.73 (s, 6H, NCC*H*$_3$), 2.24 (s, 18H, N(C*H*$_3$)$_2$), 2.46 (m, 8H, C*H*$_2$CH$_3$), 2.62 (br m, 8H, COD-*H*), 2.87 (br m, 8H, COD-*H*), 3.10 (br m, 8H, COD-*H*), 5.10 (s, 1H, (NC)$_2$C*H*), 6.13 (d, 6H, DMAP-^{meta}*H*), 7.11 (m, 6H, Dep-$^{meta/para}$*H*), 7.66 (d, 6H, DMAP-^{ortho}*H*); ^{13}C{^{1}H} NMR (400 MHz, C_6D_6, 298K): δ/ppm = 14.4, 23.8, 24.3, 35.0, 38.4, 69.9, 95.0, 107.4, 125.6, 126.6, 137.4, 146.4, 148.4, 155.0, 169.8. Elemental analysis calcd. for $C_{62}H_{87}N_8MgCo$ (Mw: 1027.67 g mol^{-1}) C 72.46 H 8.53 N 10.90; found C 72.20 H 8.02 N 10.77.

(Depnacnac)MgCo(P$_2$C$_2$*t*Bu$_2$)(COD) (4):

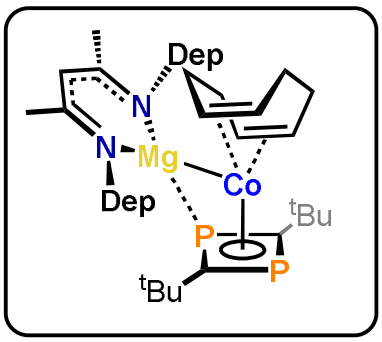

(Depnacnac)MgCo(COD)$_2$ (**2**, 1 g, 0.75 mmol) was dissolved in toluene (10 mL) and to this was added a solution of *t*BuCP in (Me$_3$Si)$_2$O (3.0 mL, 2.56 M) at room temperature, this was then left stirring overnight. Reaction progress was monitored via ^{1}H NMR spectroscopy and when the complete consumption of **2** was observed (generally after 1-2 days) all volatiles were removed *in vacuo* and *n*-hexane was added causing precipitation of a green solid. This solid was isolated via filtration and washed with *n*-hexane to yield (Depnacnac)MgCo(P$_2$C$_2$*t*Bu$_2$)(COD) as a green powder (0.81 g, 71%). X-ray quality crystals were grown from a concentrated benzene solution stored at ambient temperature. UV/vis (toluene, λ_{max} / nm, ε_{max} / L mol^{-1} cm^{-1}): 346 (27000). ^{1}H NMR (400 MHz, C_6D_6, 298 K): δ/ppm = 0.38 (s, 18H, C(C*H*$_3$)$_3$), 1.27 (br m, 12H, CH_2CH_3), 1.62 (s, 6H, NCC*H*$_3$), 2.01 (m, 2H, COD-*H*), 2.13 (m, 2H, COD-*H*), 2.58 – 3.11 (br m, 14H, C*H*$_2$CH$_3$/COD-*H*), 3.60 (br m, 2H, COD-*H*), 5.04 (s, 1H, (NC)$_2$C*H*), 6.98

(m, 6H, $^{meta/para}$Ar-*H*); $^{31}P\{^{1}H\}$ NMR (400 MHz, C_6D_6, 298 K): δ/ppm = -100.6 (s, 1P), 76.5 (s, 1P, Mg-*P*); $^{13}C\{^{1}H\}$ NMR (400 MHz, C_6D_6, 298K): δ/ppm = 14.0, 23.1, 25.0, 26.0, 31.3, 33.4, 33.9, 35.0, 55.0, 67.7, 96.3, 126.0, 126.5, 138.3, 141.0, 148.4, 170.2. Elemental analysis calcd. for $C_{43}H_{63}N_2P_2MgCo$ (Mw: 753.18 g mol^{-1}) C 68.57 H 8.43 N 3.72; found C 68.49 H 7.95 N 3.59.

(^{Dep}nacnac)Mg(THF)Co(P_2C_2tBu$_2$)$_2$ (5):

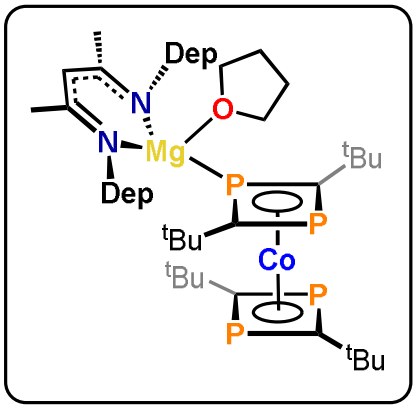

(^{Dep}nacnac)MgCo(COD)$_2$ (**2**, 0.5 g, 0.76 mmol) was dissolved in THF and to this was added a solution of *t*BuCP in $(Me_3Si)_2O$ (2.27 mL, 1.5 M) at room temperature, this was then left to stir overnight. All volatiles were removed *in vacuo* and to the orange solid was added toluene. The resulting solution was filtered, concentrated in vacuo and stored at 5 ˚C to yield (^{Dep}nacnac)Mg.THF{Co(P_2C_2tBu$_2$)$_2$} as an orange-red crystalline solid (0.5 g, 71%). UV/vis (toluene, λ_{max} / nm, ε_{max} / L mol^{-1} cm^{-1}): 287 (28000), 336 (19000). ^{1}H NMR (400 MHz, C_6D_6, 298 K): δ/ppm = 0.92 (s, 18H, PC(CH_3)$_3$), 1.14 (t, 6H, CH_2CH_3), 1.19 (t, 6H, CH_2CH_3), 1.31 (m, 4H, THF-CH_2), 1.40 (s, 9H, MgPC(CH_3)$_3$), 1.43 (s, 9H, MgC(CH_3)$_3$), 1.48 (s, 6H, NCCH_3), 2.40 (q, 4H, CH_2CH_3), 2.63 (m, 4H, CH_2CH_3), 3.88 (m, 4H, THF-OCH_2), 4.84 (s, 1H, (NC)$_2$C*H*), 6.97 – 7.08 (m, 6H, Ar*H*); $^{31}P\{^{1}H\}$ NMR (400 MHz, C_6D_6, 298 K): δ/ppm = -27.2 (s, 1P, Mg*P*(C*t*Bu)$_2$P), 13.5 (s, 2P, P_2CtBu$_2$), 29.9 (s, 1P, (s, 1P, MgP(C*t*Bu)$_2$*P*); $^{13}C\{^{1}H\}$ NMR (400 MHz, C_6D_6, 298K): δ/ppm = 12.8, 13.8, 14.3, 23.0, 23.9, 24.2, 24.7, 25.7, 31.9, 32.9, 33.5, 33.8, 34.8, 35.8, 71.7, 95.5, 125.5, 126.1, 126.7, 136.1, 137.4, 146.8, 170.0. Elemental analysis calcd. for $C_{56}H_{85}N_2OP_2MgCo$ (Mw: 1009.44 g mol^{-1}) C 66.63 H 8.49 N 2.78; found C 66.83 H 8.50 N 2.65.

[(^{Dep}nacnac)MgCoP$_4$ (P_2C_2tBu$_2$)]$_2$ (6):

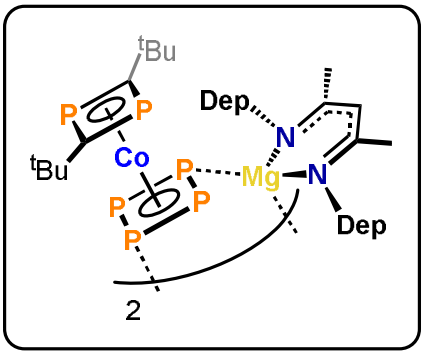

(^{Dep}nacnac)MgCo(P_2C_2tBu$_2$)(COD) (**4**, 0.1 g, 0.13 mmol) and white phosphorus (0.021 g, 0.17 mmol) were dissolved in toluene (5 mL) and heated to 80 °C for two days. The reaction mixture was filtered and left to slowly evaporate in a N_2 glove box. A small amount of orange-red crystals suitable for X-ray analysis formed after one week. The mother liquor was dried in vacuo and washed with toluene and *n*-hexane, giving [(^{Dep}nacnac)MgCoP$_4$(P_2C_2tBu$_2$)]$_2$ (**6**) as a brown-red powder (0.04 g , 39%). The product is insoluble in common organic solvents such as THF, toluene, diethyl ether, and *n*-hexane and decomposes in DMF.

Note: Due to the very low solubility of the isolated product purification and definitive NMR spectroscopic analysis was not possible. ^{1}H and ^{31}P{^{1}H} NMR spectra of partially dried reaction mixtures are shown in Figure S30 and S31. Based on the solid state structure, compound **6** should give rise to 4 signals in the ^{31}P NMR spectra, which we tentatively assign to the resonances observed at δ/ppm = –71.7, –4.3, 43.0 and 72.3.

(Cp*NiP$_2$C$_2$*t*Bu$_2$)Co(COD) (7):

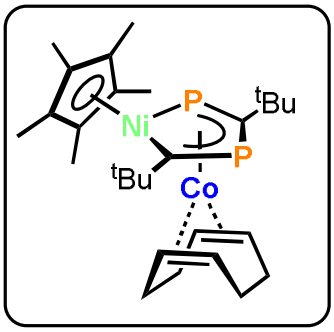

To a Schlenk flask containing (^{Dep}nacnac)MgCo(P$_2$C$_2$*t*Bu$_2$)(COD) (**4**, 0.3 g, 0.39 mmol) and Cp*Ni(acac) (0.11 g, 0.39 mmol) cooled to 0 °C was added toluene and left to stir overnight. All volatiles were removed in vacuo and the residue was extracted with *n*-hexane and stored at –20 °C to yield black-red crystals of {(Cp*)NiC$_2$P$_2$*t*Bu$_2$}Co(COD) (0.14 g, 62%). UV/vis (toluene, λ_{max} / nm, ε_{max} / L mol^{-1} cm^{-1}): 287 (46000), 324 (43000), 419 (18000). ^{1}H NMR (400 MHz, C$_6$D$_6$, 298 K): δ/ppm = 1.32 (m, 4H, COD-*H*), 1.53 (s, 24H, C(C*H*$_3$)$_3$/Cp*-*H*), 2.07 (s, 9H, C(C*H*$_3$)$_3$), 2.32 (m, 2H, COD-*H*), 3.56 (m, 2H, COD-*H*), 4.37 (m, 2H, COD-*H*); ^{31}P{^{1}H} NMR (400 MHz, C$_6$D$_6$, 298 K): 197.1 (d, 1P, $^{2}J_{PP}$ = 28 Hz), 460.3 (d, 1P, $^{2}J_{PP}$ = 28 Hz, Ni-*P*); ^{13}C{^{1}H} NMR (400 MHz, C$_6$D$_6$, 298 K): δ/ppm = 10.8, 10.9, 28.7, 35.5, 35.7, 36.1, 40.6, 50.7, 71.3, 75.2, 101.8. Elemental analysis calcd. for C$_{29}$H$_{48}$P$_2$CoNi (Mw: 576.28 g mol^{-1}) C 60.44, H 8.40; found C 60.58, H 8.04.

2. X-Ray Crystallography

Crystallographic data were recorded on a Super Nova with a Mikrofocus Cu anode and an Atlas CCD Detector. In all cases, Cu-K_α radiation (λ = 1.54184 Å) was used. Crystals were selected under mineral oil, mounted on micromount loops and quench-cooled using an Oxford Cryosystems open flow N_2 cooling device. The diffraction pattern was indexed and the total number of runs and images was based on the strategy calculation from the program CrysAlisPro (Rigaku, V1.171.40.18b, 2018). The unit cell was refined using CrysAlisPro (Rigaku, V1.171.40.18b, 2018). Either semi-empirical multi-scan absorption corrections or analytical ones were applied to the data.[6] Using Olex2,[7] the structures were solved with SHELXT[8] using intrinsic phasing and refined with SHELXL[9] using least squares refinement on F^2.[10] The hydrogen atoms were located in idealized positions and refined isotropically with a riding model. Crystallographic data for the structures in this paper have been deposited with the Cambridge Crystallographic Data Centre, CCDC, 12 Union Road, Cambridge CB21EZ, UK. Copies of these data can be obtained free of charge (http://www.ccdc.cam.ac.uk) on quoting the depository number 2038297, 2054748-2054754 and 2081284.

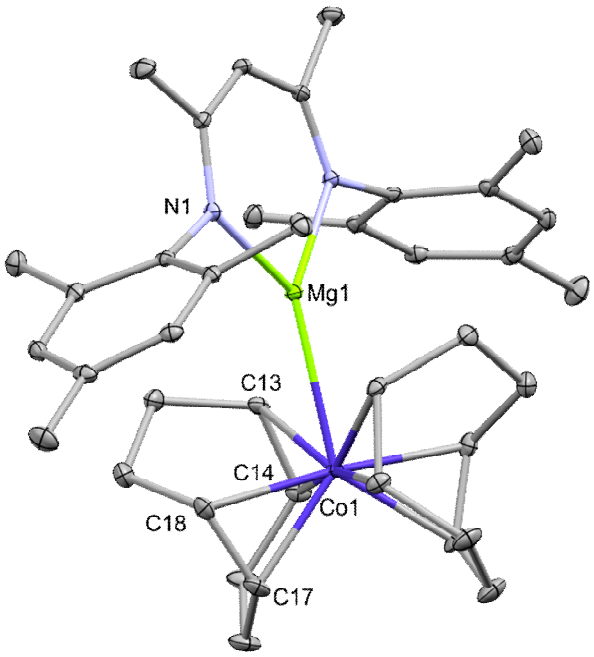

Figure S1. Thermal ellipsoid plot (30% probability surface) of **1** (hydrogens omitted) Selected bond lengths (Å) and angles (°): Co1–Mg1 2.6314(7), Mg1–N1 2.0749(13), N1– Mg1–N1' 91.69(7), N1–Mg1–Co1 134.15(4).

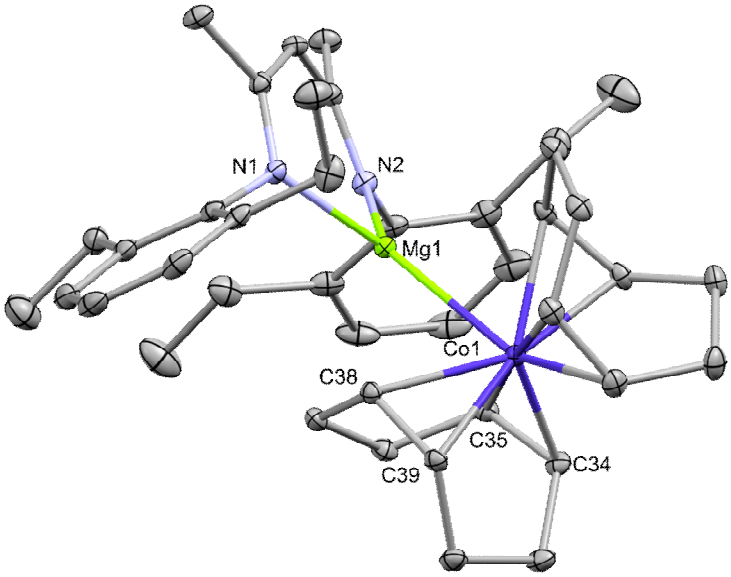

Figure S2. Thermal ellipsoid plot (30% probability surface) of **2** (hydrogens omitted) Selected bond lengths (Å) and angles (°): Co1–Mg1 2.5459(5), N1–Mg1 2.0483(12), N2–Mg1 2.0937(12), N1–Mg1–N2 92.58(5), N1–Mg1–Co1 134.19(4), N2–Mg1–Co1 132.52(4).

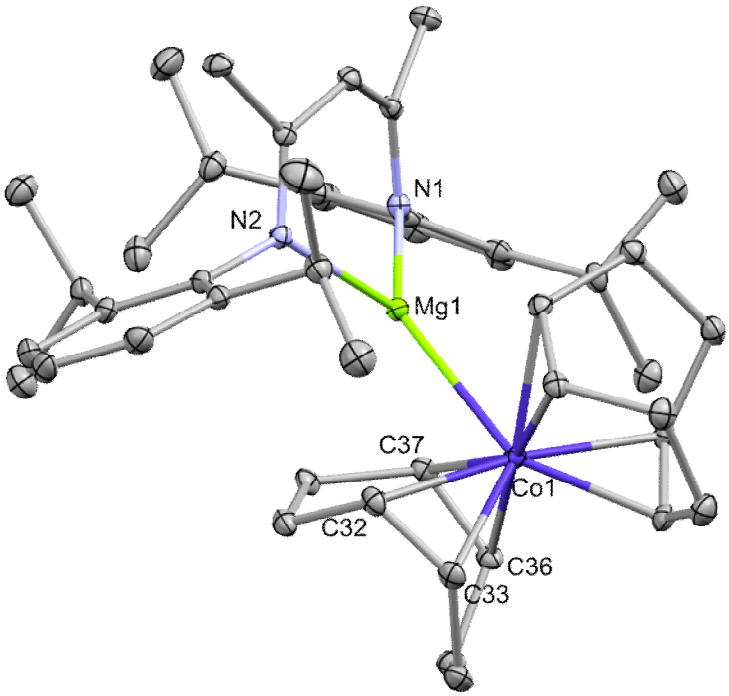

Figure S3. Thermal ellipsoid plot (30% probability surface) of **3** (hydrogens omitted) Selected bond lengths (Å) and angles (°): Co1–Mg1 2.5584(7), Mg1–N1 2.0614(18), Mg1–N2 2.1009(18), N1–Mg1–N2 96.32(7), N1–Mg1–Co1 135.45(6), N2–Mg1–Co1 127.17(6).

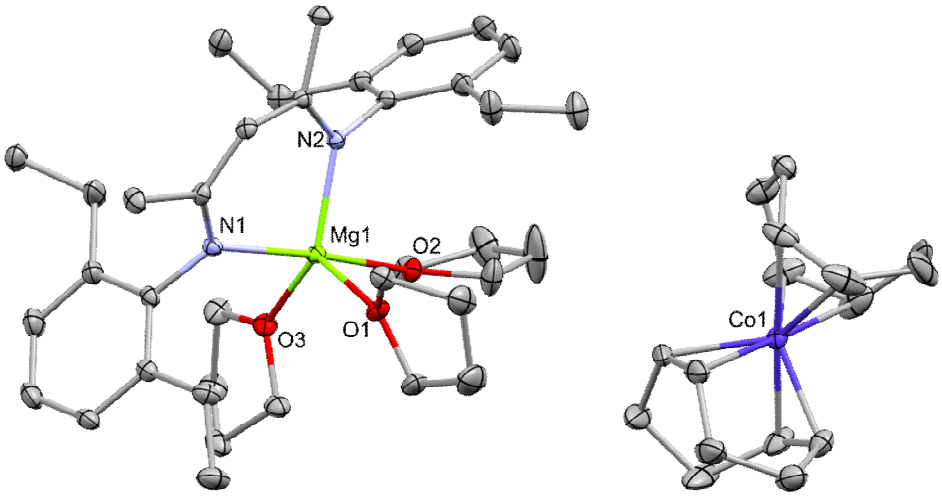

Figure S4. Thermal ellipsoid plot (30% probability surface) of **2·THF** (hydrogens omitted) Selected bond lengths (Å) and angles (°): Mg1–N1 2.1140(15), Mg–N2 2.0707(15), Mg1–O1 12.0790(13), Mg1–O2 2.1461(13), Mg1–O3 2.0806(14), Co–COD (Ave.) 2.0327(2), N1–Mg1–N2 90.01(6).

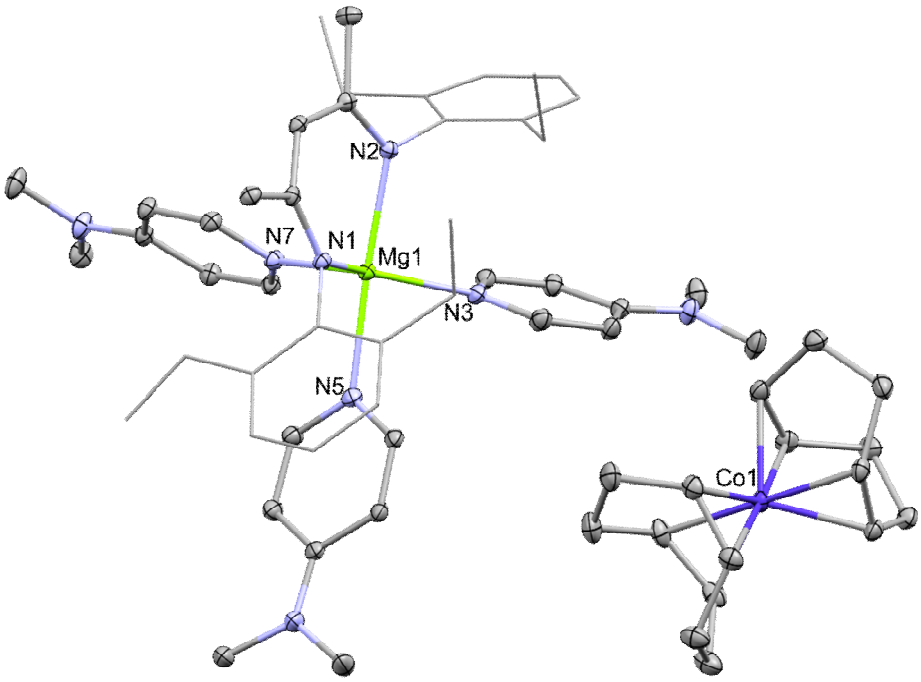

Figure S5. Thermal ellipsoid plot (30% probability surface) of **2·DMAP** (hydrogens omitted) Selected bond lengths (Å) and angles (°): Mg1–N1 2.1250(11), Mg1–N2 2.1543(11), Mg1–N3 2.1796(12), Mg1–N5 2.2167(12), Mg1–N7 2.1484(11), Co–COD (Ave.) 2.0372(14).

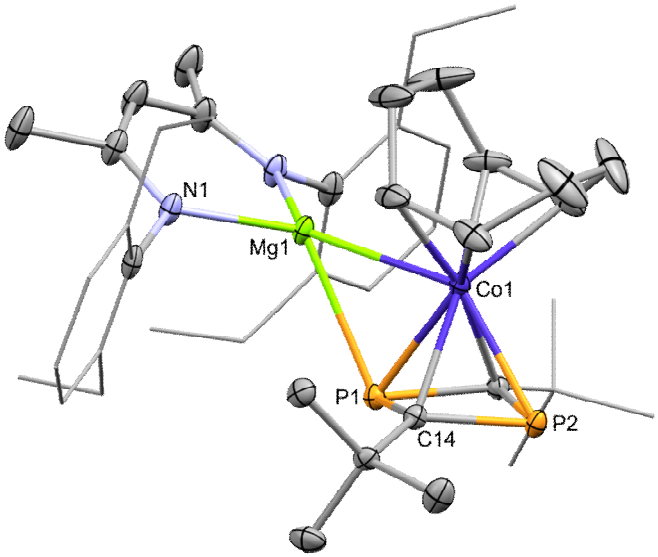

Figure S6. Thermal ellipsoid plot (30% probability surface) of **4** (hydrogens omitted) Selected bond lengths (Å) and angles (°): Mg1–Co1 2.6762(14), Mg1–P1 2.6272(16), Mg–N1 2.064(2), Co1–P1 2.3069(11), Co1–P2 2.2951(11), P1–C14 1.807(3), P2–C14 1.788(3), N1–Mg1–N1' 92.89(14), P1–Co1–P2 72.07(4).

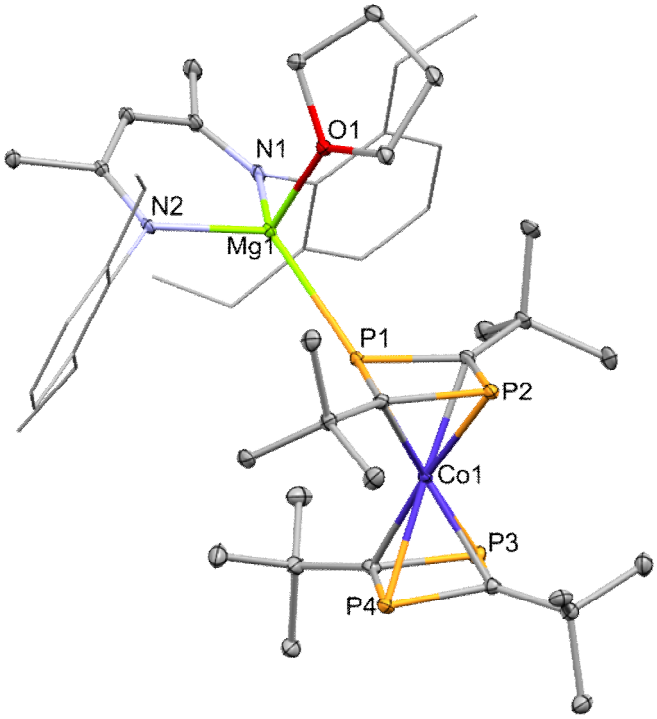

Figure S7. Thermal ellipsoid plot (30% probability surface) of **5** (hydrogens omitted) Selected bond lengths (Å) and angles (°): P1–Mg1 2.6057(11), P1–Co1 2.2235(8), P2–Co1 2.2695(8), P3–Co1 2.2544(9), P4–Co1 2.2591(8), Mg1–O1 2.024(2), Mg1–N1 2.042(2), Mg1–N2 2.019(2), N1–Mg1–N2 94.60(10), P1–Mg1–O1 99.51(7).

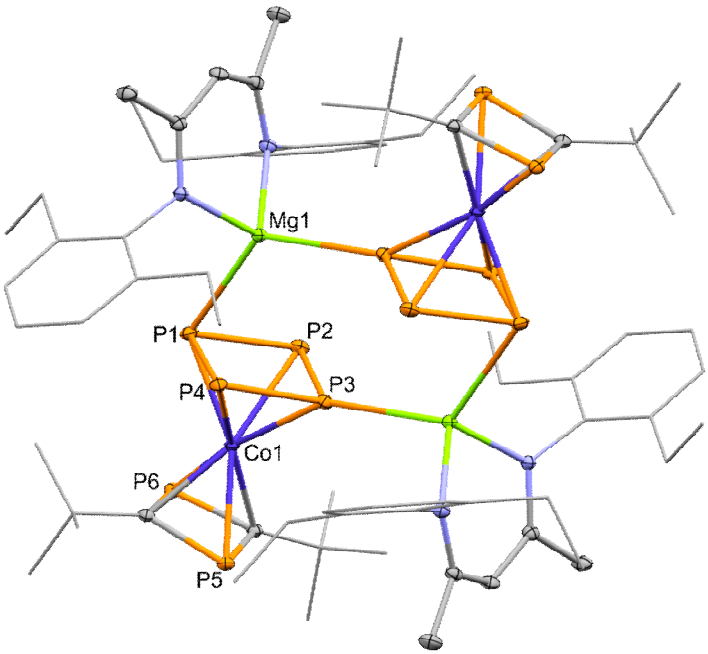

Figure S8. Thermal ellipsoid plot (30% probability surface) of **6** (hydrogens omitted) Selected bond lengths (Å) and angles (°): Co-P1 2.2460(4), Co1–P2 2.3322(4), Co1–P3 2.2520(4), Co1–P4 2.2988(4), Co1–P5 2.2514(4), Co1–P6 2.2494(4), Mg1–P1 2.6747(6), Mg1'–P3 2.6847(6), P1-P2 2.2083(5), P2-P3 2.1641(5), P3-P4 2.1740(5), P4-P1 2.2184(5), P1-P2-P3 88.553(19), P2-P3-P4 92.834(19), P3-P4-P1 88.047(19), P4-P1-P2 90.451(19).

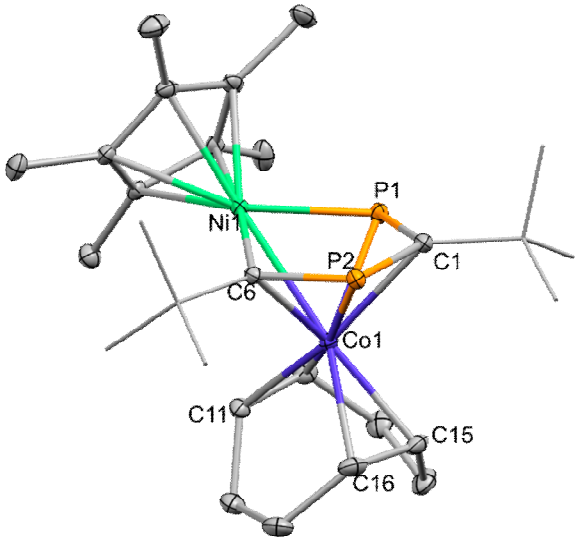

Figure S9. Thermal ellipsoid plots (30% probability surface) of **7**. Hydrogen atoms are omitted for clarity. Selected bond lengths (Å) and angles (°) for **7**: Co1-Ni1 2.5065(3), Ni1-P1 2.2051(4), Ni1-C6 1.9269(14), P1-C1 1.7388(15), C1-P2 1.7663(14), P2-C6 1.7625(14), C6-Ni1-P1 92.66(4), C6-P2-C1 101.10(7), P1-C1-P2 120.41(8).

Compound	**1**	**2**	**3**	**2·THF**
Empirical formula	$C_{39}H_{53}CoMgN_2$	$C_{41}H_{57}CoMgN_2$	$C_{45}H_{65}CoMgN_2$	$C_{57}H_{89}CoMgN_2O_4$
Formula weight	633.07	661.12	717.23	948.00
Temperature [K]	123(1)	123(1)	123(1)	123(1)
Crystal system	Monoclinic	Monoclinic	orthorhombic	triclinic
Space group	C2/c	$P2_1/c$	Pbca	P-1
a [Å]	15.0053(4)	9.06340(10)	19.3913(4)	11.6935(3)
b [Å]	15.5613(3)	13.9493(2)	16.0799(4)	14.9701(4)
c [Å]	14.1623(3)	27.4651(5)	24.4772(6)	16.3882(4)
α [°]	90	90	90	91.301(2)
β [°]	98.952(2)	92.341(2)	90	106.295(2)
γ [°]	90	90	90	109.225(2)
Volume [Å³]	3266.64(13)	3469.46(9)	7632.2(3)	2578.95(12)
Z	4	4	8	2
ρ_{calc} *[g/cm³]*	1.287	1.266	1.248	1.221
μ [mm⁻¹]	4.518	4.275	3.925	3.083
F(000)	1360.0	1424.0	3104.0	1029.0
Crystal size [mm³]	0.368 × 0.169 × 0.118	0.3 × 0.136 × 0.105	0.357 × 0.12 × 0.044	0.716 × 0.282 × 0.158
Radiation	Cu Kα (λ = 1.54184)	Cu Kα (λ = 1.54184)	Cu Kα (λ = 1.54184)	Cu Kα (λ = 1.54184)
2Θ range for data collection [°]	8.238 to 152.884	6.442 to 147.35	7.224 to 148.006	6.304 to 148.002
Index ranges	-18 ≤ h ≤ 18, -19 ≤ k ≤ 19, -17 ≤ l ≤ 14	-10 ≤ h ≤ 11, -17 ≤ k ≤ 17, -33 ≤ l ≤ 32	-19 ≤ h ≤ 23, -14 ≤ k ≤ 19, -30 ≤ l ≤ 25	-14 ≤ h ≤ 14, -18 ≤ k ≤ 18, -19 ≤ l ≤ 20
Reflections collected	19018	20055	23793	48564
Independent reflections	3389 [R_{int} = 0.0549, R_{sigma} = 0.0294]	6739 [R_{int} = 0.0211, R_{sigma} = 0.0217]	7609 [R_{int} = 0.0419, R_{sigma} = 0.0414]	10227 [R_{int} = 0.0413, R_{sigma} = 0.0250]
Data / restraints / parameters	3389/0/200	6739/0/432	7609/0/468	10227/0/603
Goodness-of-fit on F²	1.060	1.056	1.026	1.040
Final R indexes [I>=2σ (I)]	R1 = 0.0339, wR2 = 0.0922	R_1 = 0.0299, wR_2 = 0.0760	R_1 = 0.0434, wR_2 = 0.1009	R_1 = 0.0455, wR_2 = 0.1190
Final R indexes [all data]	R1 = 0.0346, wR2 = 0.0930	R_1 = 0.0328, wR_2 = 0.0777	R_1 = 0.0583, wR_2 = 0.1090	R_1 = 0.0475, wR_2 = 0.1209
Largest diff. peak/hole [e Å⁻³]	0.47/-0.46	0.43/-0.28	0.89/-0.37	0.46/-0.46

Compound	**2·DMAP**	**4**	**5**	**6**
Empirical formula	$C_{62}H_{87}CoMgN_8$	$C_{43}H_{63}CoMgN_2P_2$	$C_{56}H_{86}CoMgN_2OP_4$	$C_{35}H_{51}CoMgN_2P_6$
Formula weight	1027.63	753.13	1010.38	768.83
Temperature [K]	123(1)	123(1)	123(1)	123(1)
Crystal system	Triclinic	Orthorhombic	Monoclinic	Monoclinic
Space group	P-1	Pnma	I2/a	C2/c
a [Å]	10.8784(4)	16.8079(4)	21.8957(8)	24.9829(2)
b [Å]	16.6782(6)	20.4351(4)	12.5578(4)	18.9262(2)
c [Å]	16.6923(7)	11.6370(3)	41.1155(11)	16.1632(2)
α [°]	103.677(3)	90	90	90
β [°]	104.369(3)	90	96.235(3)	98.1100(10)
γ [°]	94.547(3)	90	90	90
Volume [Å³]	2819.80(19)	3996.97(16)	11238.3(6)	7566.04(14)
Z	2	4	8	8
ρ_{calc} [g/cm³]	1.210	1.252	1.194	1.350
μ [mm⁻¹]	2.839	4.506	3.863	6.325
F(000)	1108.0	1616.0	4344.0	3232.0
Crystal size [mm³]	0.428 × 0.294 × 0.125	0.493 × 0.311 × 0.118	0.36 × 0.18 × 0.11	0.4 × 0.15 × 0.105
Radiation	Cu Kα (λ = 1.54184)	Cu Kα (λ = 1.54184)	Cu Kα (λ = 1.54184)	Cu Kα (λ = 1.54184)
2Θ range for data collection [°]	6.78 to 148.022	8.654 to 147.496	7.364 to 145.696°	7.148 to 147.936
Index ranges	-13 ≤ h ≤ 13, -20 ≤ k ≤ 16, -20 ≤ l ≤ 20	-18 ≤ h ≤ 20, -24 ≤ k ≤ 25, -10 ≤ l ≤ 14	-27 ≤ h ≤ 26, -14 ≤ k ≤ 15, -43 ≤ l ≤ 50	-31 ≤ h ≤ 31, -23 ≤ k ≤ 22, -19 ≤ l ≤ 20
Reflections collected	42812	20188	24615	36692
Independent reflections	11287 [R_{int} = 0.0259, R_{sigma} = 0.0204]	4086 [R_{int} = 0.0355, R_{sigma} = 0.0228]	10888[R(int) = 0.0446]	7610 [R_{int} = 0.0319, R_{sigma} = 0.0192]
Data / restraints / parameters	11287/0/661	4086/0/239	10888/0/605	7610/0/418
Goodness-of-fit on F²	1.049	1.100	1.031	1.037
Final R indexes [I>=2σ (I)]	R_1 = 0.0324, wR_2 = 0.0860	R_1 = 0.0558, wR_2 = 0.1371	R_1 = 0.0590, wR_2 = 0.1550	R_1 = 0.0264, wR_2 = 0.0692
Final R indexes [all data]	R_1 = 0.0340, wR_2 = 0.0873	R_1 = 0.0577, wR_2 = 0.1384	R_1 = 0.0664, wR_2 = 0.1623	R_1 = 0.0270, wR_2 = 0.0697
Largest diff. peak/hole [e Å⁻³]	0.45/-0.28	1.39/-0.55	1.36/-0.65	0.31/-0.33

Compound	**7**
Empirical formula	$C_{28}H_{45}CoNiP_2$
Formula weight	561.22
Temperature [K]	123(1)
Crystal system	orthorhombic
Space group	Pbca
a [Å]	11.69710(10)
b [Å]	13.92030(10)
c [Å]	33.1444(2)
α [°]	90
β [°]	90
γ [°]	90
Volume [Å³]	5396.81(7)
Z	8
ρ_{calc} *[g/cm³]*	1.381
μ [mm⁻¹]	6.888
F(000)	2384
Crystal size [mm³]	0.25 × 0.13 × 0.17
Radiation	Cu Kα (λ = 1.54184)
2Θ range for data collection [°]	5.332 to 150.27
Index ranges	-14 ≤ h ≤ 14, -16 ≤ k ≤ 17, -40 ≤ l ≤ 41
Reflections collected	31428
Independent reflections	5511 [Rint = 0.0257, Rsigma = 0.0161]
Data / restraints / parameters	5511/0/300
Goodness-of-fit on F²	1.068
Final R indexes [I>=2σ (I)]	R_1 = 0.0246, wR2 = 0.0663
Final R indexes [all data]	R_1 = 0.0260, wR2 = 0.0669
Largest diff. peak/hole [e Å⁻³]	0.33/-0.22

3. NMR Spectroscopy

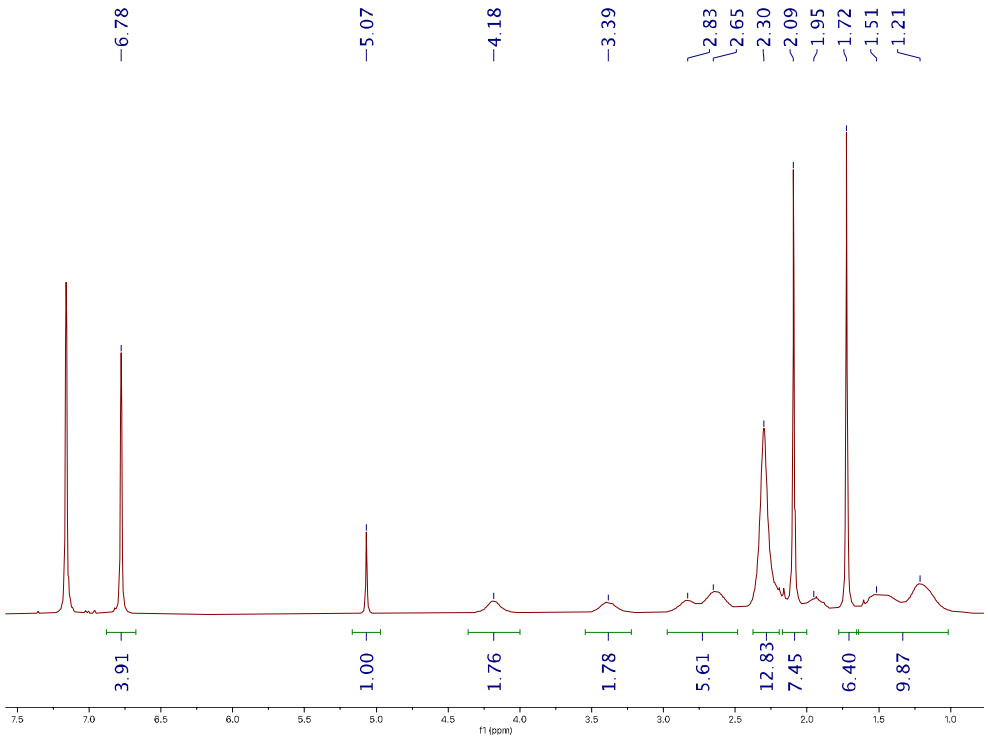

Figure S10. ^{1}H NMR Spectrum of (^{Mes}nacnac)MgCo(COD)$_2$ (**1**) in C_6D_6 at ambient temperature.

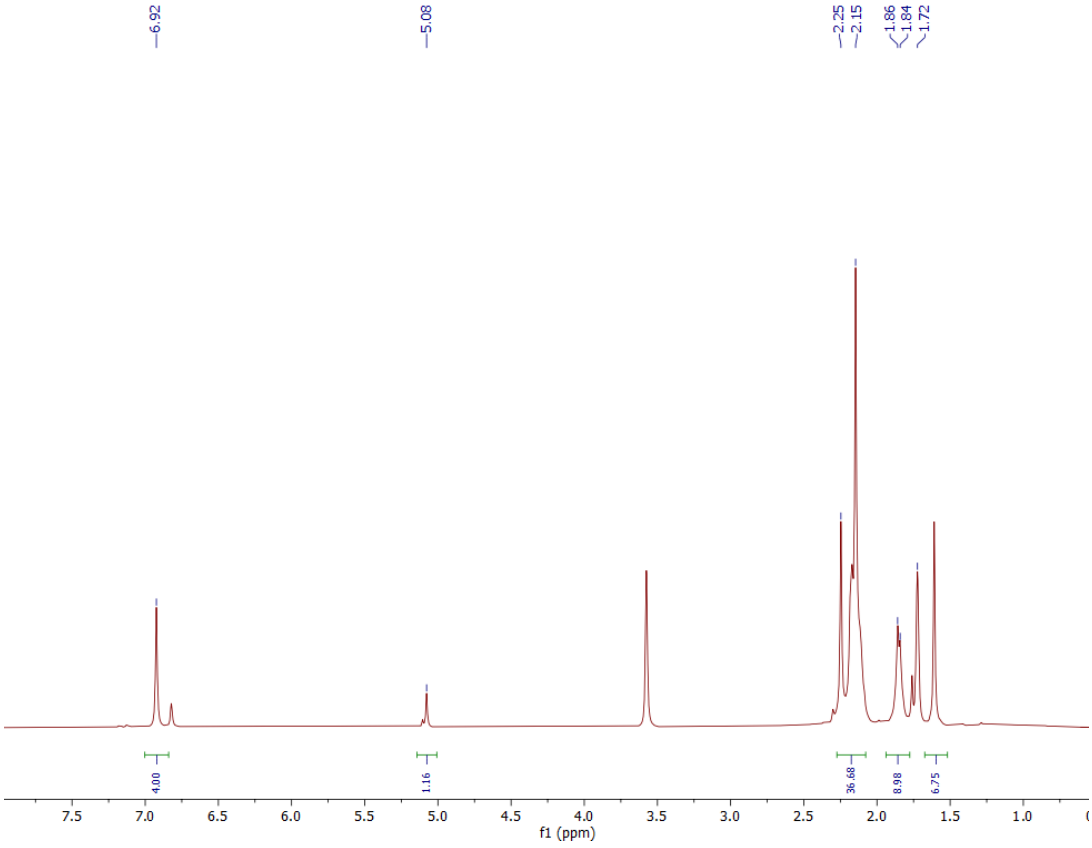

Figure S11. ^{1}H NMR Spectrum of (^{Mes}nacnac)MgCo(COD)$_2$ (**1**) in d^{8}-THF at ambient temperature.

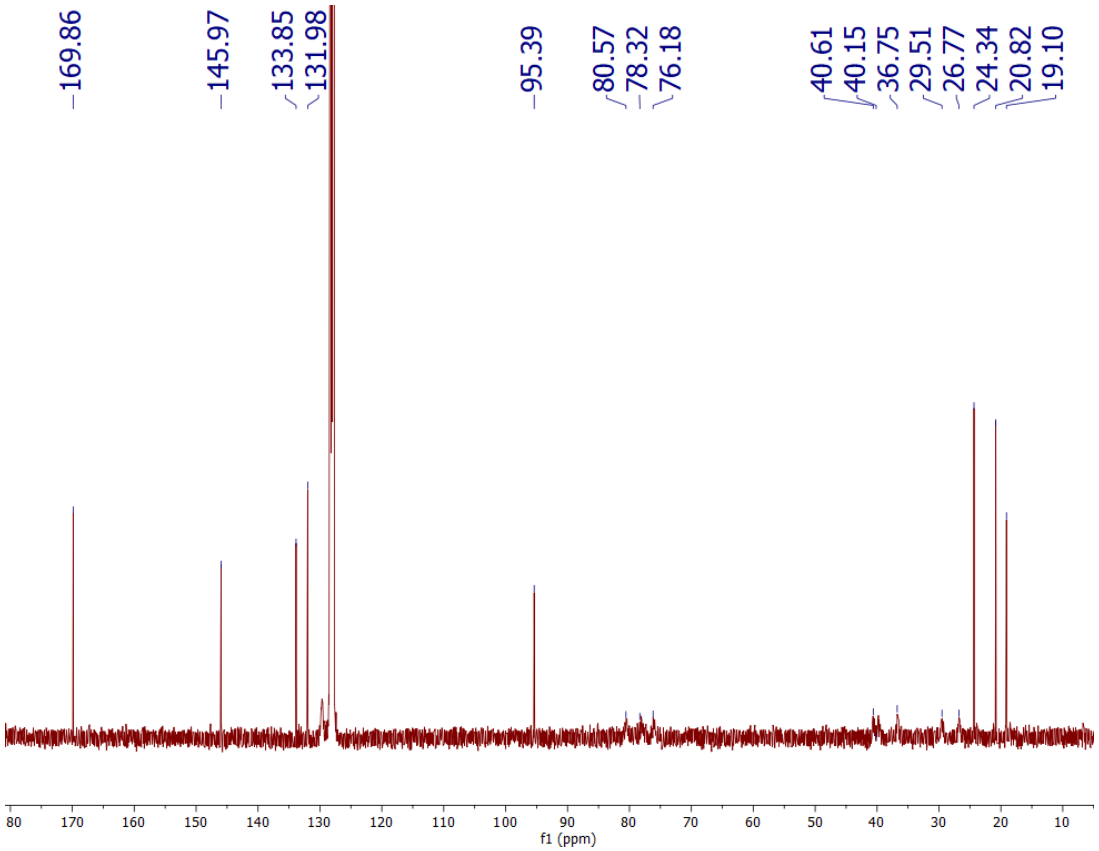

Figure S12. $^{13}C\{^{1}H\}$ NMR spectrum of (^{Mes}nacnac)MgCo(COD)$_2$ (**1**) in C_6D_6 at ambient temperature.

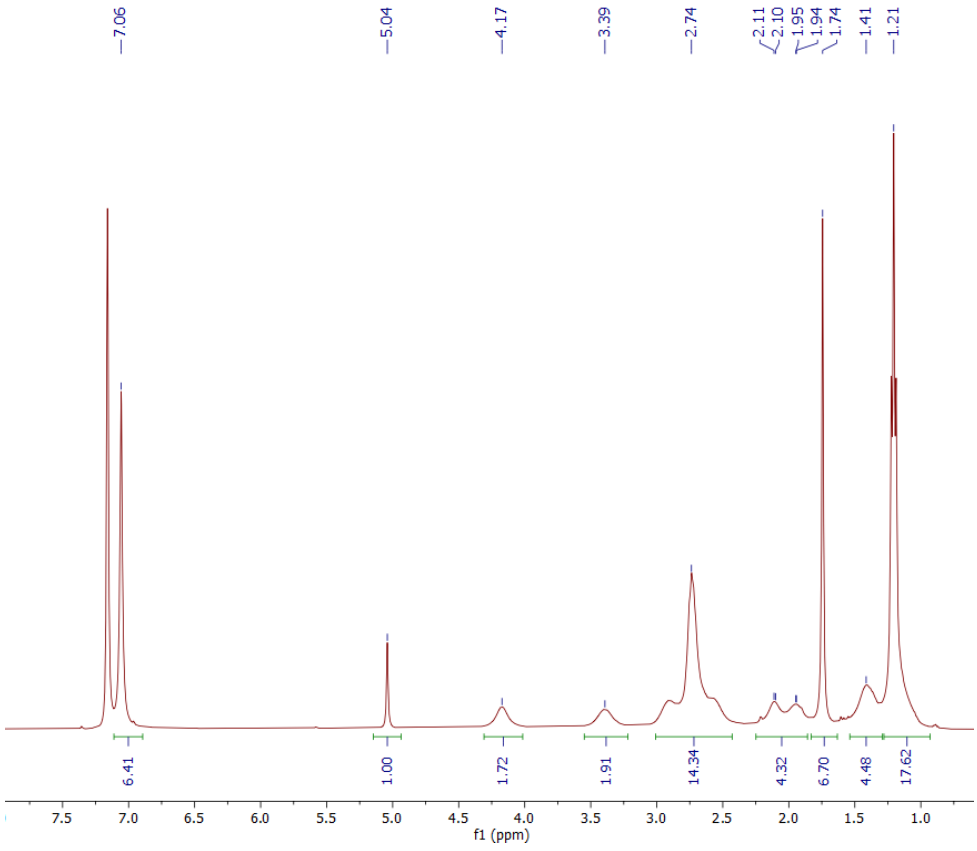

Figure S13. ^{1}H NMR spectrum of (^{Dep}nacnac)MgCo(COD)$_2$ (**2**) in C_6D_6 at ambient temperature.

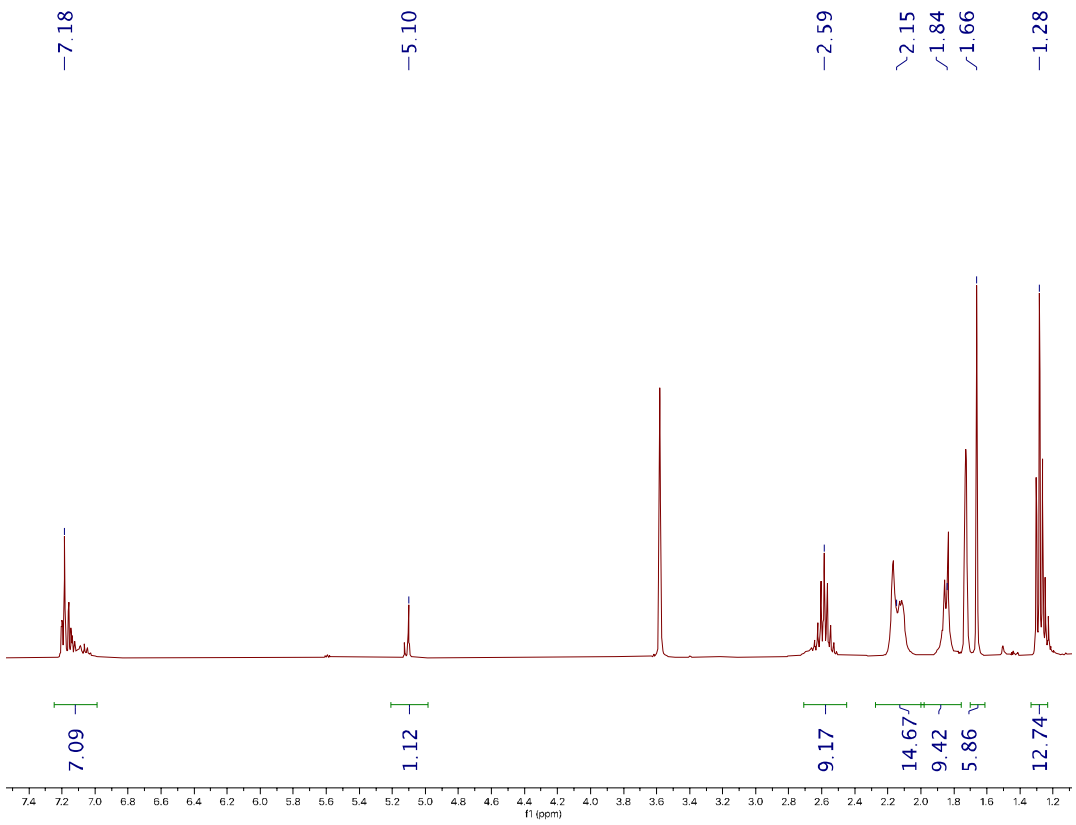

Figure S14. ^{1}H NMR spectrum of [(^{Dep}nacnac)Mg(THF)$_3$][Co(COD)$_2$] (**2·THF**) in d_8-THF at ambient temperature.

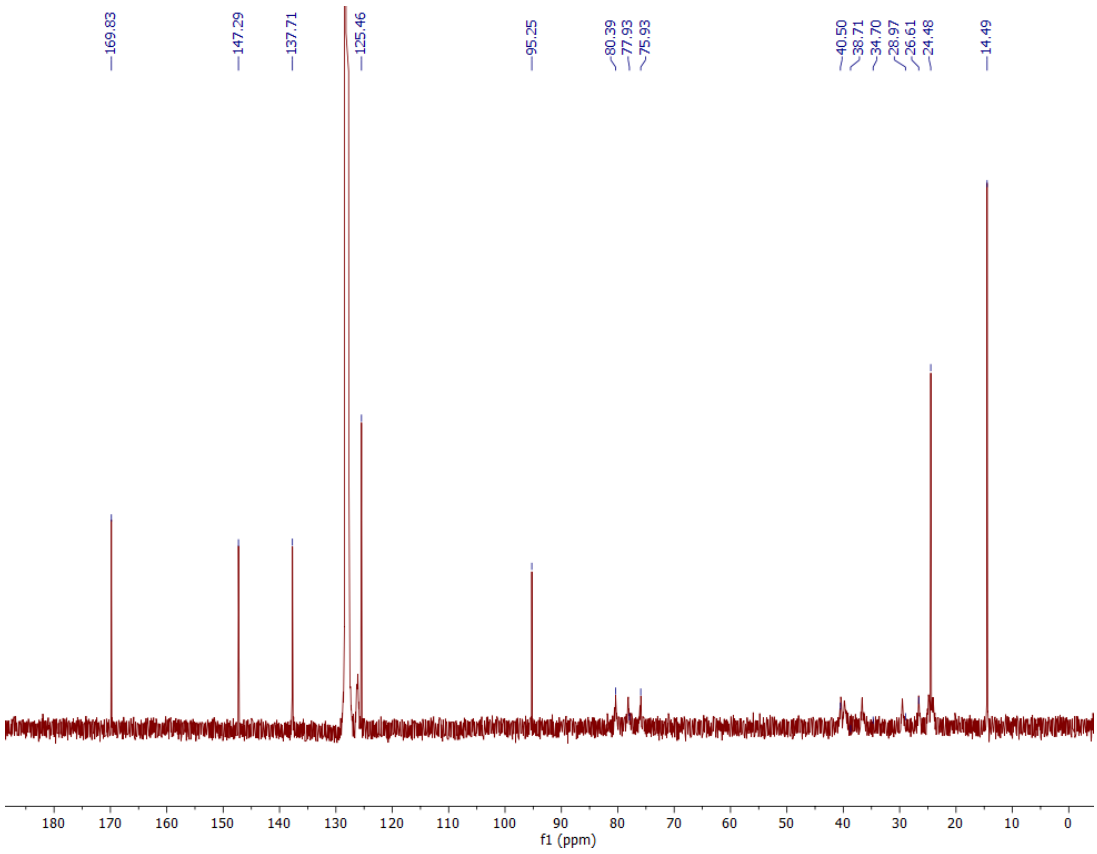

Figure S15. ^{13}C{^{1}H} NMR spectrum of (^{Dep}nacnac)MgCo(COD)$_2$ (**2**) in C_6D_6 at ambient temperature.

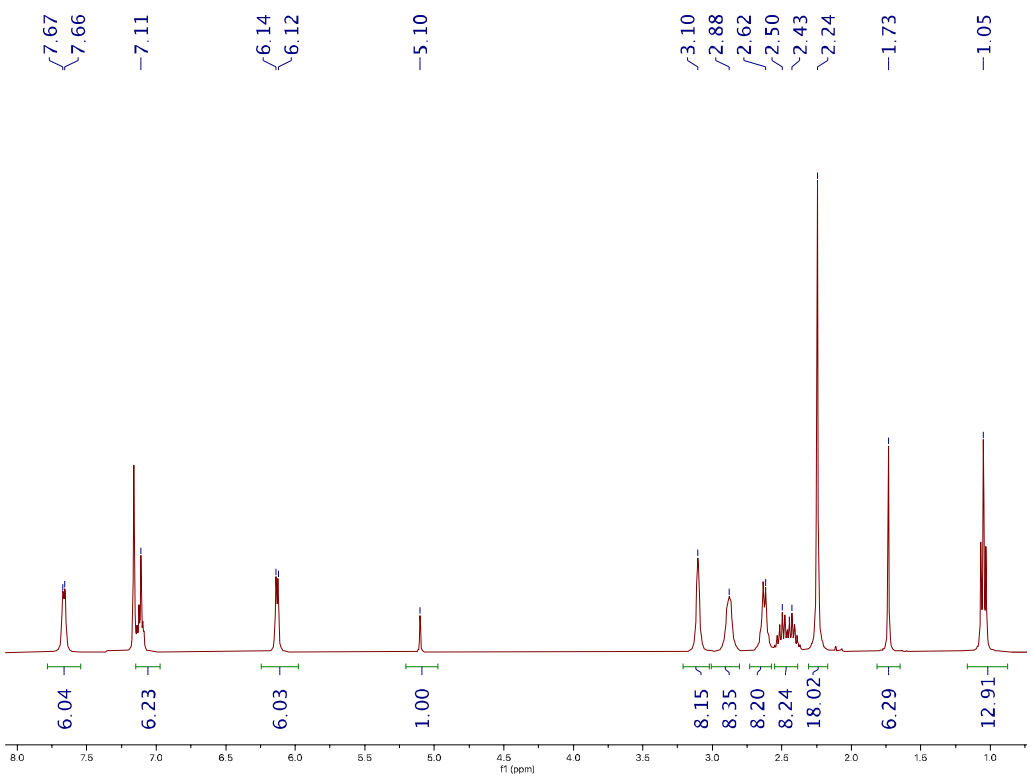

Figure S16. ^{1}H NMR spectrum of [(^{Dep}nacnac)Mg)(DMAP)$_3$][Co(COD)$_2$] (**2·DMAP**) in C_6D_6 at ambient temperature.

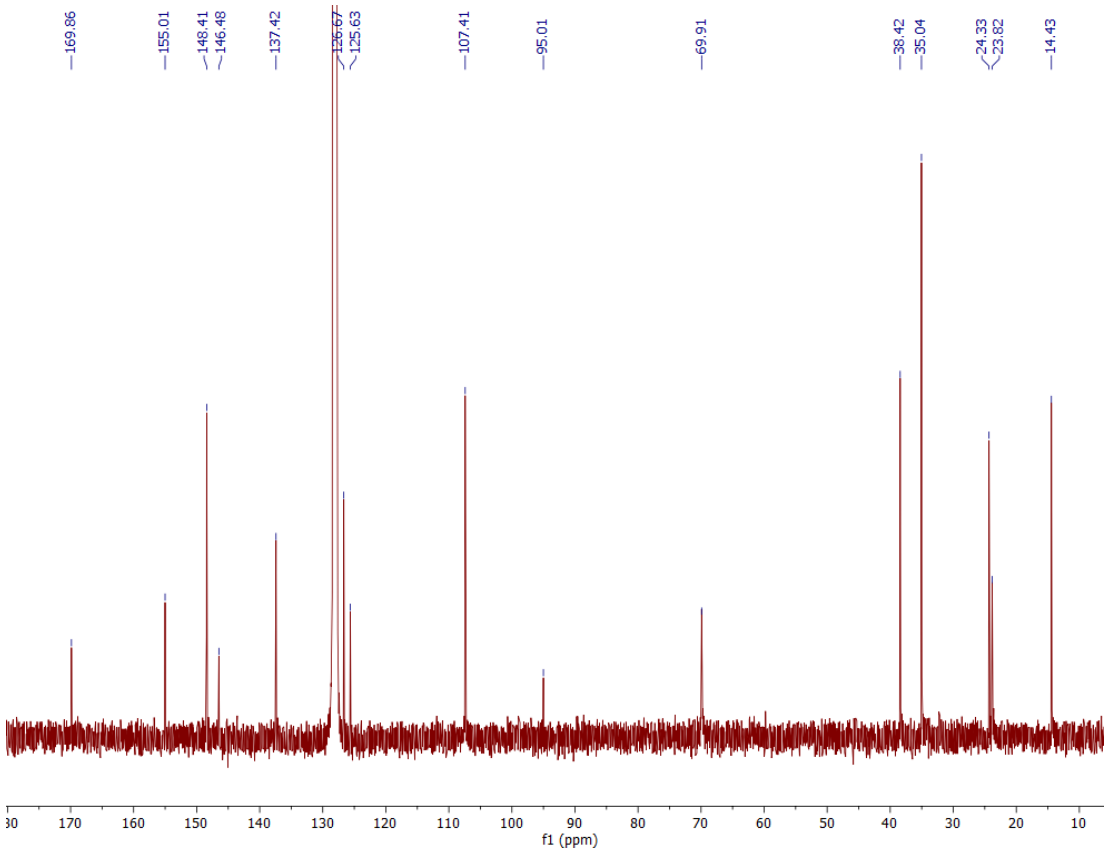

Figure S17. ^{13}C{^{1}H} NMR spectrum of [(^{Dep}nacnac)Mg)(DMAP)$_3$][Co(COD)$_2$] (**2·DMAP**) in C_6D_6 at ambient temperature.

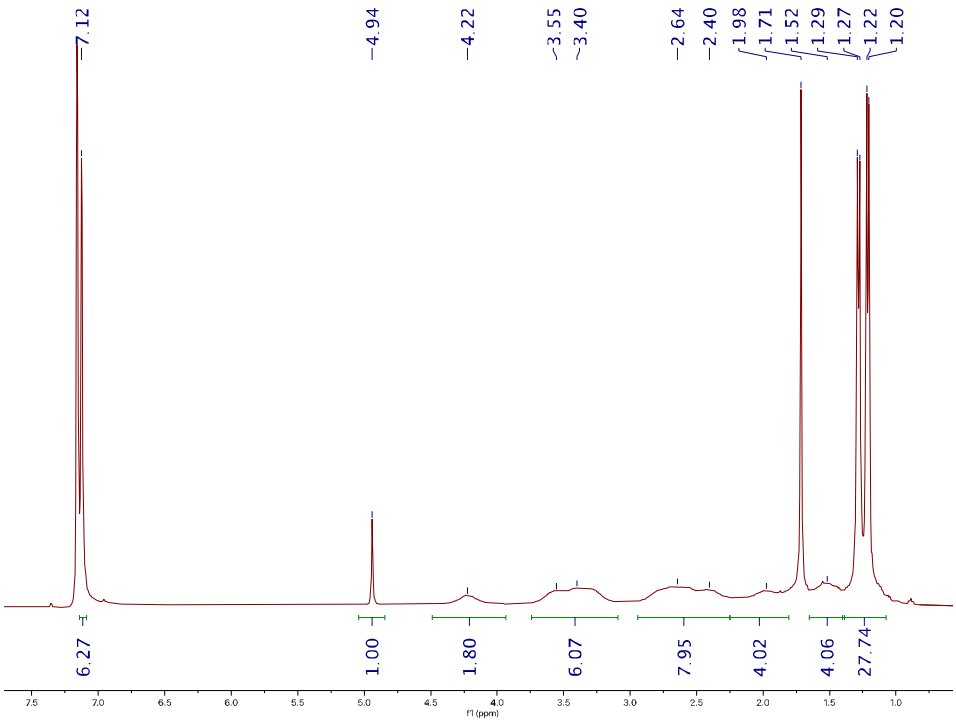

Figure S18. ^{1}H NMR spectrum of (^{Dipp}nacnac)MgCo(COD)$_2$ (**3**) in C_6D_6 at ambient temperature.

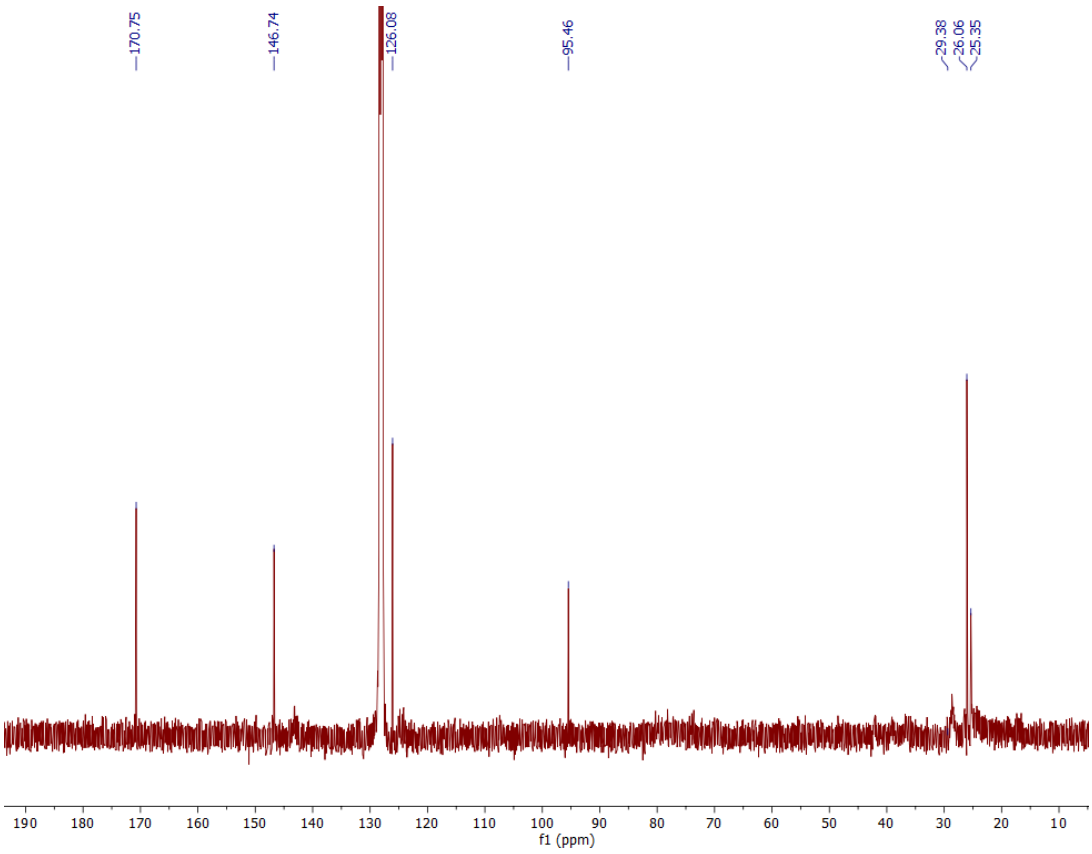

Figure S19. ^{13}C{^{1}H} NMR spectrum of (^{Dipp}nacnac)MgCo(COD)$_2$ (**3**) in C_6D_6 at ambient temperature.

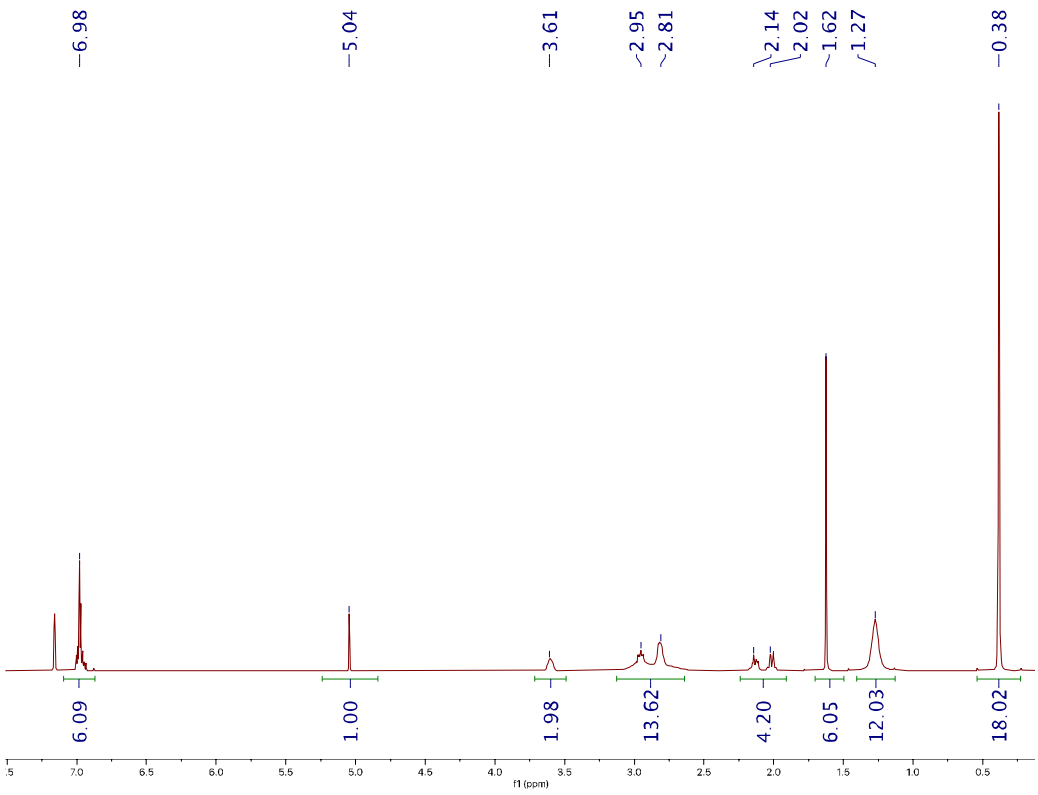

Figure S20. ^{1}H NMR spectrum of (^{Dep}nacnac)MgCo($P_2C_2tBu_2$)(COD) (**4**) in C_6D_6 at ambient temperature.

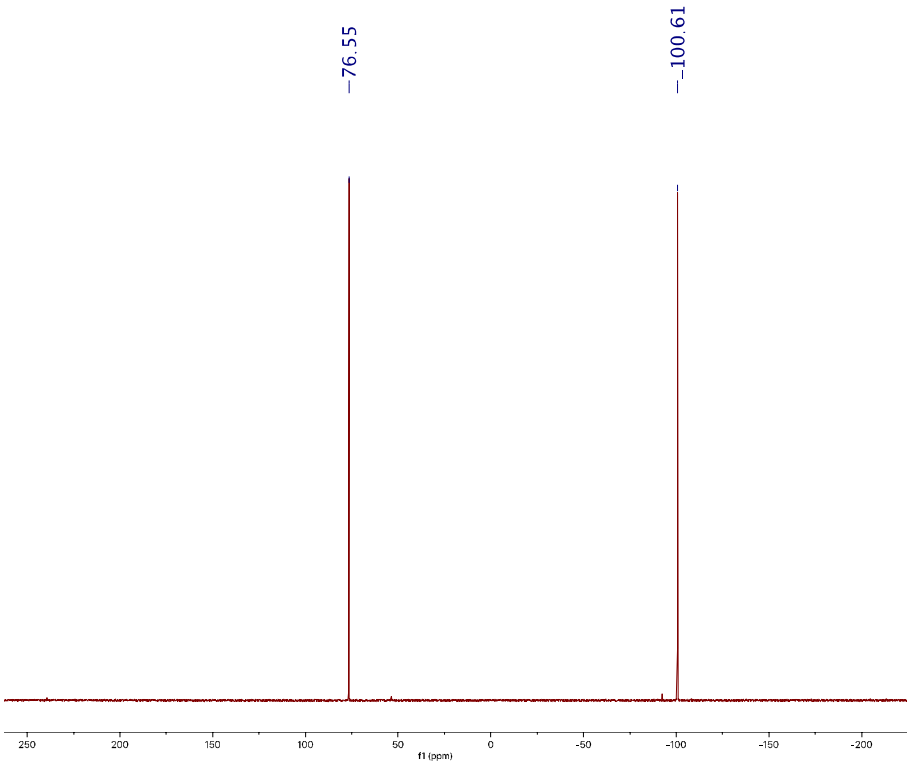

Figure S21. ^{31}P{^{1}H} NMR spectrum of (^{Dep}nacnac)MgCo($P_2C_2tBu_2$)(COD) (**4**) in C_6D_6 at ambient temperature.

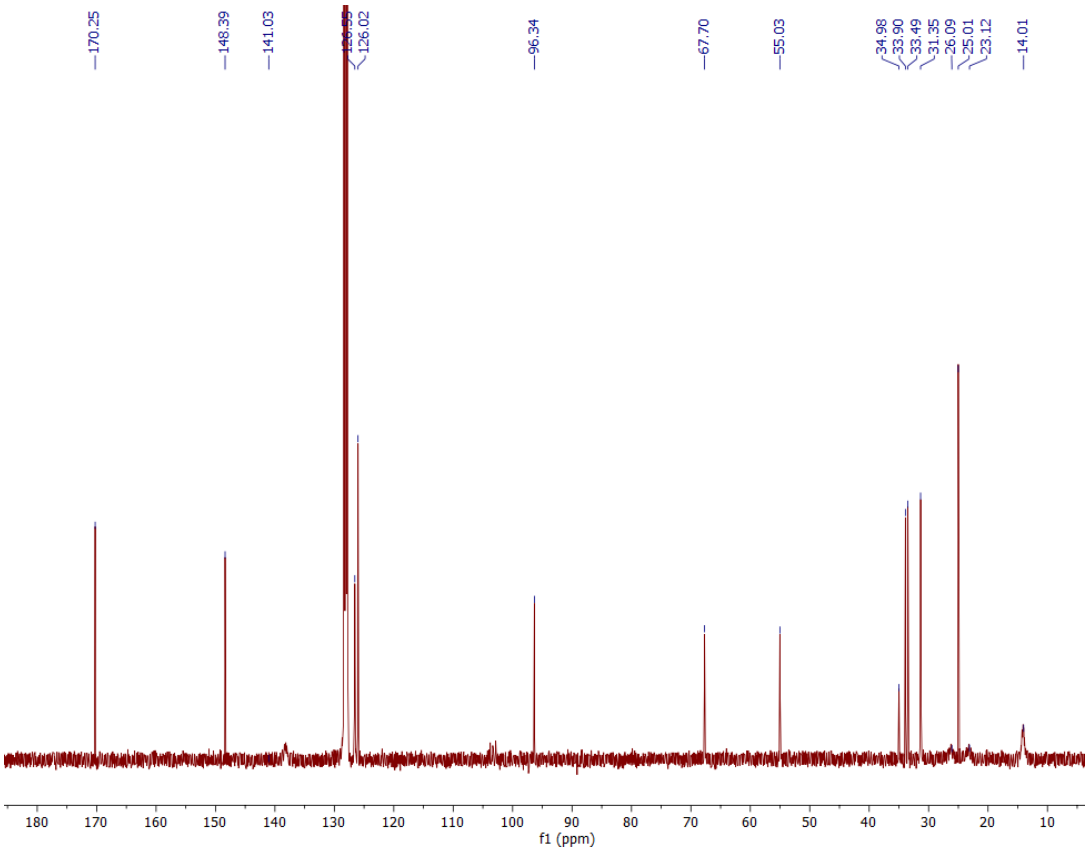

Figure S22. $^{13}C\{^{1}H\}$ NMR spectrum of (^{Dep}nacnac)MgCo($P_2C_2tBu_2$)(COD) (**4**) in C_6D_6 at ambient temperature.

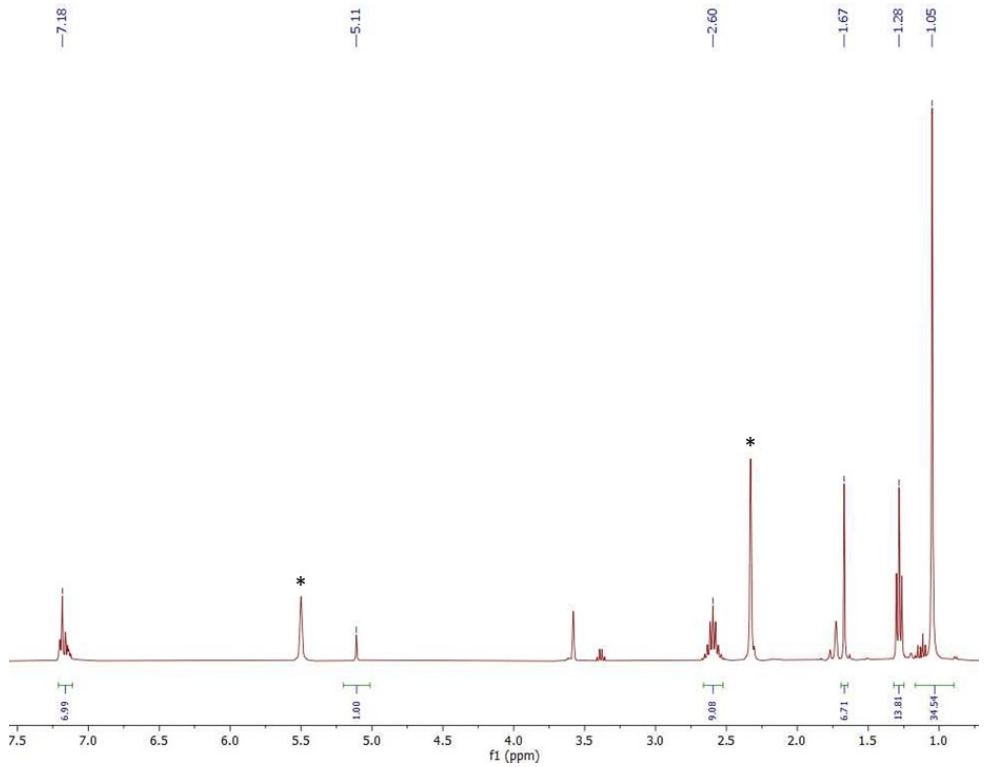

Figure S23. ^{1}H NMR spectrum of the reaction mixture of (^{Dep}nacnac)MgCo$(COD)_2$ + *t*BuCP (4 equiv., in TMS_2O) in d^8-THF at ambient temperature (*: COD).

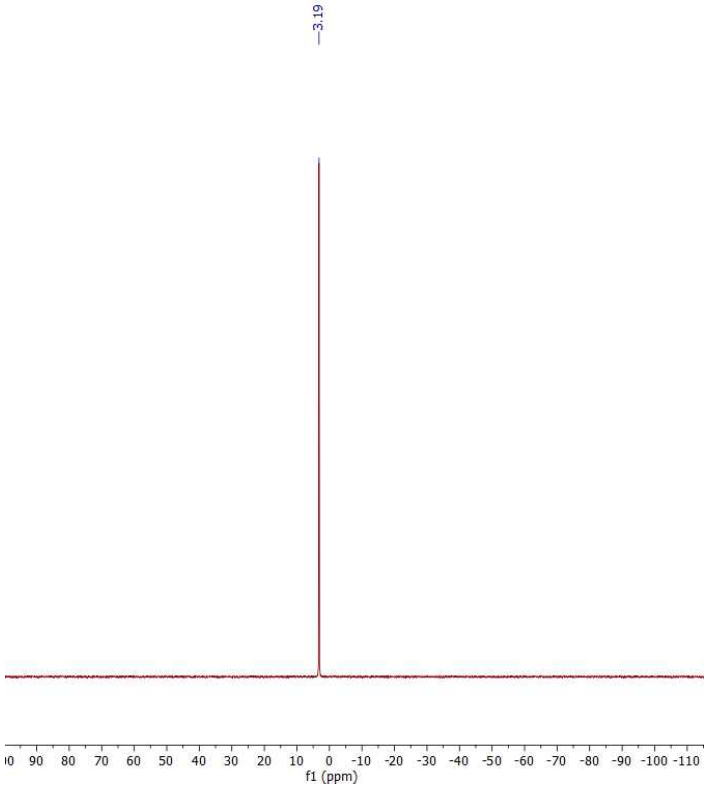

Figure S24. $^{31}P\{^{1}H\}$ NMR spectrum of the reaction mixture of (^{Dep}nacnac)MgCo(COD)$_2$ + *t*BuCP (4 equiv., in TMS_2O) in d^8-THF at ambient temperature.

Figure S25. ^{1}H NMR spectrum of (^{Dep}nacnac)Mg(THF)Co($P_2C_2tBu_2$)$_2$ (**5**) in C_6D_6 at ambient temperature.

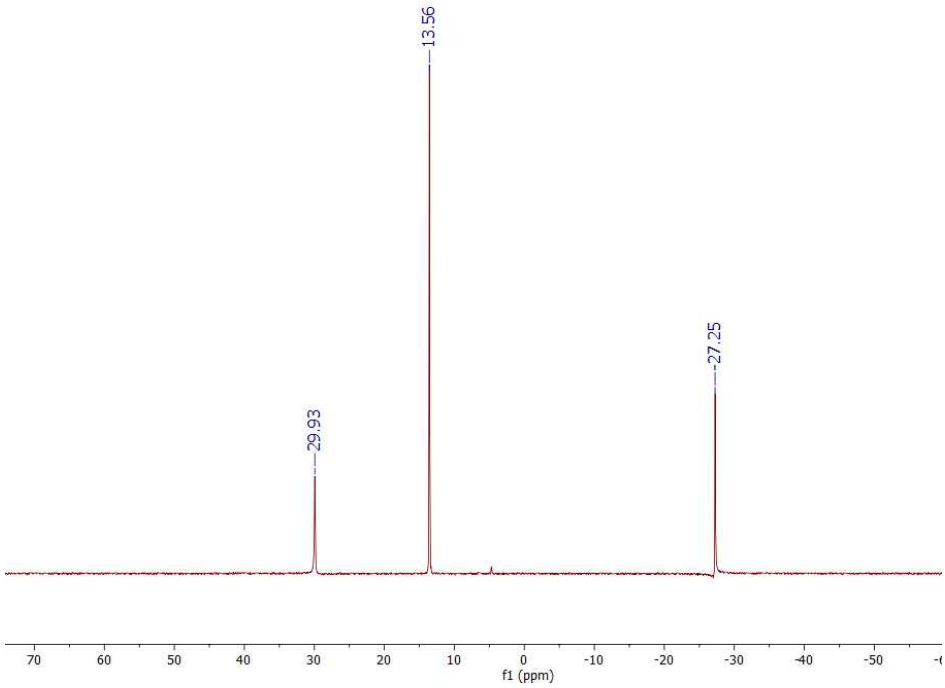

Figure S26. $^{31}P\{^{1}H\}$ NMR Spectrum of (^{Dep}nacnac)Mg(THF)Co(P_2C_2tBu$_2$)$_2$ (**5**) in C_6D_6 at ambient temperature.

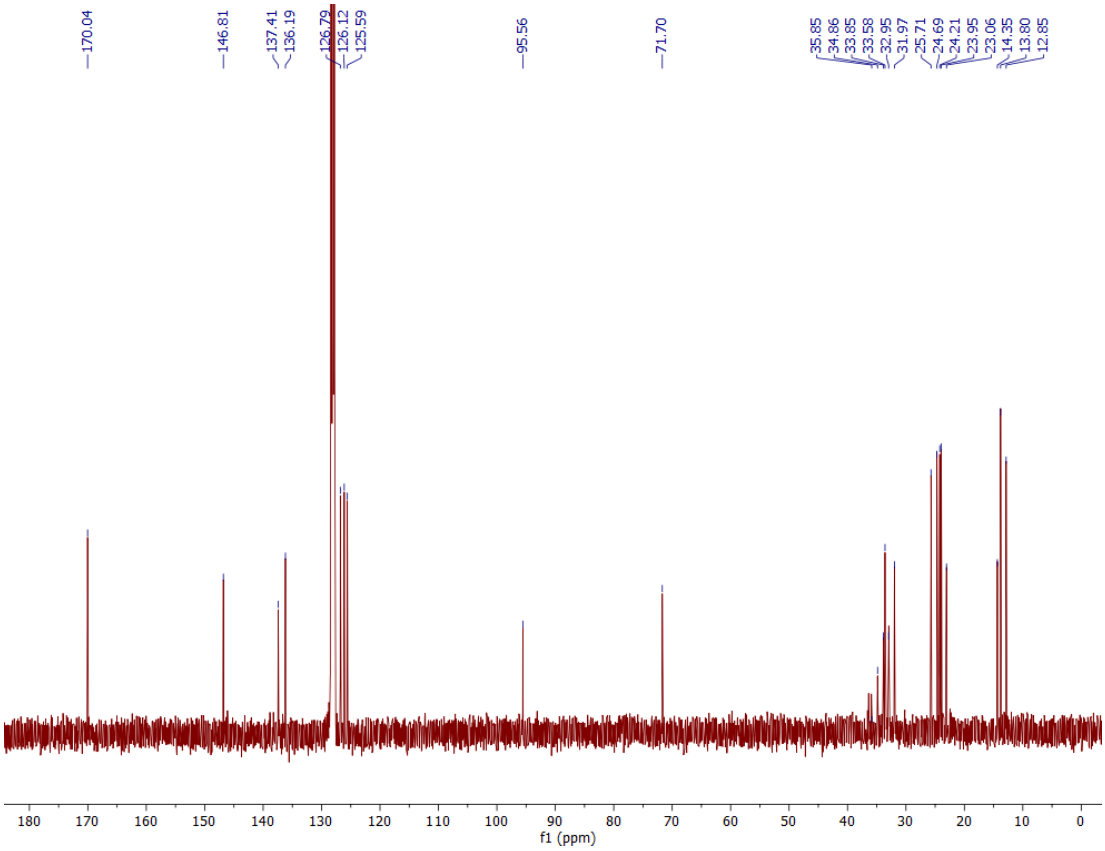

Figure S27. $^{13}C\{^{1}H\}$ NMR spectrum of (^{Dep}nacnac)Mg(THF)Co(P_2C_2tBu$_2$)$_2$ (**5**) in C_6D_6 at ambient temperature.

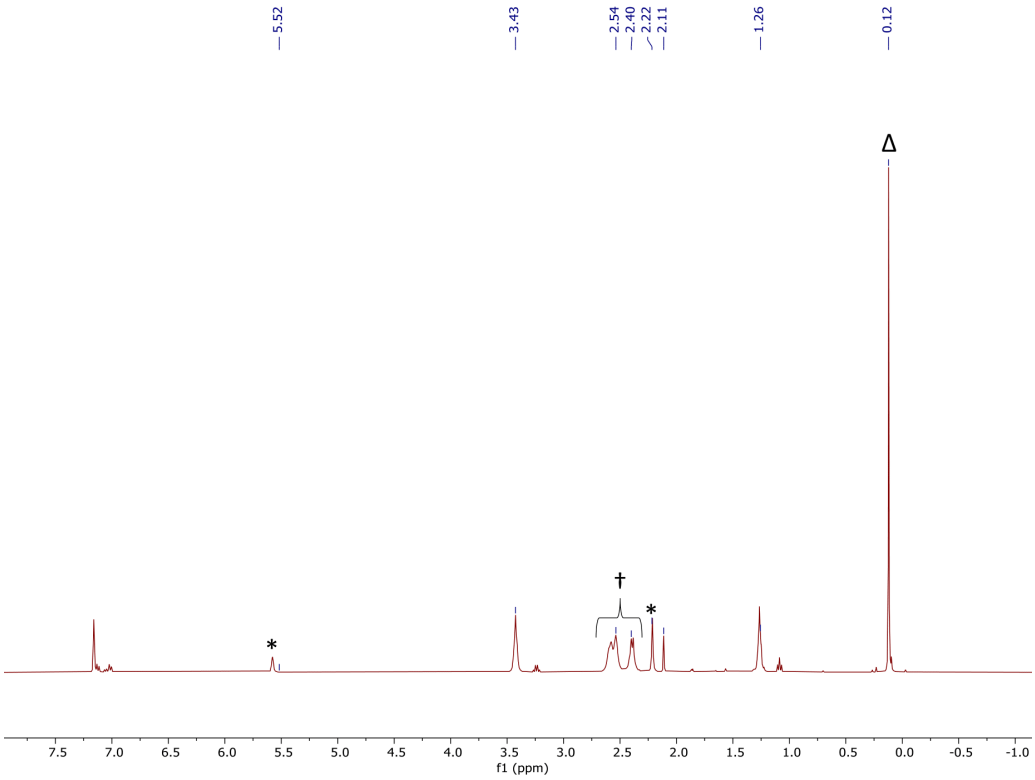

Figure S28. ^{1}H NMR spectrum of the reaction mixture of [Li(THF)$_2$][Co(η^4-COD)$_2$] (**D**) + *t*BuCP (two equiv.) in C_6D_6 at ambient temperature. (*: free COD, Δ: [Li(THF)$_2$][Co(P$_2$C$_2$*t*Bu$_2$)]/(Me$_3$Si$_2$)O, †: **D**)

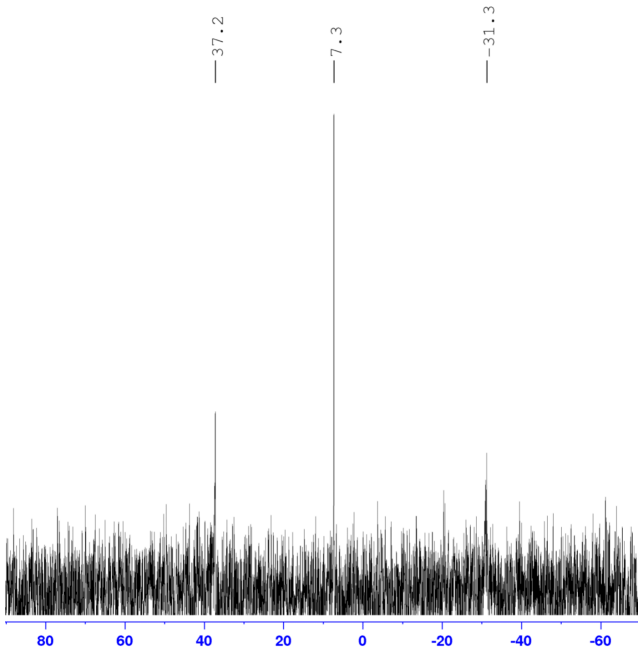

Figure S29. ^{31}P{^{1}H} NMR spectrum of the reaction mixture of [Li(THF)$_2$][Co(η^4-COD)$_2$] (**D**) + *t*BuCP (two equiv.) in C_6D_6 at ambient temperature.

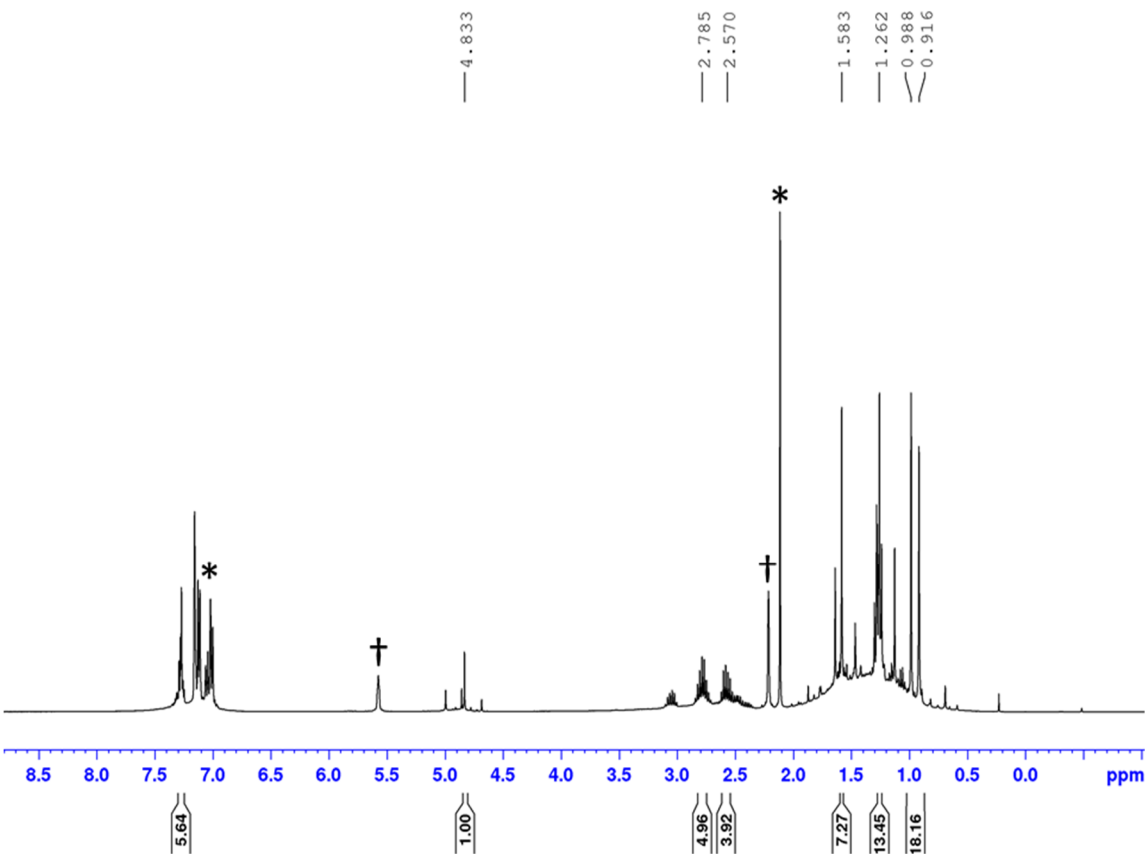

Figure S30. ^{1}H NMR spectrum of the reaction mixture of **4** and P_4 after two days stirring at 80 °C in C_6D_6 at ambient temperature (*: toluene, †: COD).

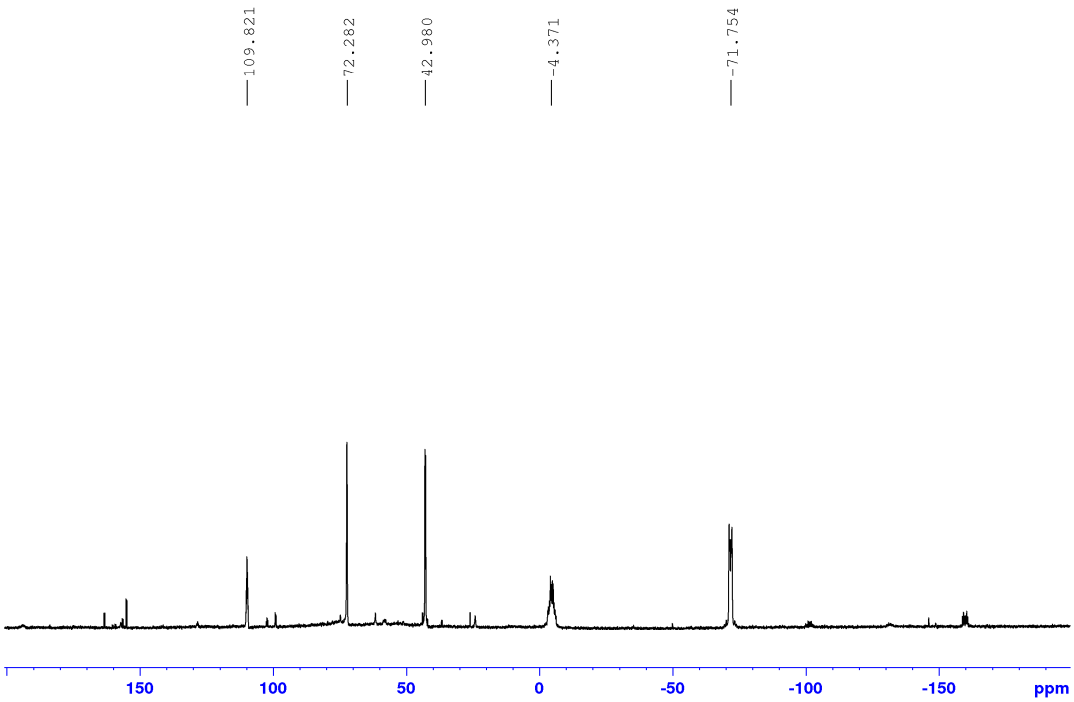

Figure S31. $^{31}P\{^{1}H\}$ NMR spectrum of the reaction mixture of **4** and P_4 after two days stirring at 80 °C in C_6D_6 at ambient

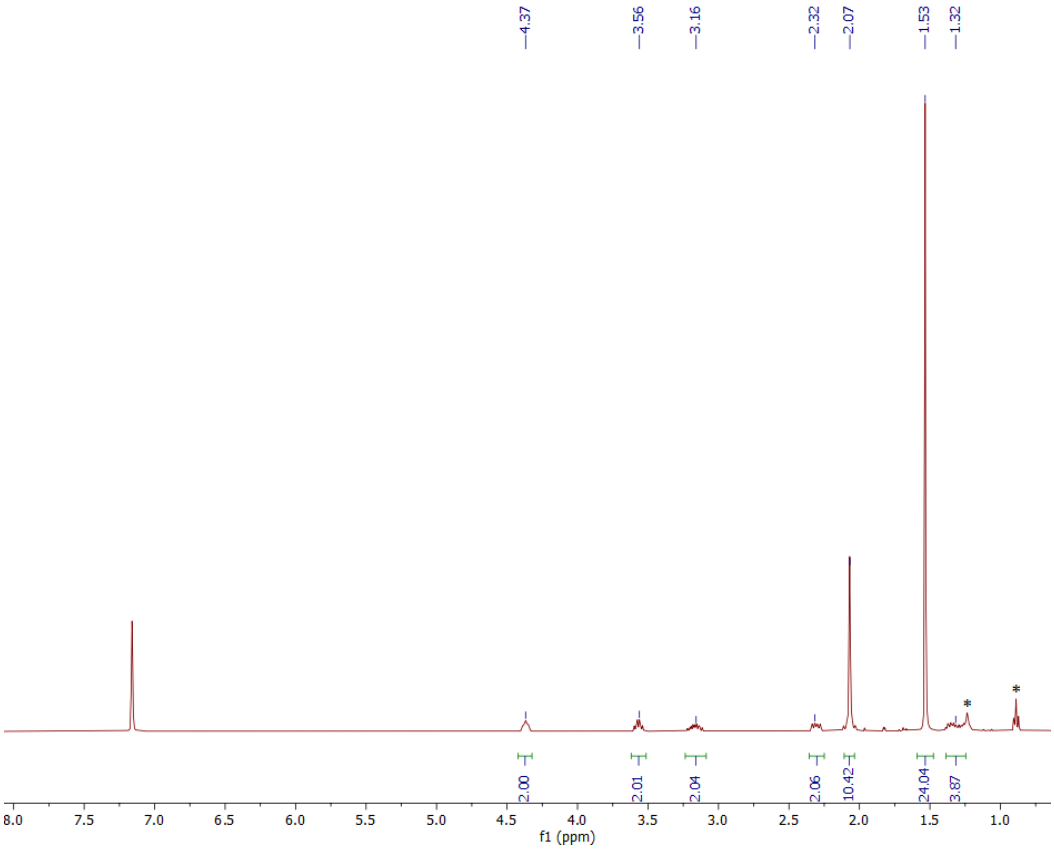

Figure S32. ^{1}H NMR spectrum of (Cp*NiC$_2$P$_2$^{t}Bu$_2$)Co(COD) (**7**) in C$_6$D$_6$ at ambient temperature (*: *n*-hexane).

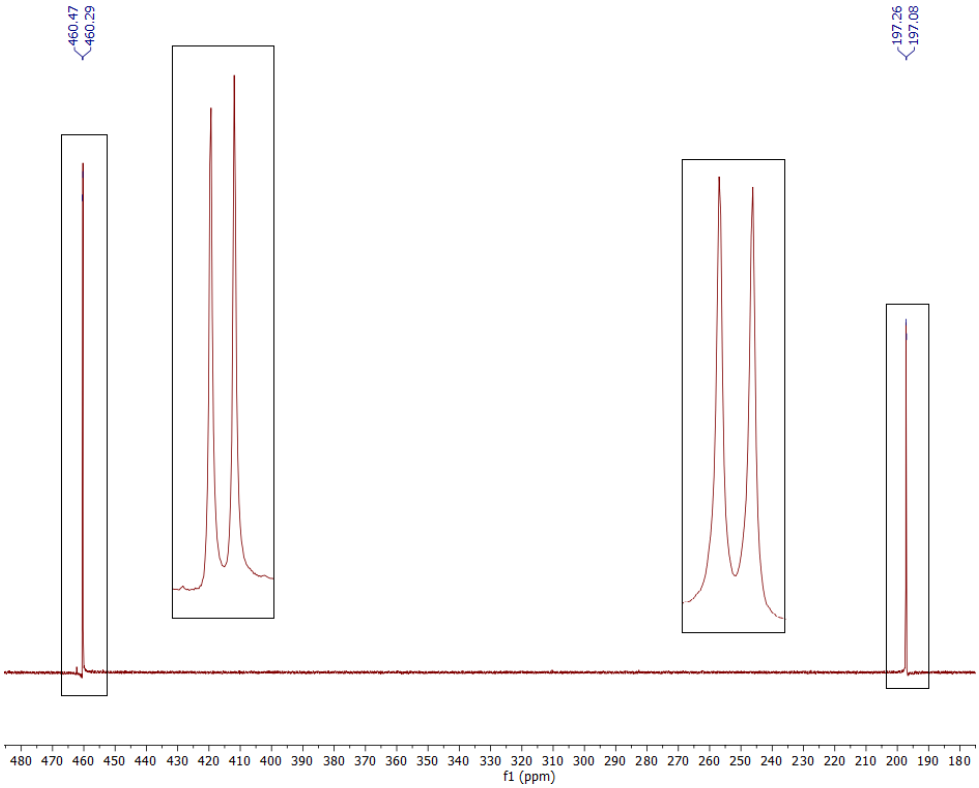

Figure S33. ^{31}P{^{1}H} NMR spectrum of (Cp*NiC$_2$P$_2$*t*Bu$_2$)Co(COD) (**7**) in C$_6$D$_6$ at ambient temperature.

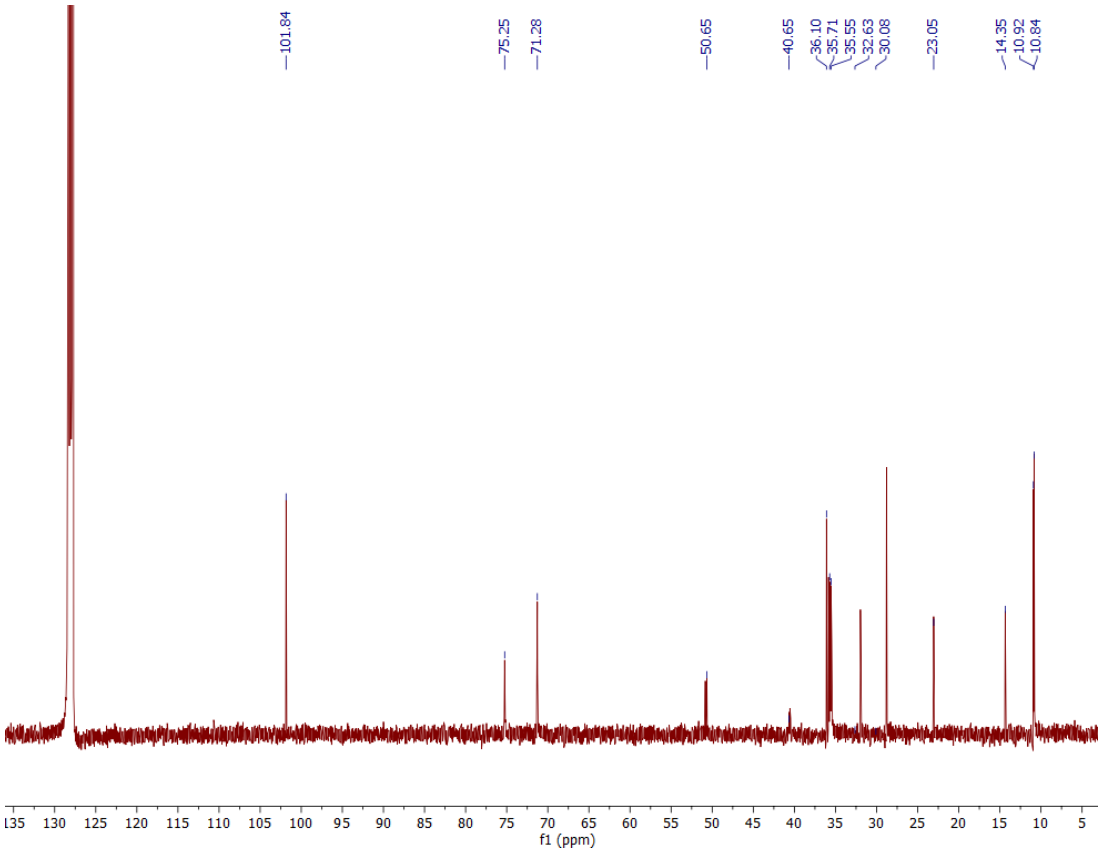

Figure S34. $^{13}C\{^{1}H\}$ NMR spectrum of (Cp*$NiC_2P_2tBu_2$)Co(COD) (**7**) in C_6D_6 at ambient temperature.

DOSY NMR Spectroscopy

General information

Diffusion ordered NMR spectroscopy experiments were performed on Bruker Avance III HD 600 MHz spectrometer, equipped with a 5 mm CPPBBO BB-1H/19F. All measurements were performed at 298 K and temperature was controlled by BVT 3000 and BVTE 3900. NMR Data were processed, evaluated and plotted with TopSpin 3.2 software. Further analysis of the measurements was performed with Microsoft Excel (Version 16.0.10359.20023 64 Bit).

Sample preparation for diffusion-ordered spectroscopy

The samples were prepared by dissolving the sample in the appropriate solvent (C_6D_6 or THF-d_8) in a Young's NMR tube. Tetramethyl silane (TMS) was used as a reference and was added by withdrawing 1 mL from the headspace of the TMS bottle, just above the surface of the liquid and injected into the NMR tube, which was then sealed immediately afterwards.

Diffusion ordered spectroscopy (DOSY)

The DOSY measurements were performed with the convection suppressing DSTE (double stimulated echo) pulse sequence developed by Jerschow and Müller in a pseudo 2D mode.[11] The diffusion time delay was set to 45 ms. Smoothed square (SMSQ10.100) gradient shapes and a linear gradient ramp with 20 increments between 5% and 95% of the maximum gradient strength (5.35 G/mm) were used. For the homospoil gradient strengths, values of 100, –13.17, 20 and –17.13% were used. For each compound in the sample, gradient pulse lengths were first optimized to obtain a sigmoidal signal decay for increasing gradient strength (0.9 ms for TMS, 1.5 ms for the compounds). NMR spectra were processed with Bruker TopSpin 3.2 (T1/T2 relaxation package) and diffusion coefficients were derived according to Jerschow and Müller.[11]

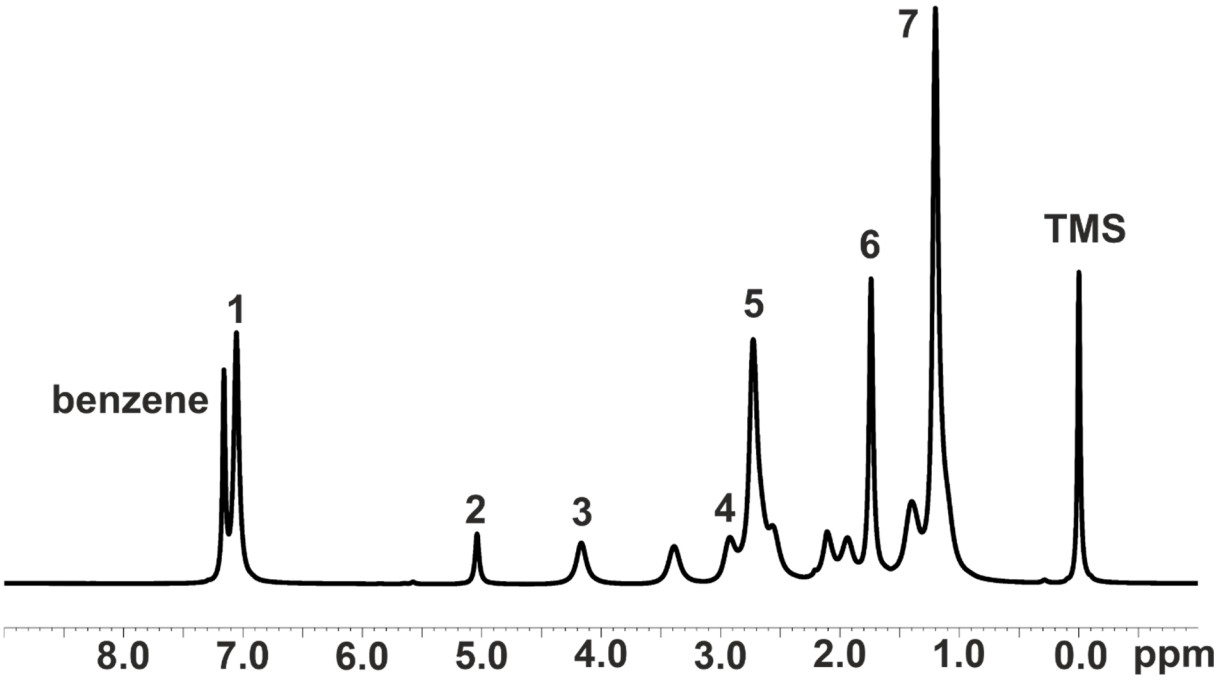

Figure S35. Section of the ^{1}H NMR spectrum of **2** at 298 K and 600 MHz in C_6D_6, showing the signals 1-7 used for the DOSY analysis. The signals at 3.40, 2.11, 1.94 and 1.40 ppm not indicated with a number could not be used in the DOSY measurements due to their line width, low signal intensity and partial overlap as they gave an insufficiently good fitting in the respective double logarithmic plots.

Table S1. Self-diffusion coefficients of signals 1-7 of **2** in benzene. Signals 3 and 4 correspond to the COD ligand, the other signals to the nacnac ligand.

Signal	Chemical Shift [ppm]	Self diffusion coefficient D [10^{-10} /m^2 s^{-1}]
1	7.05	6.58
2	5.04	6.63
3	4.17	6.66
4	2.92	6.57
5	2.73	6.52
6	1.74	6.51
7	1.20	6.47
Averaged value:		6.56

DOSY Plots:

DOSY plots (signal intensity against gradient strength or double logarithmic plot of $\ln(I/I_0)$ against Q[11]) of signals 1-7 of **2** in benzene. The slope in the double logarithmic plot corresponds to the self diffusion constants.

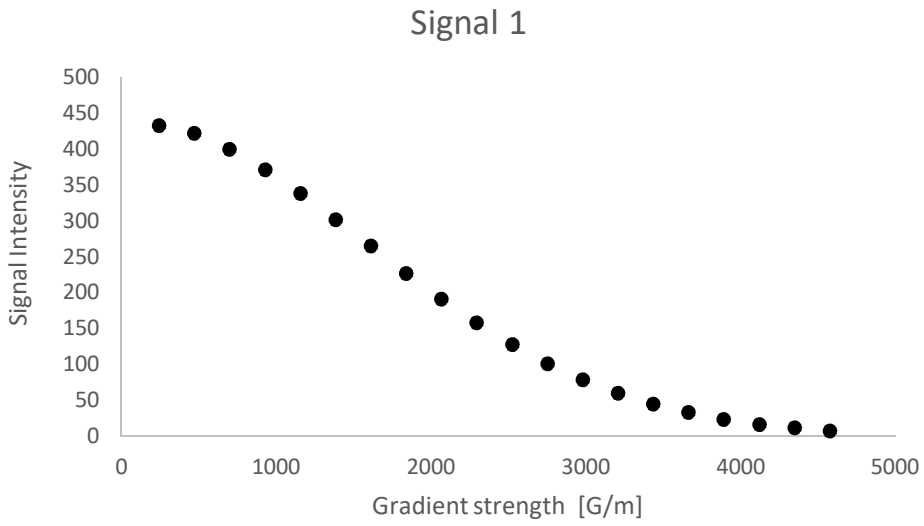

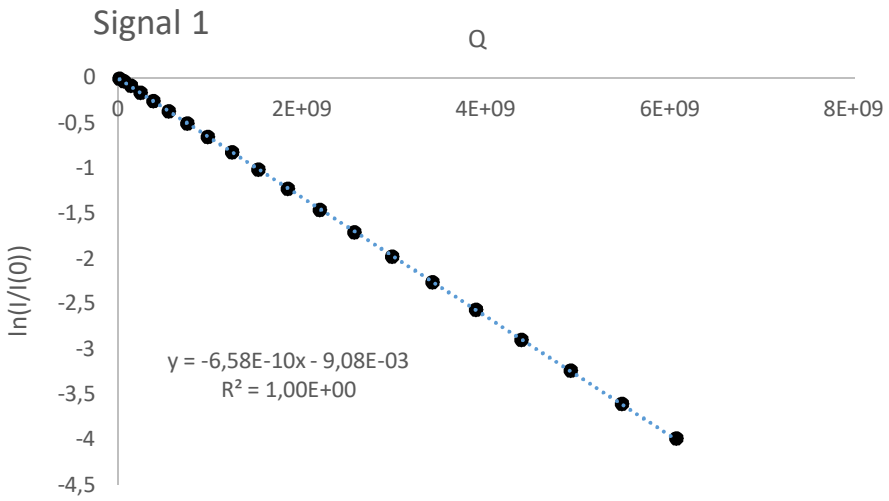
Signal 1
Q
0
-0,5
-1
-1,5
-2
-2,5
-3
-3,5
-4
-4,5
0
2E+09
4E+09
6E+09
8E+09
ln(I/I(0))
y = -6,58E-10x - 9,08E-03
R² = 1,00E+00

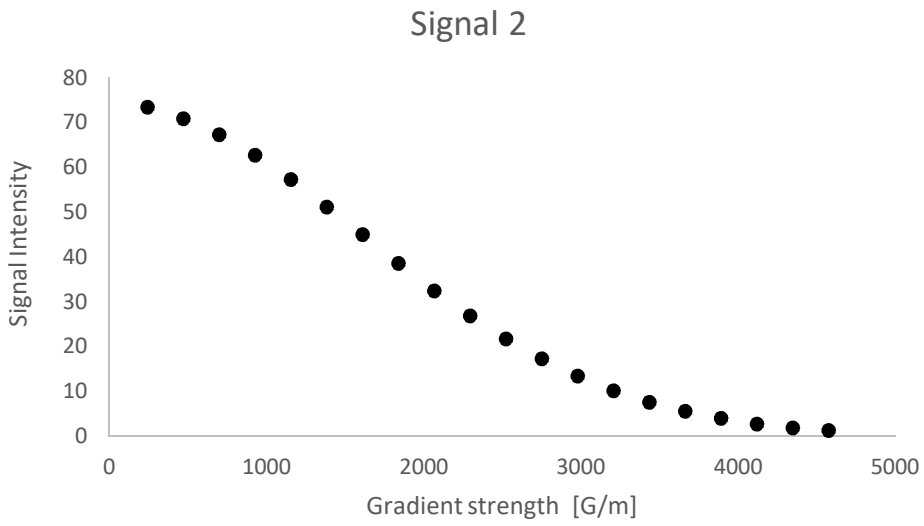
Signal 2
Signal Intensity
80
70
60
50
40
30
20
10
0
0
1000
2000
3000
4000
5000
Gradient strength [G/m]

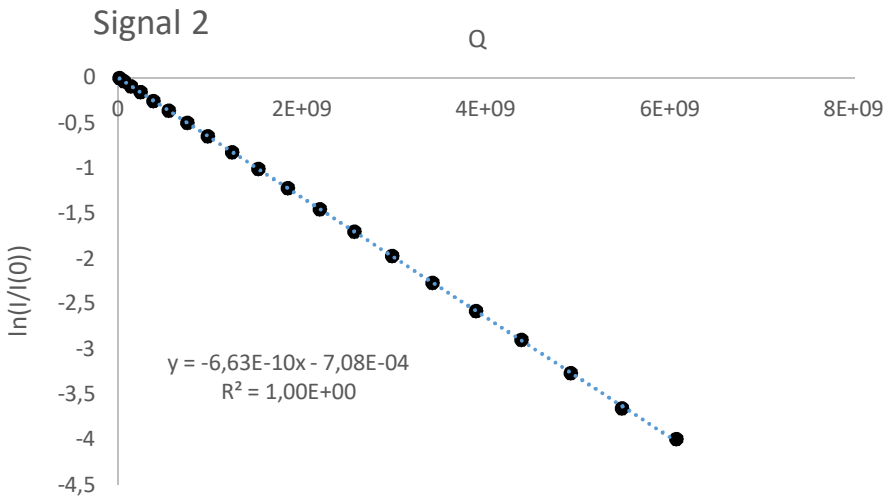
Signal 2
Q
0
-0,5
-1
-1,5
-2
-2,5
-3
-3,5
-4
-4,5
0
2E+09
4E+09
6E+09
8E+09
ln(I/I(0))
y = -6,63E-10x - 7,08E-04
R² = 1,00E+00

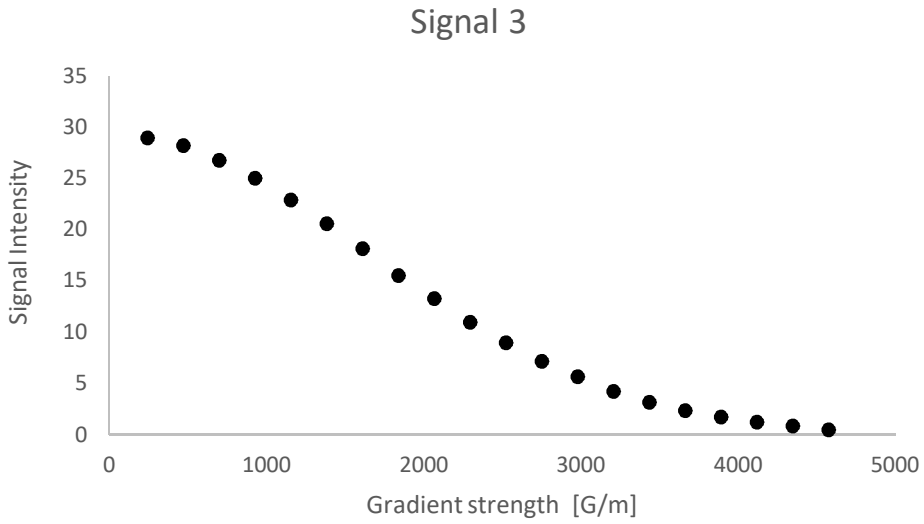
Signal 3
35
30
25
20
15
10
5
0
0
1000
2000
3000
4000
5000
Signal Intensity
Gradient strength [G/m]

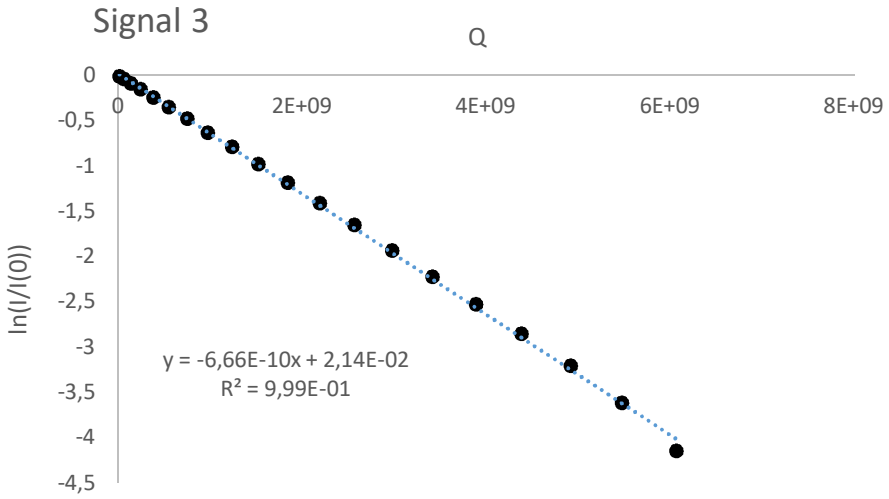
Signal 3
Q
0
-0,5
-1
-1,5
-2
-2,5
-3
-3,5
-4
-4,5
0
2E+09
4E+09
6E+09
8E+09
ln(I/I(0))
y = -6,66E-10x + 2,14E-02
R² = 9,99E-01

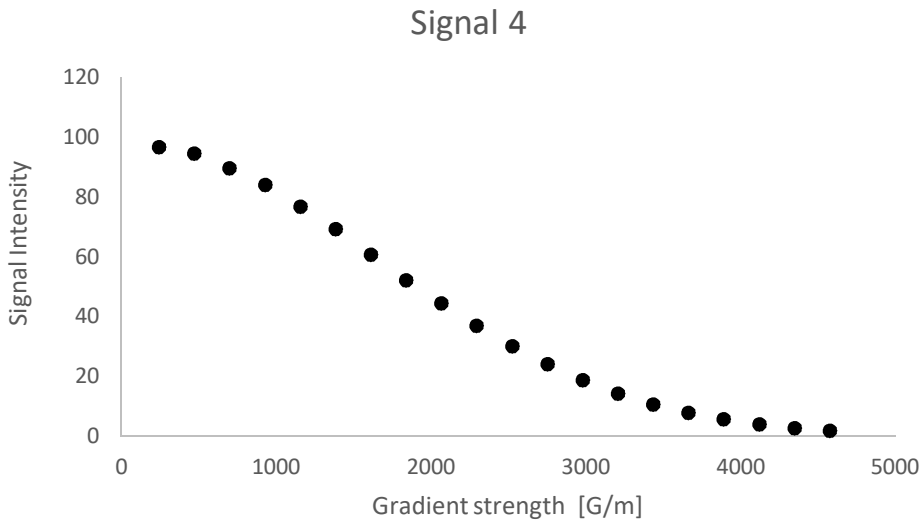
Signal 4
Signal Intensity
120
100
80
60
40
20
0
0
1000
2000
3000
4000
5000
Gradient strength [G/m]

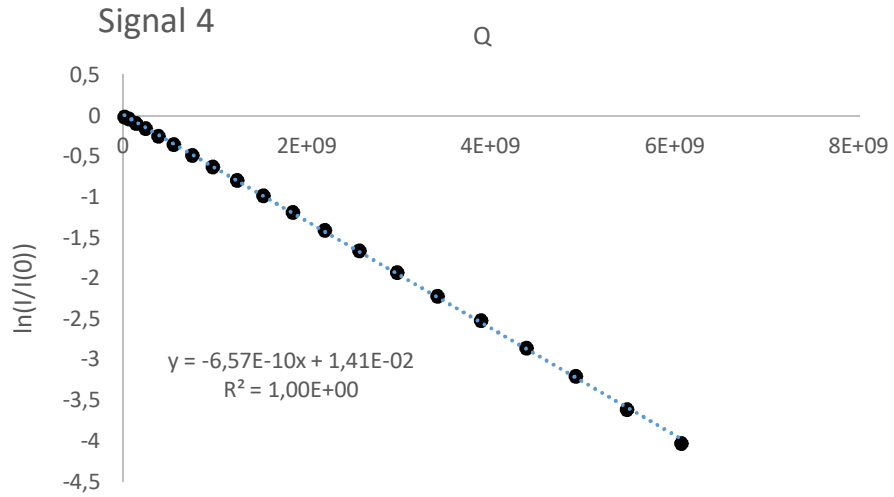
Signal 4
Q
ln(I/I(0))
0,5
0
-0,5
-1
-1,5
-2
-2,5
-3
-3,5
-4
-4,5
0
2E+09
4E+09
6E+09
8E+09
y = -6,57E-10x + 1,41E-02
R² = 1,00E+00

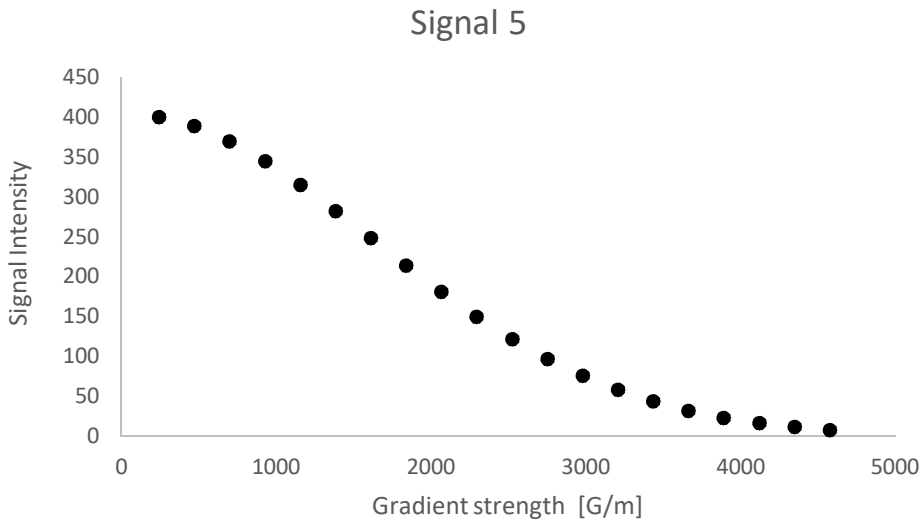
Signal 5
Signal Intensity
450
400
350
300
250
200
150
100
50
0
0
1000
2000
3000
4000
5000
Gradient strength [G/m]

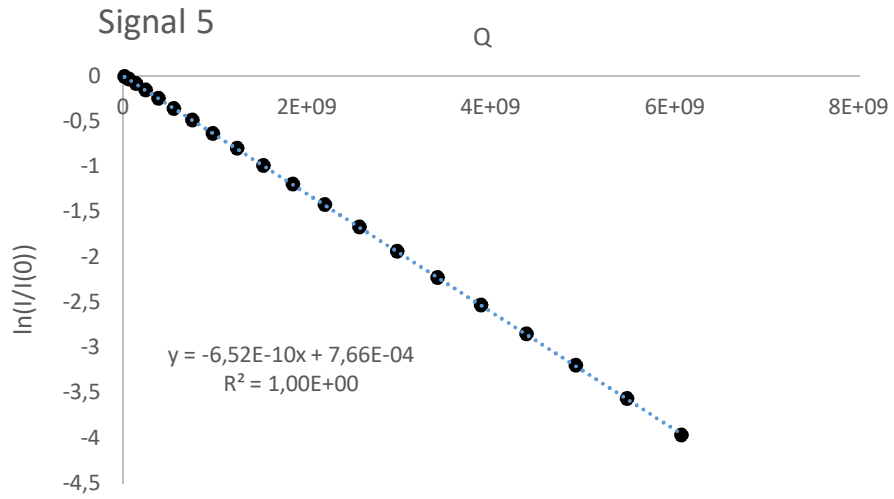
Signal 5
Q
ln(I/I(0))
0
-0,5
-1
-1,5
-2
-2,5
-3
-3,5
-4
-4,5
0
2E+09
4E+09
6E+09
8E+09
y = -6,52E-10x + 7,66E-04
R² = 1,00E+00

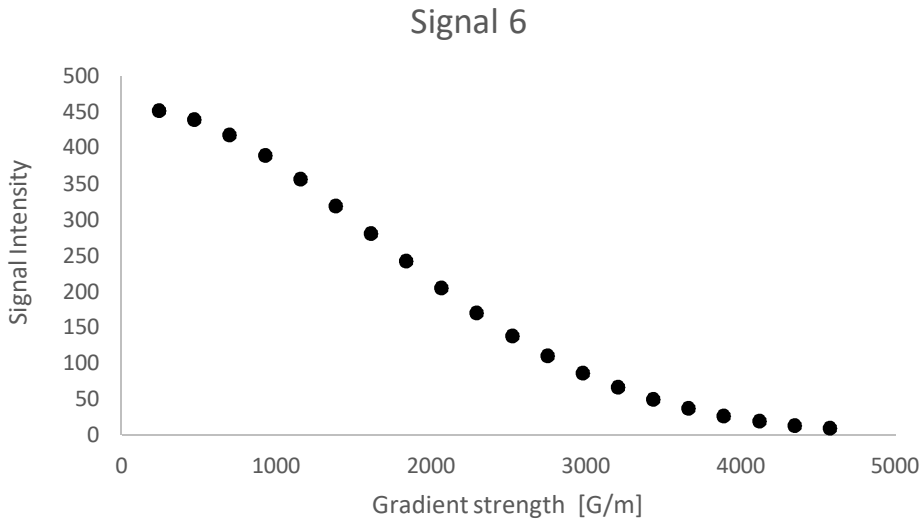
Signal 6
Signal Intensity
500
450
400
350
300
250
200
150
100
50
0
0
1000
2000
3000
4000
5000
Gradient strength [G/m]

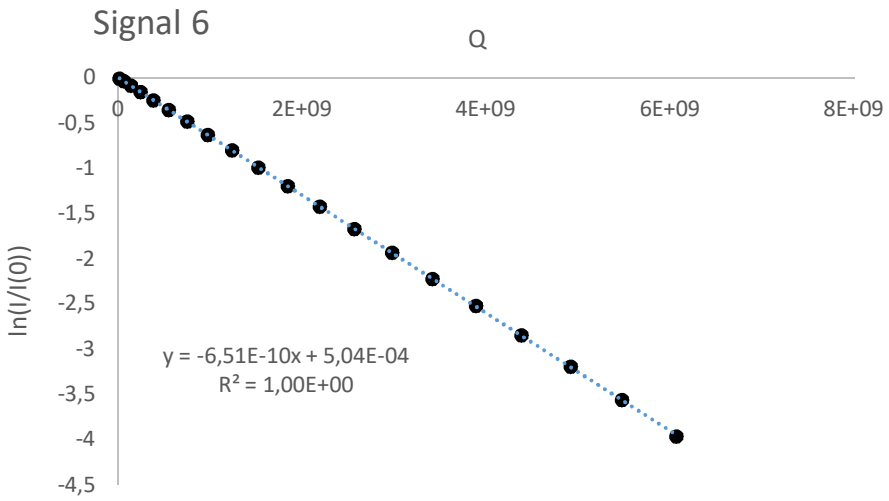
Signal 6
Q
0
-0,5
-1
-1,5
-2
-2,5
-3
-3,5
-4
-4,5
0
2E+09
4E+09
6E+09
8E+09
ln(I/I(0))
y = -6,51E-10x + 5,04E-04
R² = 1,00E+00

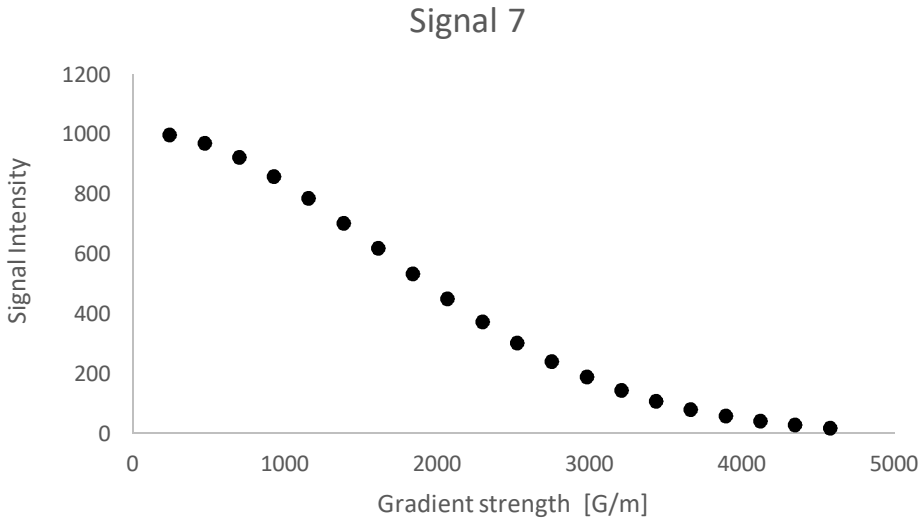
Signal 7
1200
1000
800
600
400
200
0
0
1000
2000
3000
4000
5000
Signal Intensity
Gradient strength [G/m]

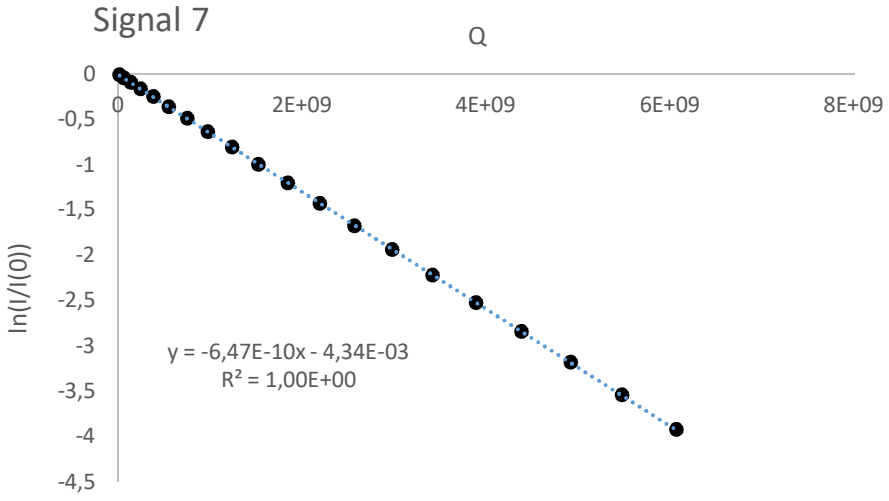
Signal 7
Q
0
-0,5
-1
-1,5
-2
-2,5
-3
-3,5
-4
-4,5
0
2E+09
4E+09
6E+09
8E+09
ln(I/I(0))
y = -6,47E-10x - 4,34E-03
R² = 1,00E+00

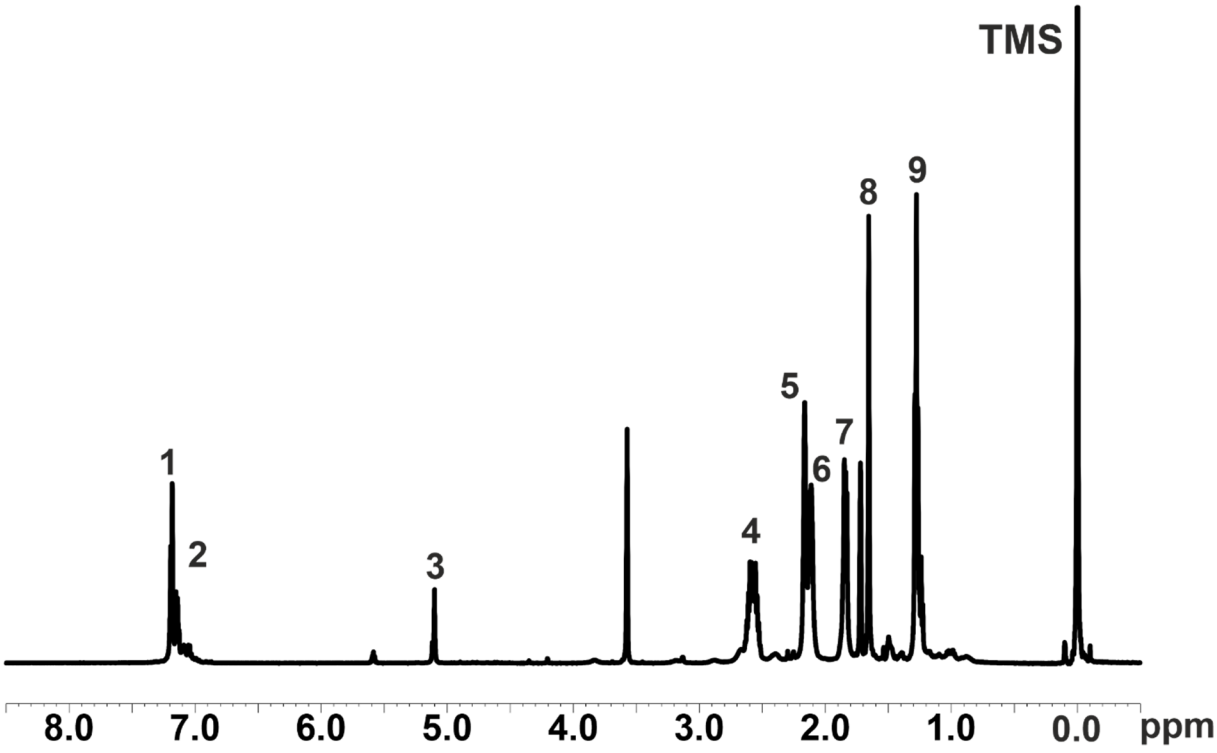

Figure S36. Section of the ^{1}H NMR spectrum of **2.THF** at 298 K and 600 MHz in THF-d_8, showing the signals 1-9 used for the DOSY analysis.

Table S2. Self-diffusion coefficients D of signals 1-9 of [**2.THF**] in THF.

Signal	Chemical Shift [ppm]	Self diffusion coefficient D [10^{-10} /m_2 s^{-1}]
1	7.19	6.63
2	7.14	6.63
3	5.10	6.67
4	2.58	6.68
5	2.17	7.50
6	2.11	7.62
7	1.84	7.58
8	1.66	6.63
9	1.28	6.66

Note: In contrast to the measurement in benzene, where similar self-diffusion coefficients were observed for all signals, in THF a significant offset is observed between the signals of the COD ligand (signals 5, 6 and 7; D ≈ 7.56*10^{-10} m^2/s) and the remaining signals for the nacnac ligand (signal 1-4, 8 and 9; D ≈ 6.65*10^{-10} m^2/s). This demonstrates that in THF the COD and nacnac ligands are part of separate species in solution.

DOSY Plots:

DOSY plots (signal intensity against gradient strength or double logarithmic plot of $\ln(I/I_0)$ against Q[11]) of signals 1-9 of **2·THF** in THF. The slope in the double logarithmic plot corresponds to the self diffusion constants.

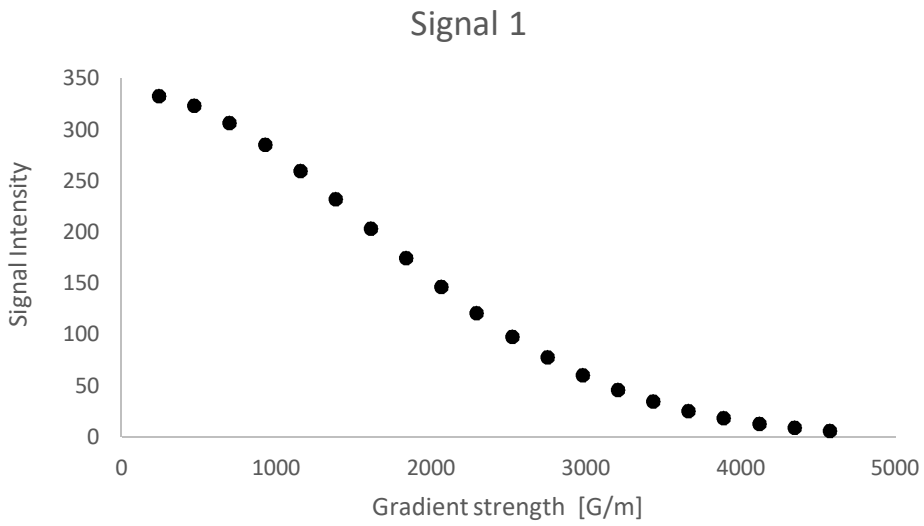

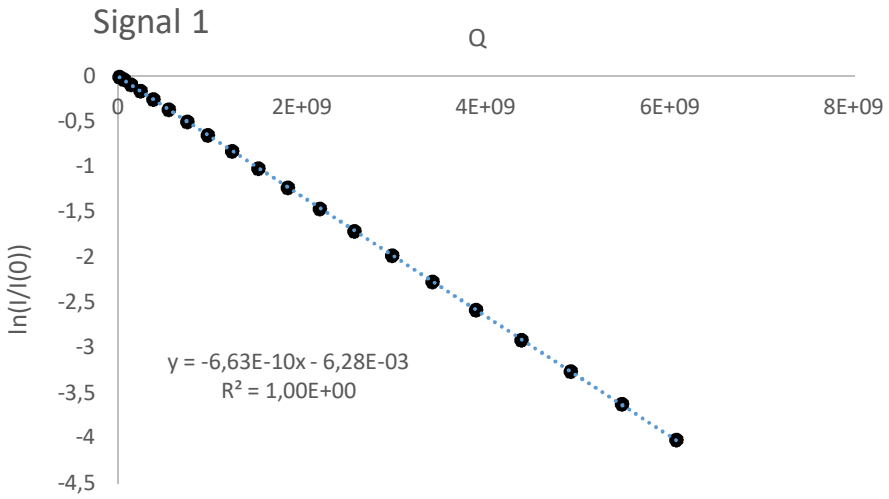

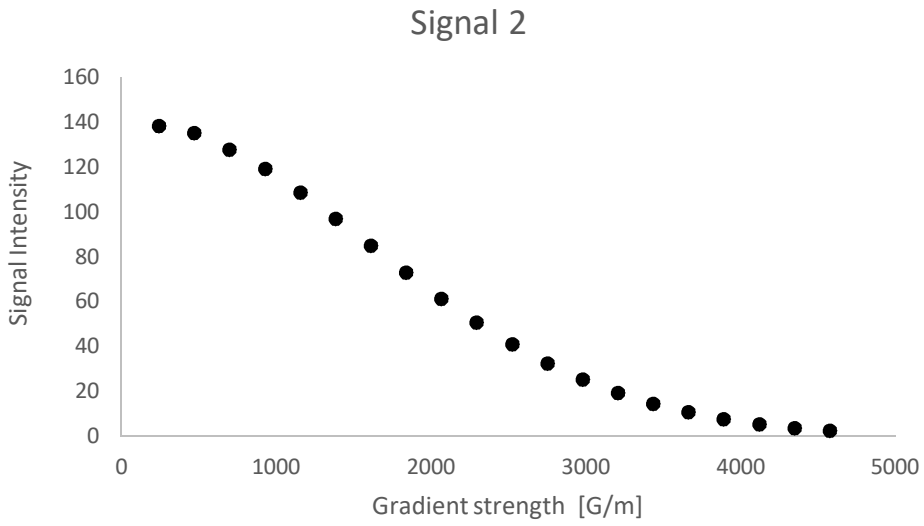
Signal 2
Signal Intensity
160
140
120
100
80
60
40
20
0
0
1000
2000
3000
4000
5000
Gradient strength [G/m]

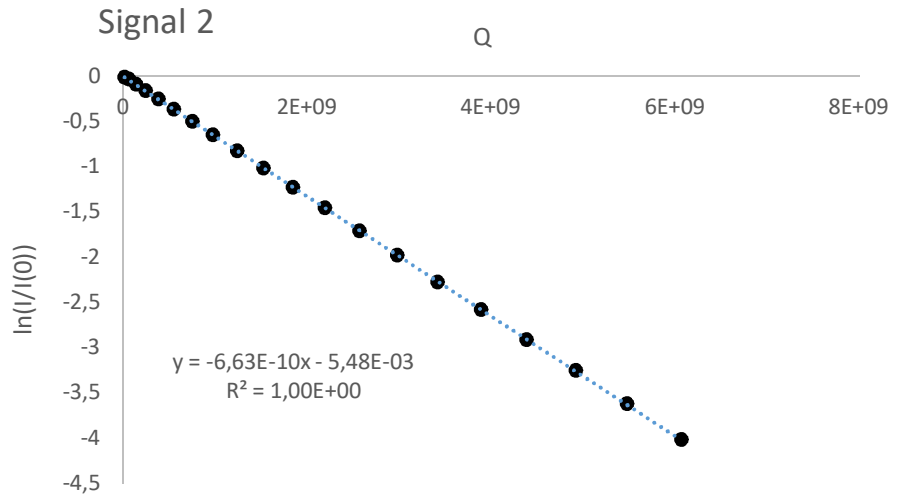
Signal 2
Q
ln(I/I(0))
0
-0,5
-1
-1,5
-2
-2,5
-3
-3,5
-4
-4,5
0
2E+09
4E+09
6E+09
8E+09
y = -6,63E-10x - 5,48E-03
R² = 1,00E+00

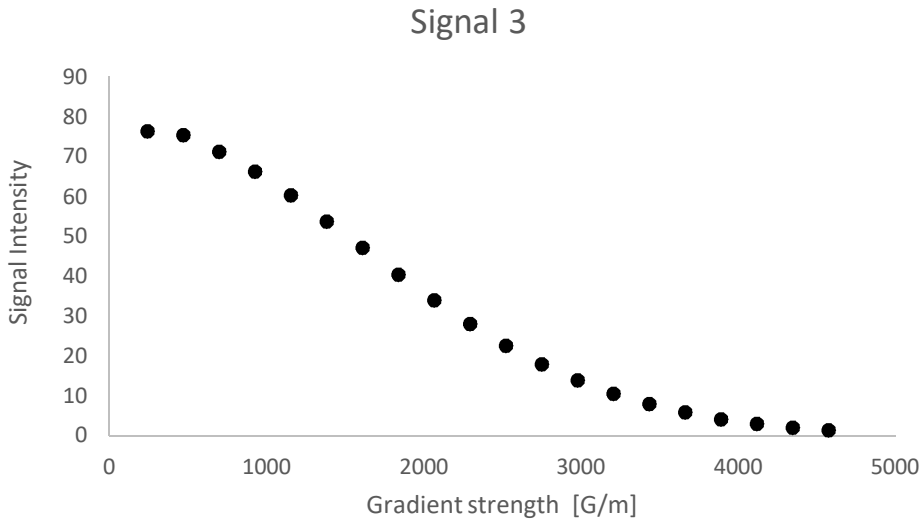
Signal 3
Signal Intensity
90
80
70
60
50
40
30
20
10
0
0
1000
2000
3000
4000
5000
Gradient strength [G/m]

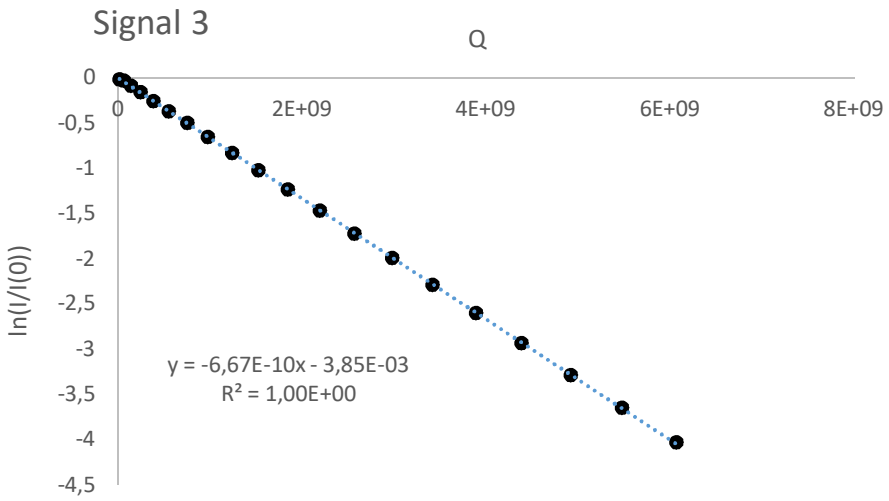
Signal 3
Q
0
-0,5
-1
-1,5
-2
-2,5
-3
-3,5
-4
-4,5
0
2E+09
4E+09
6E+09
8E+09
ln(I/I(0))
y = -6,67E-10x - 3,85E-03
R² = 1,00E+00

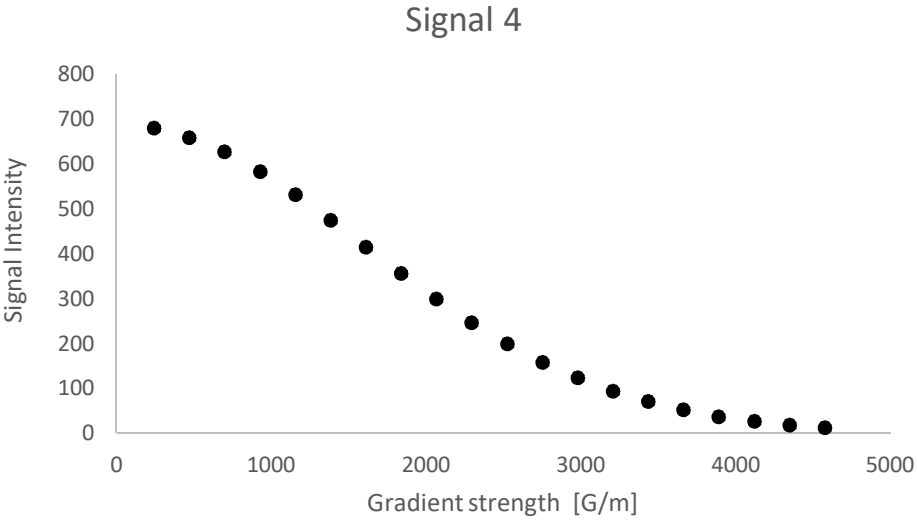
Signal 4
800
700
600
500
400
300
200
100
0
0
1000
2000
3000
4000
5000
Signal Intensity
Gradient strength [G/m]

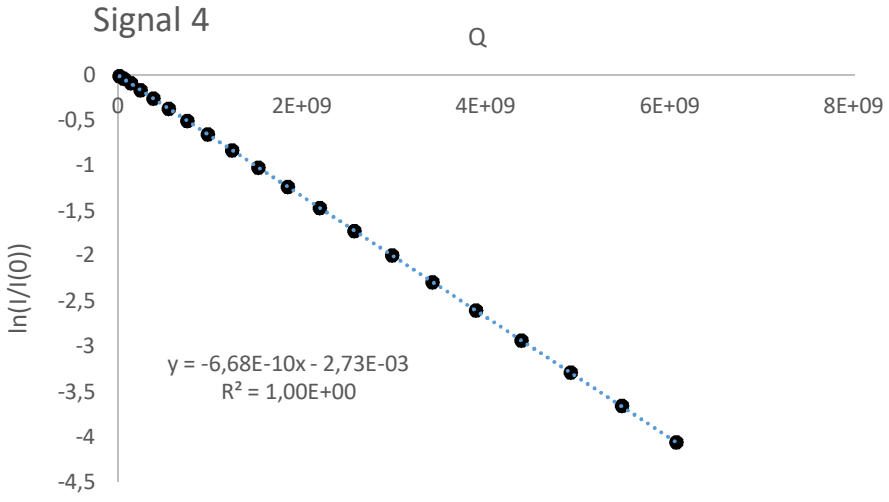
Signal 4
Q
0
-0,5
-1
-1,5
-2
-2,5
-3
-3,5
-4
-4,5
0
2E+09
4E+09
6E+09
8E+09
ln(I/I(0))
y = -6,68E-10x - 2,73E-03
R² = 1,00E+00

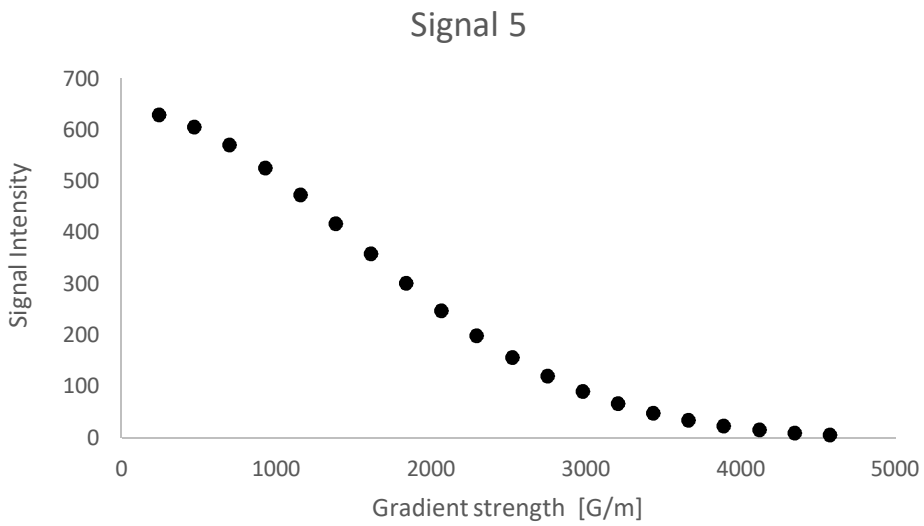
Signal 5
Signal Intensity
700
600
500
400
300
200
100
0
0
1000
2000
3000
4000
5000
Gradient strength [G/m]

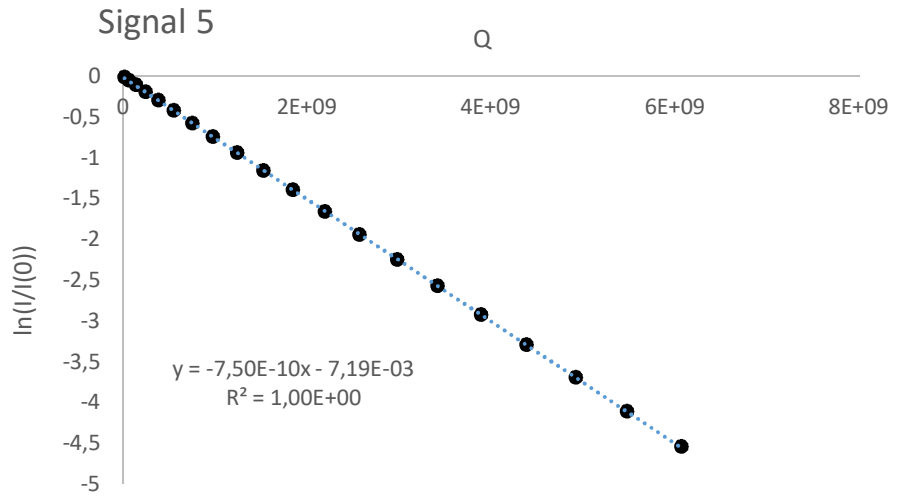
Signal 5
Q
ln(I/I(0))
0
-0,5
-1
-1,5
-2
-2,5
-3
-3,5
-4
-4,5
-5
0
2E+09
4E+09
6E+09
8E+09
y = -7,50E-10x - 7,19E-03
R² = 1,00E+00

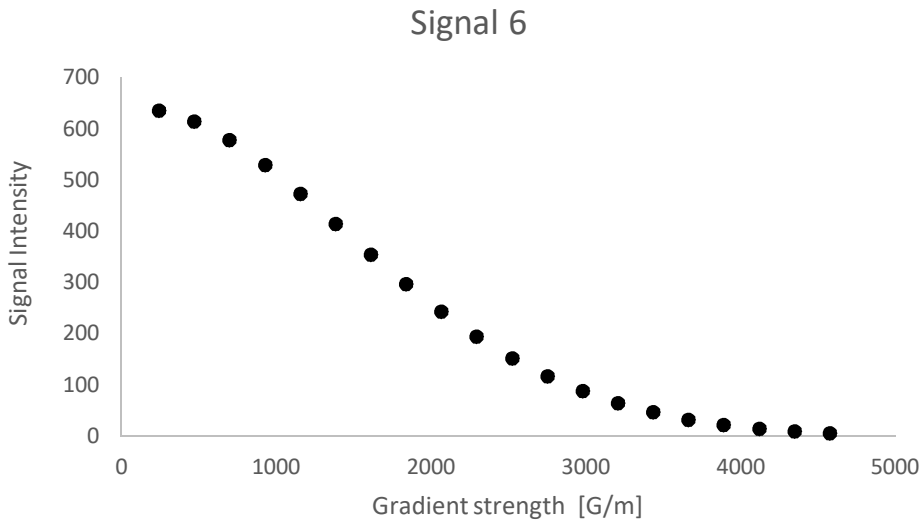
Signal 6
Signal Intensity
700
600
500
400
300
200
100
0
0
1000
2000
3000
4000
5000
Gradient strength [G/m]

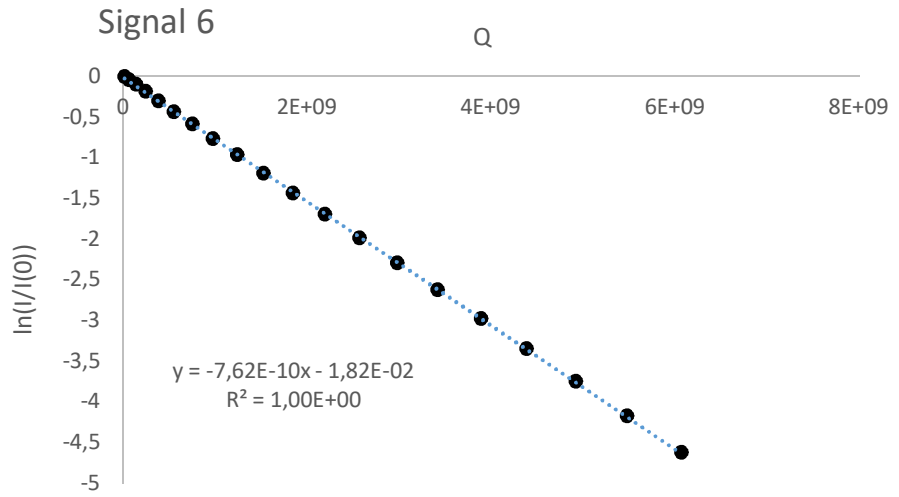
Signal 6
Q
ln(I/I(0))
0
-0,5
-1
-1,5
-2
-2,5
-3
-3,5
-4
-4,5
-5
0
2E+09
4E+09
6E+09
8E+09
y = -7,62E-10x - 1,82E-02
R² = 1,00E+00

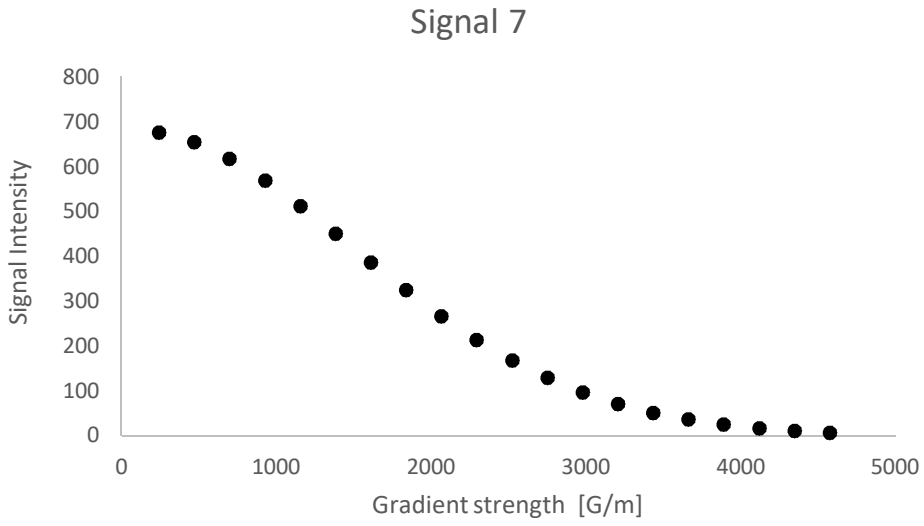
Signal 7
Signal Intensity
800
700
600
500
400
300
200
100
0
0
1000
2000
3000
4000
5000
Gradient strength [G/m]

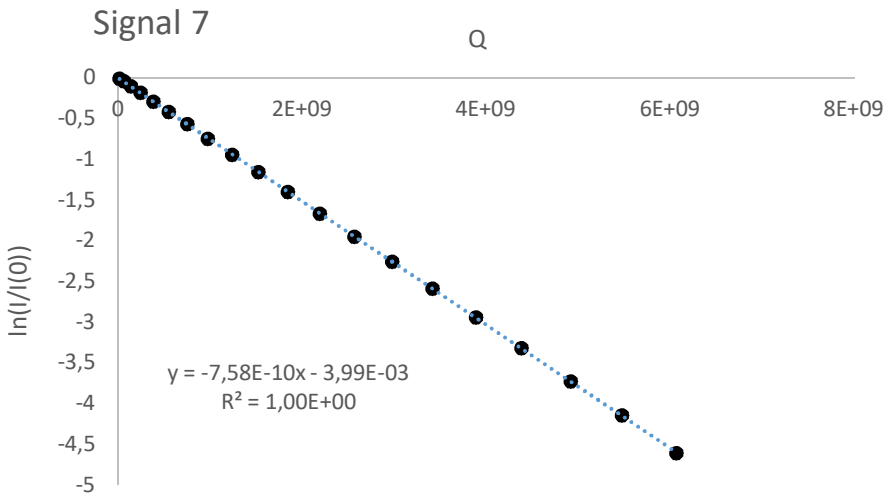
Signal 7
Q
0
-0,5
-1
-1,5
-2
-2,5
-3
-3,5
-4
-4,5
-5
0
2E+09
4E+09
6E+09
8E+09
ln(I/I(0))
y = -7,58E-10x - 3,99E-03
R² = 1,00E+00

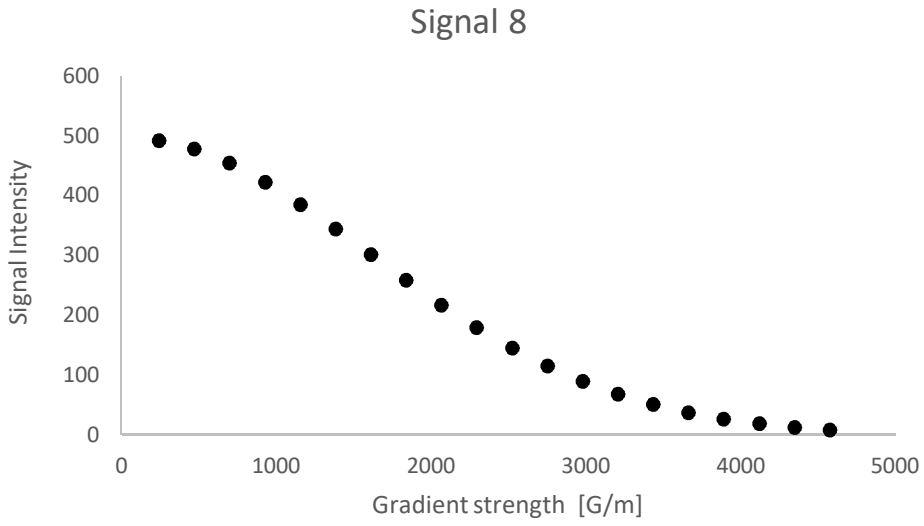
Signal 8
600
500
400
300
200
100
0
0
1000
2000
3000
4000
5000
Signal Intensity
Gradient strength [G/m]

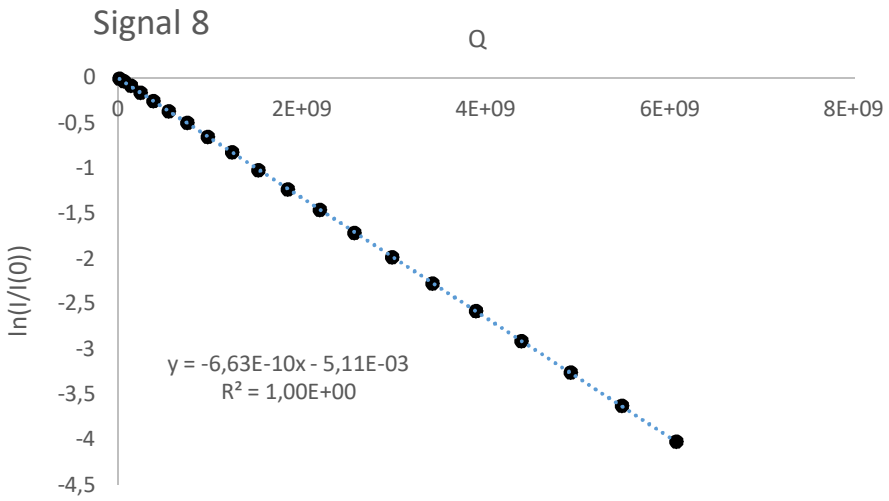
Signal 8
Q
0
-0,5
-1
-1,5
-2
-2,5
-3
-3,5
-4
-4,5
0
2E+09
4E+09
6E+09
8E+09
ln(I/I(0))
y = -6,63E-10x - 5,11E-03
R² = 1,00E+00

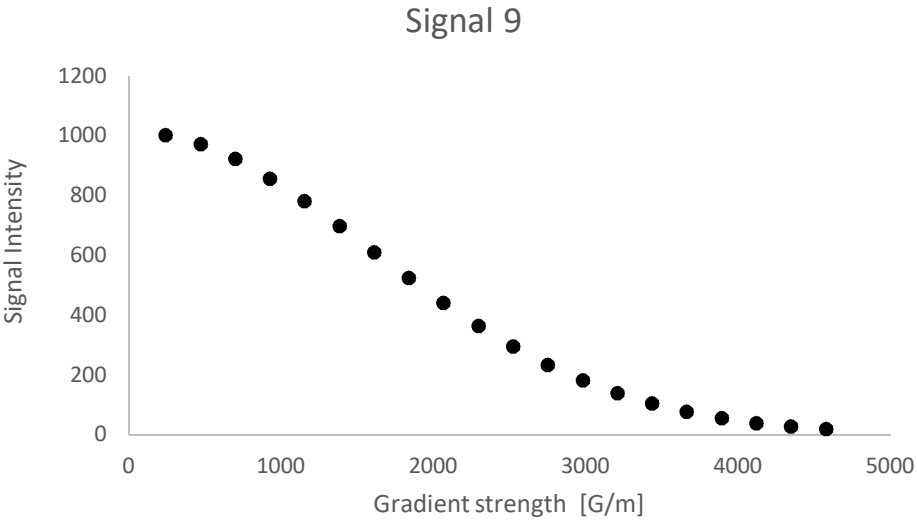
Signal 9
1200
1000
800
600
400
200
0
Signal Intensity
0
1000
2000
3000
4000
5000
Gradient strength [G/m]

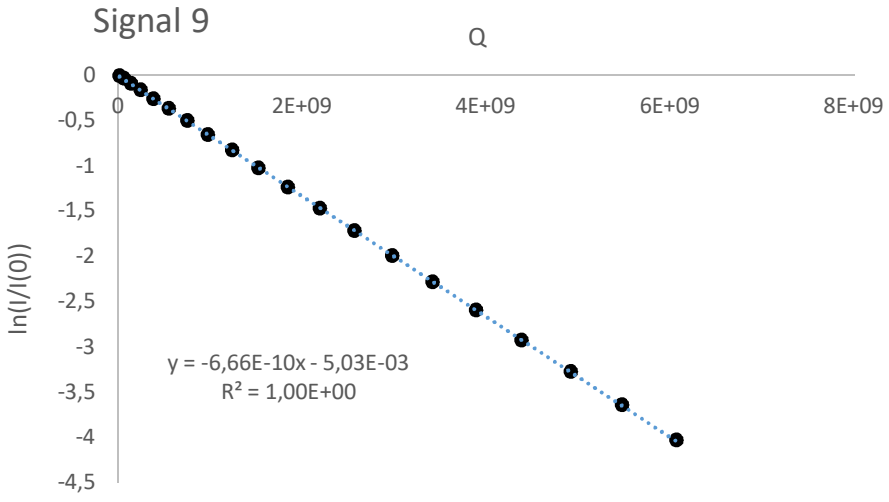
Signal 9
Q
0
-0,5
-1
-1,5
-2
-2,5
-3
-3,5
-4
-4,5
0
2E+09
4E+09
6E+09
8E+09
ln(I/I(0))
y = -6,66E-10x - 5,03E-03
R² = 1,00E+00

5. UV-Vis Spectra

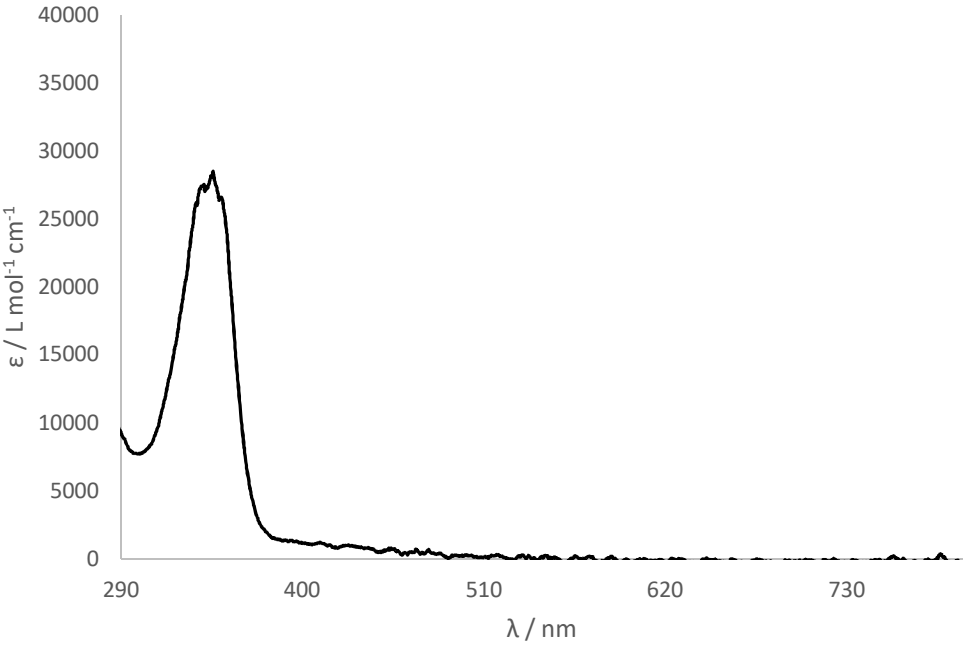

Figure S37. UV/Vis of (^{Mes}nacnac)MgCo(COD)$_2$ (**1**) in toluene.

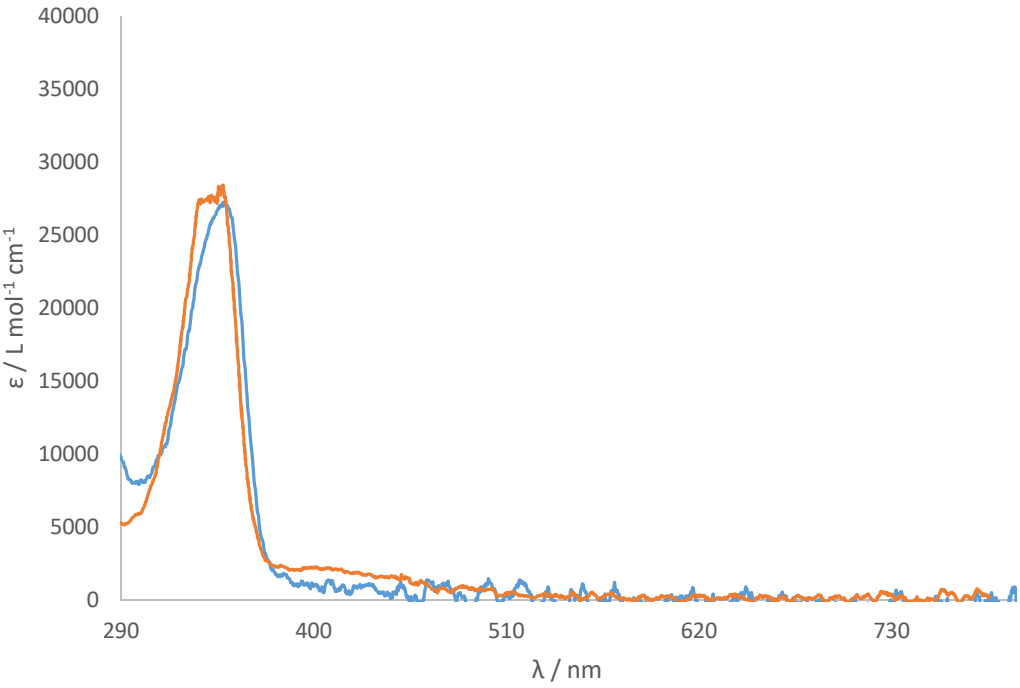

Figure S38. UV/Vis of (^{Dep}nacnac)MgCo(COD)$_2$ (**2**) in toluene (blue) and THF (orange).

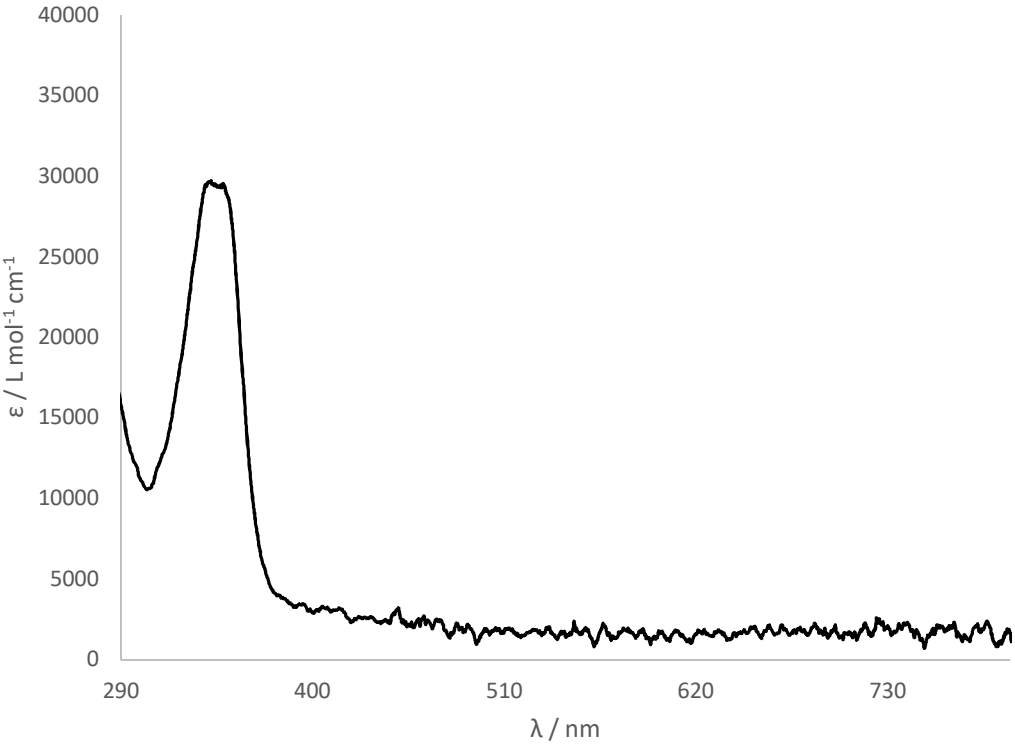

Figure S39. UV/Vis of [(^{Dep}nacnac)Mg(DMAP)$_3$][Co(COD)$_2$] (**2·DMAP**) in toluene.

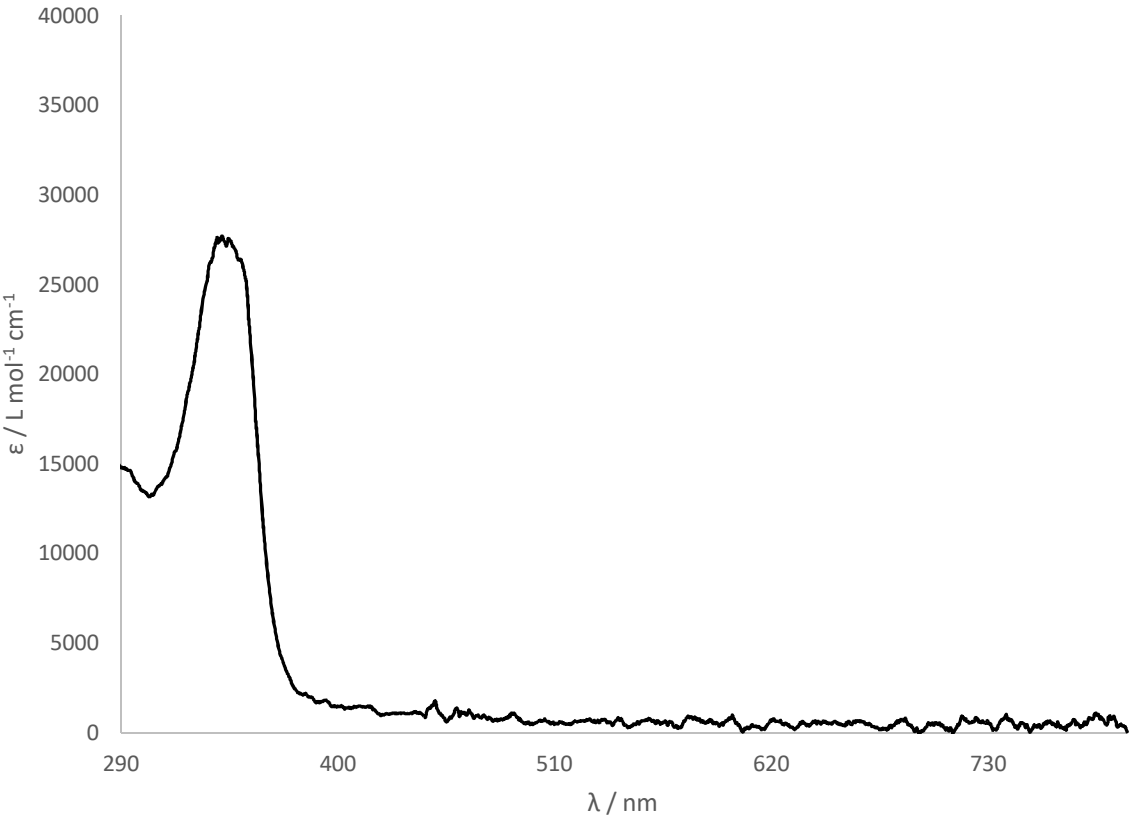

Figure S40. UV/Vis of (^{Dep}nacnac)MgCo(P_2C_2tBu$_2$)(COD) (**4**) in toluene.

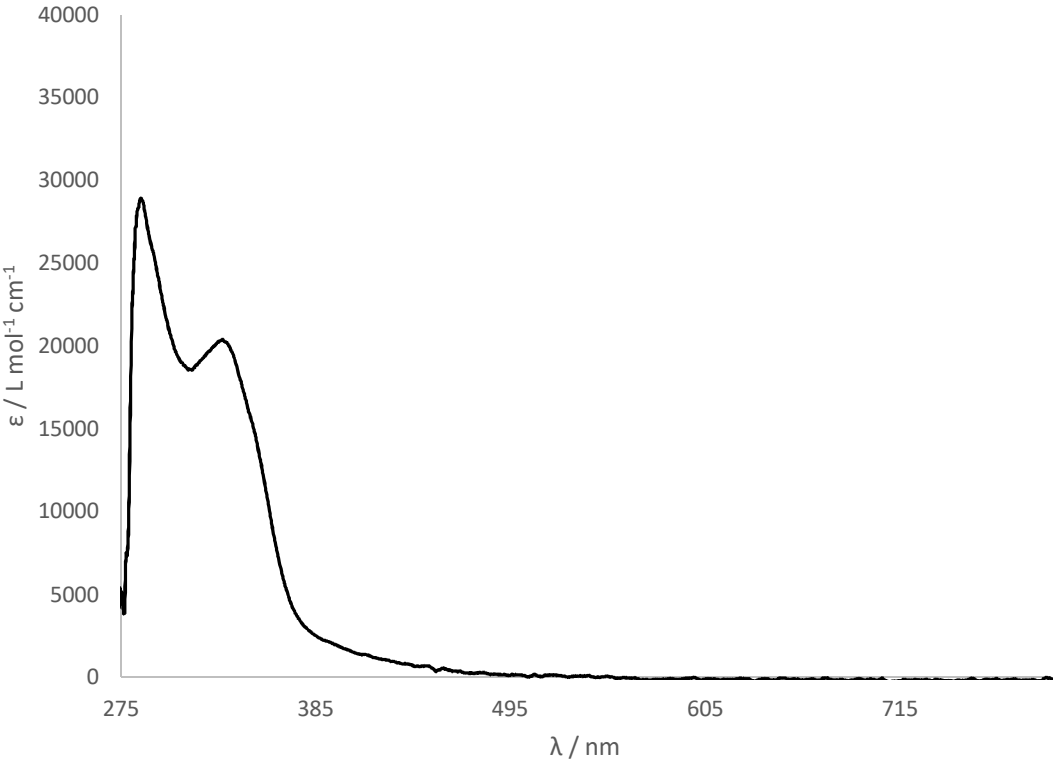

Figure S41. UV/Vis of (^{Dep}nacnac)Mg(THF)Co($P_2C_2tBu_2$)$_2$ (**5**) in toluene.

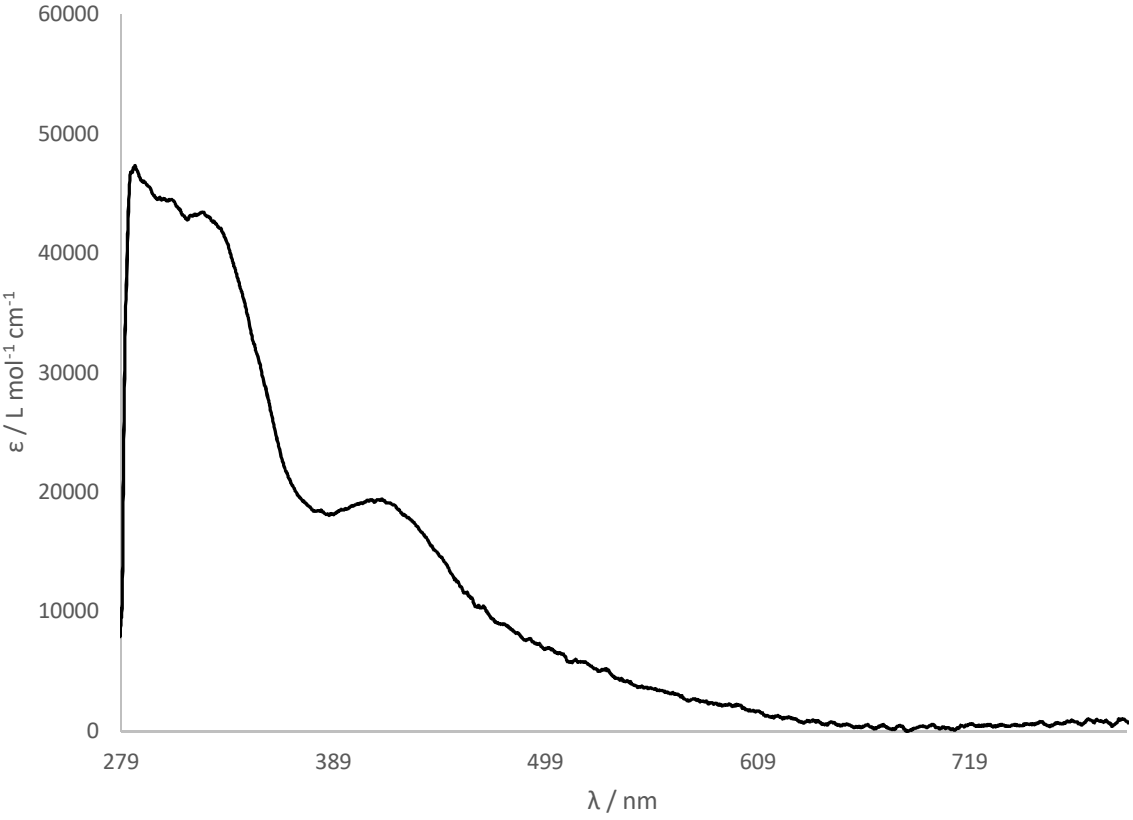

Figure S42. UV/Vis of (Cp*Ni$P_2C_2tBu_2$)Co(COD) (**7**) in toluene.

6. Quantum Chemical Calculations

General Methods

Geometry optimisation and intrinsic bond orbital (IBO) calculations were carried out with ORCA 4.1 and were performed at the TPSS-D3BJ/def2-TZVP level of theory in the gas phase.[12] Density fitting techniques, also called resolution-of-identity approximation (RI),[13] were used for density functional theory (DFT) calculations. Natural bond order (NBO) analysis was performed using Gaussian09 program package (Revision E.01) also at the TPSS-D3BJ/def2-TZVP level of theory.[14] Atoms in molecules (AIM) analysis was performed using the Multiwfn software.[15] ChemCraft was used to visualise IBOs.

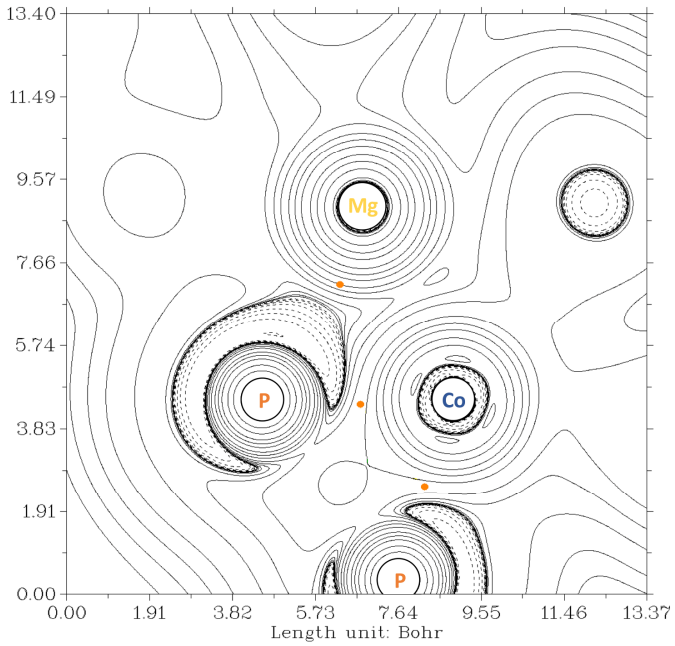

Figure S43. A Laplacian contour plot of the DFT-calculated electron density of **4**; bond critical points are shown in orange.

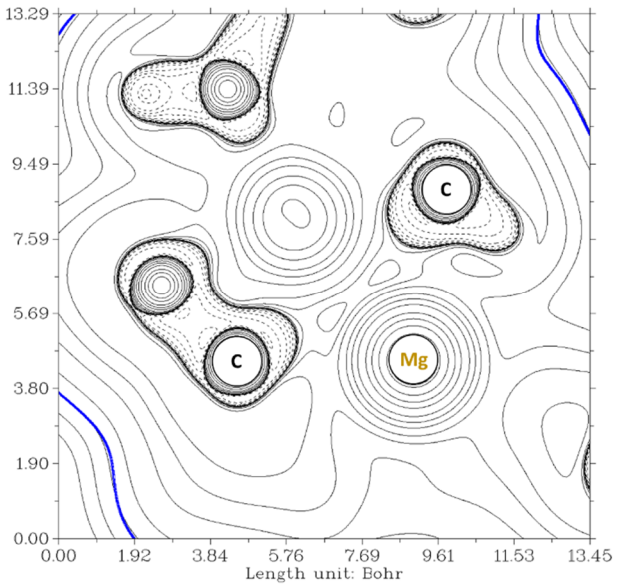

Figure S44. A Laplacian contour plot of the DFT-calculated electron density of **2**; showing the Mg centre and vinyl carbons in close proximity.

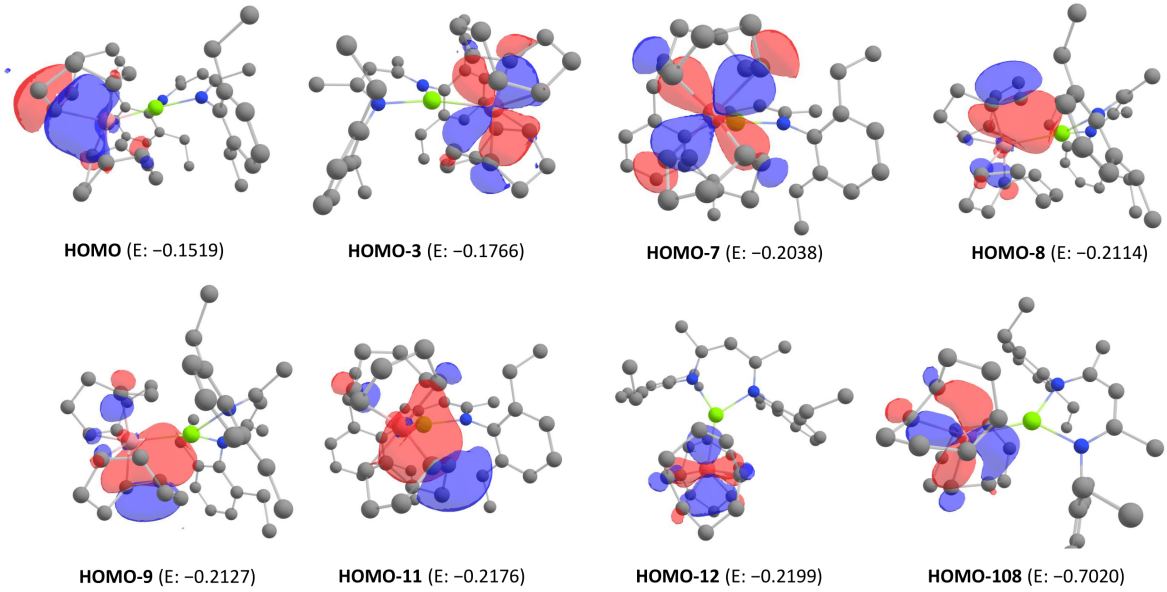

Figure S45. All cobalt centred IBOs (TPSS-D3BJ/def2-TZVP) for (^{Dep}nacnac)MgCo(COD)$_2$ (**2**). Contour value = 0.03, energy (E) in Hartree-Fock (HF).

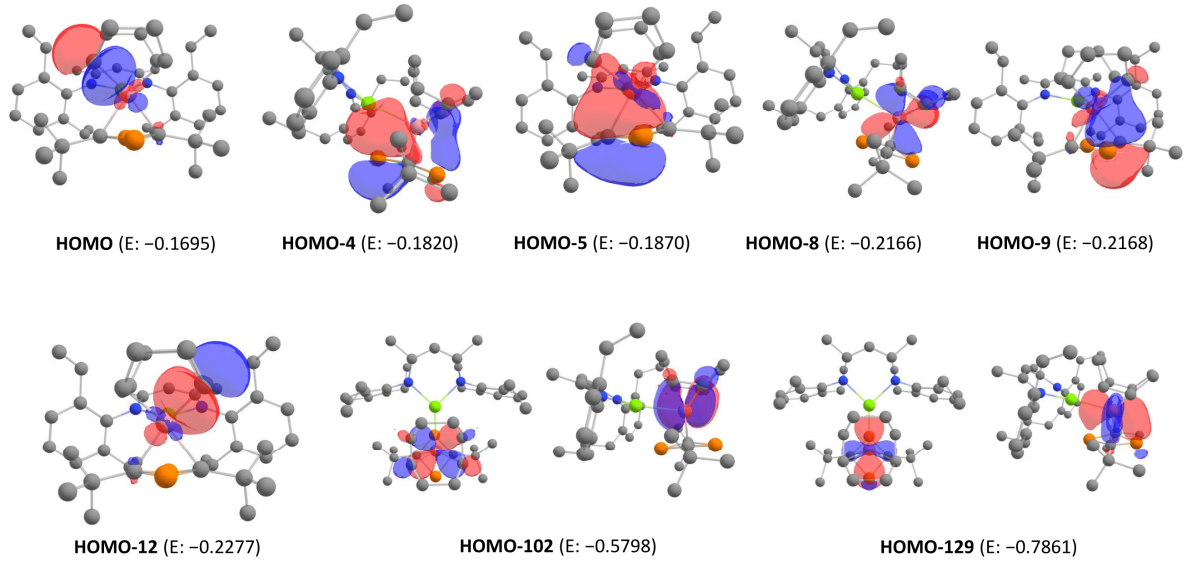

Figure S46. All cobalt centred IBOs (TPSS-D3BJ/def2-TZVP) for (^{Dep}nacnac)MgCo(P_2C_2tBu$_2$)(COD) (**4**). Contour value = 0.03, energy (E) in Hartree-Fock (HF).

Calculated atomic charges of **2**:

```
-----------------------
MULLIKEN ATOMIC CHARGES
-----------------------
   0 Co:   -0.722216
   1 Mg:    0.328801
   2 N :   -0.533399
   3 N :   -0.461291

-----------------------
LOEWDIN ATOMIC CHARGES
-----------------------
   0 Co:   -0.358699
   1 Mg:    0.064246
   2 N :    0.157918
   3 N :    0.158358

-------------------
IAO PARTIAL CHARGES
-------------------
Warning!!! IAOs HAVE MEANING, only when all occupied MOs are involved.
   0 Co:    0.820230
   1 Mg:    1.482659
   2 N :   -0.505487
   3 N :   -0.521540
```

Excerpt from IBO analysis of **2**:

```
--------------------------------------------------------------------------------
                  LOCALIZED MOLECULAR ORBITAL COMPOSITIONS
--------------------------------------------------------------------------------

The Mulliken populations for each LMO on each atom are computed
The LMO`s will be ordered according to atom index and type
  (A) Strongly localized MO`s have populations of >=0.950 on one atom
  (B) Two center bond orbitals have populations of >=0.850 on two atoms
  (C) Other MO`s are considered to be `delocalized`

FOUND  -  59 strongly local MO`s
       - 105 two center bond MO`s
       -  14 significantly delocalized MO`s
More delocalized orbitals:
MO 177:  0Co- 0.135 20C - 0.341 23C - 0.427
MO 176:  5C - 0.493 18C - 0.216 42C - 0.217
MO 175:  42C - 0.212 48C - 0.221 57C - 0.505
MO 174:  0Co- 0.720 9C - 0.083 16C - 0.088
MO 173:  14C - 0.233 22C - 0.479 66C - 0.216
MO 172:  18C - 0.199 46C - 0.505 48C - 0.232
MO 171:  14C - 0.198 50C - 0.480 81C - 0.253
MO 170:  0Co- 0.571 9C - 0.113 16C - 0.148 20C - 0.076
MO 169:  0Co- 0.196 1Mg- 0.079 16C - 0.149 19C - 0.499
MO 168:  0Co- 0.168 9C - 0.189 13C - 0.529
MO 167:  4C - 0.186 6C - 0.601 8C - 0.195
MO 166:  0Co- 0.181 11C - 0.321 15C - 0.424
MO 165:  0Co- 0.800
MO 164:  66C - 0.244 81C - 0.207 83C - 0.496
```

Excerpt from NBO analysis of **2**:

Wiberg bond index matrix in the NAO basis:

Atom	1	2	3	4	5	6	7	8	9
1. Co	0.0000	0.0270	0.0013	0.0013	0.0006	0.0004	0.0003	0.0000	0.0005
2. Mg	0.0270	0.0000	0.0551	0.0572	0.0053	0.0044	0.0030	0.0011	0.0054
3. N	0.0013	0.0551	0.0000	0.0576	1.4406	0.0024	0.0846	0.0109	0.0541
4. N	0.0013	0.0572	0.0576	0.0000	0.0513	1.0452	0.0869	0.0116	1.4182

Mulliken charges:

		1
1	Co	-0.717005
2	Mg	0.338551
3	N	-0.534684
4	N	-0.460789

Summary of Natural Population Analysis:

Atom	No	Natural Charge	Natural Population			
			Core	Valence	Rydberg	Total
Co	1	0.25416	17.99982	8.69828	0.04774	26.74584
Mg	2	1.78734	9.99993	0.17979	0.03294	10.21266
N	3	-0.74461	1.99999	5.71752	0.02710	7.74461
N	4	-0.76635	1.99999	5.73909	0.02726	7.76635

SECOND ORDER PERTURBATION THEORY ANALYSIS OF FOCK MATRIX IN NBO BASIS

Threshold for printing: 0.50 kcal/mol
(Intermolecular threshold: 0.05 kcal/mol)

Donor (L) NBO	Acceptor (NL) NBO	E(2) kcal/mol	E(NL)-E(L) a.u.	F(L,NL) a.u.
within unit 1				
58. LP (1)Co 1	306. RY (13)Co 1	0.84	2.61	0.042
60. LP (3)Co 1	179. LV (1)Co 1	1.67	0.57	0.027
60. LP (3)Co 1	294. RY (1)Co 1	0.93	1.34	0.032
60. LP (3)Co 1	308. RY (15)Co 1	0.71	2.55	0.038
61. LP (4)Co 1	297. RY (4)Co 1	0.58	1.44	0.026
61. LP (4)Co 1	307. RY (14)Co 1	0.56	2.94	0.036
61. LP (4)Co 1	309. RY (16)Co 1	1.38	2.81	0.056
62. LP (5)Co 1	179. LV (1)Co 1	0.84	0.59	0.020
62. LP (5)Co 1	298. RY (5)Co 1	0.95	2.22	0.041
62. LP (5)Co 1	310. RY (17)Co 1	0.62	3.33	0.041
62. LP (5)Co 1	311. RY (18)Co 1	0.59	2.64	0.035
from unit 1 to unit 2				
58. LP (1)Co 1	328. RY (5)Mg 2	0.06	1.43	0.009
59. LP (2)Co 1	180. LV (1)Mg 2	0.10	0.39	0.005
59. LP (2)Co 1	326. RY (3)Mg 2	0.51	1.38	0.024
59. LP (2)Co 1	328. RY (5)Mg 2	0.15	1.42	0.013
59. LP (2)Co 1	332. RY (9)Mg 2	0.11	2.47	0.015
59. LP (2)Co 1	333. RY (10)Mg 2	0.21	2.46	0.020
59. LP (2)Co 1	337. RY (14)Mg 2	0.07	2.40	0.011
59. LP (2)Co 1	338. RY (15)Mg 2	0.15	2.16	0.016
60. LP (3)Co 1	180. LV (1)Mg 2	0.33	0.39	0.010
60. LP (3)Co 1	326. RY (3)Mg 2	0.09	1.38	0.010
60. LP (3)Co 1	332. RY (9)Mg 2	0.14	2.47	0.017
60. LP (3)Co 1	333. RY (10)Mg 2	0.14	2.46	0.017
60. LP (3)Co 1	337. RY (14)Mg 2	0.10	2.40	0.014
61. LP (4)Co 1	329. RY (6)Mg 2	0.19	1.34	0.014
61. LP (4)Co 1	330. RY (7)Mg 2	0.12	1.55	0.012
61. LP (4)Co 1	331. RY (8)Mg 2	0.15	1.45	0.013
62. LP (5)Co 1	180. LV (1)Mg 2	0.13	0.41	0.006
62. LP (5)Co 1	324. RY (1)Mg 2	0.08	1.37	0.009
62. LP (5)Co 1	333. RY (10)Mg 2	0.10	2.48	0.014

Excerpt from IBO analysis of **4**:

```
-----------------------
MULLIKEN ATOMIC CHARGES
-----------------------
   0 Co:   -0.385495
   1 P :   -0.191911
   2 P :   -0.048914
   3 Mg:    0.269259
   4 N :   -0.486697
```

```
----------------------
LOEWDIN ATOMIC CHARGES
----------------------
   0 Co:   -0.523141
   1 P :    0.624501
   2 P :    0.565782
   3 Mg:   -0.046355
   4 N :    0.150318

--------------------
IAO PARTIAL CHARGES
--------------------
Warning!!! IAOs HAVE MEANING, only when all occupied MOs are involved.
   0 Co:    0.740780
   1 P :    0.003207
   2 P :    0.179479
   3 Mg:    1.414189
   4 N :   -0.523334

-------------------------------------------------------------------------------
                    LOCALIZED MOLECULAR ORBITAL COMPOSITIONS
-------------------------------------------------------------------------------

The Mulliken populations for each LMO on each atom are computed
The LMO`s will be ordered according to atom index and type
  (A) Strongly localized MO`s have populations of >=0.950 on one atom
  (B) Two center bond orbitals have populations of >=0.850 on two atoms
  (C) Other MO`s are considered to be `delocalized`

FOUND  -  72 strongly local MO`s
       - 117 two center bond MO`s
       -  13 significantly delocalized MO`s

More delocalized orbitals:
MO 201:  0Co- 0.208 28C - 0.201 43C - 0.540
MO 200:  30C - 0.232 32C - 0.220 34C - 0.497
MO 199:  5C - 0.226 13C - 0.477 32C - 0.240
MO 198:  74C - 0.238 75C - 0.473 81C - 0.228
MO 197:  0Co- 0.106 1P - 0.554 3Mg- 0.135
MO 196:  0Co- 0.264 2P - 0.207 59C - 0.536
MO 195:  14C - 0.595 16C - 0.195 77C - 0.195
MO 194:  81C - 0.232 83C - 0.220 85C - 0.497
MO 193:  0Co- 0.731 28C - 0.081 102C - 0.081
MO 192:  0Co- 0.264 2P - 0.206 6C - 0.536
MO 191:  74C - 0.226 76C - 0.477 83C - 0.240
MO 190:  5C - 0.238 8C - 0.473 30C - 0.228
MO 189:  0Co- 0.208 102C - 0.201 104C - 0.540
```

Excerpt from NBO analysis of **4**:

```
 Mulliken charges:
                1
     1  Co  -0.381016
     2  P   -0.186694
     3  P   -0.046590
     4  Mg   0.271004
     5  N   -0.487770
```

Summary of Natural Population Analysis:

Atom	No	Natural Charge	Natural Population			
			Core	Valence	Rydberg	Total
Co	1	0.12563	17.99978	8.81392	0.06067	26.87437
P	2	0.24421	9.99995	4.69594	0.05991	14.75579
P	3	0.53582	9.99995	4.41862	0.04562	14.46418
Mg	4	1.73012	9.99994	0.23330	0.03664	10.26988
N	5	-0.76179	1.99999	5.73407	0.02773	7.76179

Wiberg bond index matrix in the NAO basis:

Atom	1	2	3	4	5	6	7	8	9
1. Co	0.0000	0.2507	0.2214	0.0268	0.0011	0.0002	0.3765	0.0100	0.0002
2. P	0.2507	0.0000	0.1495	0.1350	0.0045	0.0006	1.0546	0.0124	0.0002
3. P	0.2214	0.1495	0.0000	0.0231	0.0017	0.0002	1.1015	0.0124	0.0001
4. Mg	0.0268	0.1350	0.0231	0.0000	0.0573	0.0038	0.0043	0.0008	0.0036
5. N	0.0011	0.0045	0.0017	0.0573	0.0000	1.0357	0.0005	0.0000	0.0325

SECOND ORDER PERTURBATION THEORY ANALYSIS OF FOCK MATRIX IN NBO BASIS

Threshold for printing: 0.50 kcal/mol
(Intermolecular threshold: 0.05 kcal/mol)

Donor (L) NBO	Acceptor (NL) NBO	E(2) kcal/mol	E(NL)-E(L) a.u.	F(L,NL) a.u.
from unit 1 to unit 2				
70. LP (1)Co 1	419. RY (6)Mg 4	0.08	1.49	0.009
70. LP (1)Co 1	423. RY (10)Mg 4	0.08	2.09	0.011
70. LP (1)Co 1	427. RY (14)Mg 4	0.06	2.26	0.010
71. LP (2)Co 1	204. LV (1)Mg 4	0.61	0.37	0.013
71. LP (2)Co 1	423. RY (10)Mg 4	0.43	2.07	0.027
71. LP (2)Co 1	425. RY (12)Mg 4	0.32	1.85	0.022
71. LP (2)Co 1	428. RY (15)Mg 4	0.25	2.33	0.022
71. LP (2)Co 1	433. RY (20)Mg 4	0.15	3.56	0.021
72. LP (3)Co 1	416. RY (3)Mg 4	0.06	1.17	0.007
72. LP (3)Co 1	417. RY (4)Mg 4	0.45	1.26	0.021
72. LP (3)Co 1	420. RY (7)Mg 4	0.06	1.38	0.008
73. LP (4)Co 1	414. RY (1)Mg 4	0.10	1.23	0.010
73. LP (4)Co 1	418. RY (5)Mg 4	0.15	1.49	0.013
73. LP (4)Co 1	419. RY (6)Mg 4	0.18	1.49	0.015
73. LP (4)Co 1	425. RY (12)Mg 4	0.07	1.86	0.010
74. LP (1) P 2	204. LV (1)Mg 4	10.18	0.51	0.064
74. LP (1) P 2	414. RY (1)Mg 4	0.35	1.35	0.019
74. LP (1) P 2	421. RY (8)Mg 4	0.19	1.42	0.015
74. LP (1) P 2	422. RY (9)Mg 4	0.14	1.78	0.014
74. LP (1) P 2	423. RY (10)Mg 4	0.18	2.21	0.018
74. LP (1) P 2	430. RY (17)Mg 4	0.07	2.71	0.012
75. LP (1) P 3	204. LV (1)Mg 4	0.09	0.49	0.006
75. LP (1) P 3	418. RY (5)Mg 4	0.05	1.60	0.008
75. LP (1) P 3	422. RY (9)Mg 4	0.09	1.77	0.011
76. LP (2) P 3	204. LV (1)Mg 4	0.56	0.30	0.011
76. LP (2) P 3	418. RY (5)Mg 4	0.09	1.40	0.010
76. LP (2) P 3	422. RY (9)Mg 4	0.15	1.57	0.014
76. LP (2) P 3	423. RY (10)Mg 4	0.25	2.00	0.020
76. LP (2) P 3	425. RY (12)Mg 4	0.11	1.77	0.013
76. LP (2) P 3	427. RY (14)Mg 4	0.09	2.16	0.012
76. LP (2) P 3	432. RY (19)Mg 4	0.06	2.84	0.011
76. LP (2) P 3	433. RY (20)Mg 4	0.10	3.48	0.017
80. BD (1)Co 1- C 60	204. LV (1)Mg 4	0.80	0.45	0.017
80. BD (1)Co 1- C 60	417. RY (4)Mg 4	0.05	1.34	0.008

Cartesian coordinates of (^{Dep}nacnac)MgCo(COD)$_2$ (**2**) optimised with Orca 4.1 at the TPSS-D3BJ/def2-TZVP level of theory.

Energy: -3288.184966712858

Co	6.19349674542942	7.29295677600773	10.66427174445875
Mg	5.97213312889920	9.76534827966438	10.13201879879395
N	5.82273192292791	10.76266674149047	8.28158566023418

N	6.05316121644345	11.58674366543890	11.13642642872760
C	6.28337352714837	12.00979995879023	8.10166041429133
C	5.51498556175873	11.67360990731831	12.45419908659053
C	6.71043797814815	12.85521324227472	9.15621777669574
H	7.11909698154539	13.82491113626170	8.84262350281146
C	6.48706871097405	12.71677035310737	10.54673140260913
C	4.87755292200627	7.11735348455063	12.19086284293018
H	5.43394137500293	6.98569077204785	13.13385175586201
C	4.94281021796653	5.95238010004906	9.73965571975854
H	5.49822880779639	5.30909684573901	9.03549203754816
C	4.79595047118955	8.47944778117247	11.74166753734785
C	5.24650000753078	10.05050377650472	7.18584645552764
C	4.62407920001286	7.26924285829183	9.29271840872017
C	7.50080519690795	6.96912220496431	9.16183851945687
H	6.93870332500646	6.89178403757028	8.21469921976088
C	4.21324233086274	12.22128067496877	12.64312161863827
C	7.71875126577038	8.31860912262714	9.61689944936747
C	7.71060396691798	7.09281069789064	12.05282906413735
H	7.32310230268177	7.41293320977262	13.03486280155444
C	6.03557536766432	9.23672969592633	6.32844187391255
C	7.28148859964363	5.81341648596097	11.59882840315516
H	6.64390113328083	5.22882892752884	12.28449997573807
C	3.57019652246755	8.92305462614528	10.93312112232090
C	8.93035236755327	8.68090779932977	10.47134359802021
H	8.82860011350490	9.72990840644075	10.82357916925074
H	9.86158468189169	8.67054191403995	9.85622978629544
C	4.11084357235077	5.18973851256126	10.75282092093125
H	4.69659378119080	4.30466408783760	11.07845664211683
H	3.17979018274651	4.77912464365651	10.29122628124097
C	3.42275909331756	12.76728903942488	11.46677994760058
H	3.87087018009409	12.38258503828395	10.52913089395857
H	3.56059175786444	13.87226050387014	11.41534259541919
C	6.69048977990164	13.96298297145406	11.38888815270880
H	5.72107996889120	14.47464966511462	11.56217260601859
H	7.36028430555293	14.67952481071290	10.87802399435650
H	7.10377009692496	13.71970183837701	12.38604997372227
C	9.04997506910246	7.72890083616962	11.68060708103350
H	9.79801736632431	6.93630587761882	11.47055518165294
H	9.44726733950857	8.27884595977019	12.55823051475234

C	6.23059613526369	11.11509971262720	13.54883205167046
C	3.78829465955432	6.06714422757534	11.98005866351765
H	2.79678283101959	6.55499071319223	11.87099978235866
H	3.70588838990423	5.43607915080334	12.88848130952017
C	3.67229496335101	12.23469071705723	13.94391407728792
H	2.66797432315449	12.65481663291619	14.10536930722261
C	4.38375170985019	11.71680319490094	15.03429018159221
H	3.94237082039936	11.73787284988936	16.04226984277619
C	3.82973649908487	10.10689994178683	7.03183596861861
C	3.34223551449277	7.99371162964058	9.71786193012532
H	2.54807049569765	7.25526175393696	9.94862294421251
H	2.96313109470364	8.57444805752417	8.85661794890422
C	8.48307574171367	5.82157360380092	9.38774224484999
H	9.50907820445107	6.21985581705058	9.53362024466167
H	8.53630344649889	5.19329550339226	8.47492157474676
C	5.65200852032805	11.15522442414085	14.83057357745924
H	6.20819583057864	10.72310644184808	15.67776452419624
C	6.31254675417248	12.58763895056540	6.69998374116657
H	6.94913023837914	11.97811312088731	6.02892002563479
H	6.68506856715336	13.62762029802273	6.69588204787213
H	5.29669469515397	12.57141527543702	6.25461254395730
C	8.04588222300688	4.97154840856753	10.59612658698254
H	7.37543316895324	4.15721681853153	10.24934484126759
H	8.91757856429112	4.46085652667804	11.07310067462556
C	5.37358500402052	8.39882576781640	5.40615656689825
H	5.97227096925666	7.73817427938325	4.75952521000304
C	7.57217342457025	10.45087890901067	13.33667634679457
H	7.48075378895304	9.74876520133855	12.48146543711974
H	7.79307227883036	9.81780142756740	14.22077973770996
C	3.03584042020563	11.08055738002985	7.88340292386215
H	3.37958344668679	12.11421003117184	7.65383826193813
H	3.32994162378919	10.94277752115657	8.94546060361959
C	8.75073979605099	11.40135783952890	13.08306386875964
H	8.62767228818589	11.95469962980323	12.13206652146869
H	9.70245431098397	10.83522496596381	13.01772998724220
H	8.85391083555973	12.14312038717797	13.90143158167130
C	7.55360667755442	9.27329894543586	6.33885040303154
H	7.89996474924090	10.00594443359102	7.09347756527788
H	7.94368017939497	8.28855566873434	6.67449594684843

C	3.21553425260046	9.26625216388859	6.08754781896676
H	2.12254230239924	9.28365795963061	5.97167435328877
C	3.97911453900034	8.39401574264415	5.29618093158586
H	3.48291221565175	7.72222069937369	4.57959766606046
C	1.92222204482390	12.45320510765108	11.48240934967719
H	1.43322365317811	12.85121322747978	10.57058879598976
H	1.40226327789848	12.90254769532888	12.35231522379254
H	1.74296272104199	11.35938882187895	11.51511310502809
C	1.51501186420394	11.00636313384534	7.75952224555928
H	1.16963264364059	11.22343299686265	6.72797171437216
H	1.03495891561410	11.74359213728539	8.43264257118496
H	1.13148883015089	10.00318522676964	8.03858264998835
C	8.16907754565805	9.61765371572114	4.97261703064387
H	7.81073607838377	10.60022163893762	4.60156508849999
H	7.91044042010746	8.86452438250954	4.20140032435305
H	9.27524488384395	9.66130030324883	5.03837536597340
H	5.13831143894856	9.22499452066069	12.48293229487346
H	4.97804756074539	7.53912223310478	8.28211982579833
H	7.53659360383933	9.06746631970169	8.81654837484010
H	3.68996310615841	9.98143448257645	10.58996114279207
H	2.66935447496795	8.97724506569155	11.58773956923172

Cartesian coordinates of (^{Dep}nacnac)MgCo(P_2C_2tBu$_2$)(COD) (**4**) optimised with Orca 4.1 at the TPSS-D3BJ/def2-TZVP level of theory.

Energy: -4050.605413934357

Co	11.75571057181409	15.32629312187485	7.36153338672293
P	9.91814985049013	15.32635378496130	5.92679134870104
P	9.87573767791349	15.32612091145847	8.69338427978463
Mg	12.32918108410306	15.32639308231155	4.83266328915346
N	12.88758844145378	13.79599702100452	3.50325597054157
C	12.35775211968460	12.47287828924110	3.65164591784919
C	10.05124284887493	14.14768260683437	7.32560476131343
C	9.71636504371063	12.65798371389870	7.39708589447847
C	13.13542448785552	11.39660846968435	4.16763844321760
C	10.78595225436333	11.74018031604682	6.78328904777463
H	11.06028409855575	12.07552526226095	5.76957330460524
H	10.40224173520714	10.70392343865906	6.69833824381992

H	11.70350691904490	11.70358122700397	7.39929850862253
C	11.00276333030689	12.25313672575998	3.26862763469061
C	14.10428263708151	15.32640987231161	2.03171532648222
H	14.76478183382709	15.32641346168832	1.15521121526305
C	13.67237337892985	14.03969038294349	2.43638769741010
C	14.58993653479897	11.55727471752971	4.56995068666269
H	14.87407688963893	12.62340369350636	4.48764412208535
H	15.22192393075316	11.02085211308898	3.82577269699511
C	9.48495549674002	12.24312598437932	8.86616788370412
H	10.38672449595659	12.42467666354495	9.48695304207136
H	9.24491073285209	11.16135494883546	8.92742453947633
H	8.64695670314019	12.80967315010461	9.32120466819615
C	8.39868714969679	12.45910886657324	6.60789859741640
H	7.60394714648368	13.13265742342058	6.98800929441634
H	8.04483604310952	11.40990974215446	6.69403433610818
H	8.55282197042327	12.68436724374741	5.53272386306824
C	12.86291745313935	16.68523486226677	8.33400582631199
H	12.22365477041863	17.51840422660679	8.66289759623545
C	12.53929547612112	10.12308689825215	4.27196176481605
H	13.13867995085444	9.28640206556607	4.66296429621556
C	10.45251375556533	10.96378458058340	3.39091379135876
H	9.40477589682376	10.80412112661718	3.09060797548389
C	11.21314044119074	9.89774927819159	3.88669938216092
H	10.77129669944713	8.89421642281731	3.97974011789198
C	14.09444363221778	12.88989202754236	1.53775024752022
H	14.81191227338570	12.22058131421489	2.05245192267380
H	14.57029631386800	13.26123468712528	0.61267071574426
H	13.22229854638020	12.26319241038154	1.26539859521352
C	10.16465911413269	13.35295710388670	2.65697308739542
H	9.09420250226077	13.11930614131285	2.83268671305392
H	10.35060187038197	14.31447400151380	3.17839192076602
C	13.23679732728384	16.67986532689977	6.95029246349000
C	14.93635981783566	11.03417234187071	5.97203318800898
H	14.75580451629852	9.94425647924209	6.06415222433323
H	14.33204552970031	11.54054198782805	6.74984911582992
H	16.00636314568280	11.21223394448779	6.20175088401225
C	13.73985583644467	16.10153645238187	9.43033194413169
H	14.77762676241688	16.49797936741123	9.33694812244479
H	13.36370138771304	16.46914193022353	10.40512513341886

C	14.58886292468412	16.10065841679883	6.52585531097398
H	14.83586296143221	16.46568277353357	5.50864421682460
H	15.39212535116796	16.50162374069784	7.18187337235285
C	10.41299322706911	13.52855906930652	1.15040378267160
H	10.31548977259231	12.56012461630729	0.61818618850391
H	11.42708372023951	13.92826061647378	0.95279590828226
H	9.68411048954517	14.23472919702730	0.70639295497486
H	12.88677390763303	17.53950499625215	6.35616769392898
C	10.05116962173543	16.50478547613093	7.32580560541121
C	9.71624412151691	17.99445014169497	7.39751895900715
C	10.78569149111370	18.91233144968396	6.78361614325446
H	11.05995869903859	18.57700587880585	5.76987541816371
H	10.40190411003885	19.94856190538999	6.69870356581843
H	11.70328506125717	18.94899562138043	7.39955374172412
C	9.48508383875178	18.40913161089871	8.86668694519136
H	10.38696616673570	18.22755556461942	9.48729731771509
H	9.24499340393159	19.49088335880499	8.92810517762984
H	8.64719052166079	17.84249383501891	9.32180667957552
C	8.39840332141364	18.19335318794815	6.60860502505551
H	7.60375509913915	17.51974956221105	6.98881087296819
H	8.04454831651181	19.24253828680092	6.69490309728075
H	8.55232852777758	17.96818937606538	5.53338028150621
N	12.88756368725894	16.85680032019054	3.50325040941802
C	12.35753214175746	18.17984904423503	3.65152236728530
C	13.13494944380206	19.25617282503400	4.16777141363851
C	11.00265335214026	18.39948894842280	3.26804976396585
C	13.67233601619358	16.61312266127671	2.43637472422762
C	14.58932496075654	19.09561080182664	4.57061285238229
H	14.87356305228873	18.02949153744239	4.48846846687435
H	15.22149965753294	19.63204524405375	3.82660361463616
C	12.53868507219019	20.52964418286387	4.27193008842107
H	13.13786679294399	21.36635832673418	4.66318479490401
C	10.45224830132542	19.68878557916162	3.39021520931248
H	9.40460336025344	19.84837587753321	3.08954781734236
C	11.21262889508013	20.75487636239188	3.88626450770231
H	10.77065999340153	21.75836277636393	3.97920486634826
C	14.09433824378236	17.76293273769761	1.53772093971251
H	14.81178865386739	18.43228736793522	2.05239442871771
H	14.57017844921922	17.39160644079997	0.61262837011604

H	13.22215371960776	18.38958700152394	1.26539244604090
C	10.16483944130448	17.29962283874057	2.65606908827048
H	9.09431329287129	17.53318255596569	2.83146470035189
H	10.35069987318168	16.33809959944680	3.17751129911382
C	14.93529607125857	19.61882998545224	5.97276116256681
H	14.75458298388394	20.70873026999733	6.06476622133769
H	14.33085640957742	19.11243166487207	6.75044741898837
H	16.00526104324503	19.44090997793646	6.20276984686687
C	10.41363983374307	17.12407395438300	1.14956584079485
H	10.31632690872420	18.09252902478329	0.61735141908622
H	11.42777984930146	16.72435028860449	0.95226117457972
H	9.68487723004435	16.41793742153644	0.70530576912374
C	12.86300671133743	13.96737824123461	8.33394130818033
H	12.22376400426848	13.13417898505637	8.66280284924781
C	13.23686701779217	13.97281891443432	6.95022216714930
C	13.73993239644362	14.55107848454650	9.43027652843320
H	14.77773926789651	14.15474750676530	9.33682498897885
H	13.36384947559538	14.18336585933772	10.40505660039784
C	14.58888918700721	14.55211428068264	6.52576928849732
H	14.83584400405115	14.18720576755161	5.50850246283273
H	15.39220426037166	14.15110273405689	7.18169583559993
H	12.88686486333966	13.11320371522509	6.35604766059947

5. References

(1) S. J. Bonyhady, C. Jones, S. Nembenna, A. Stasch, A. J. Edwards, G. J. McIntyre, *Chem. Eur. J.* **2010**, *16*, 938.

(2) R. Lalrempuia, C. E. Kefalidis, S. J. Bonyhady, B. Schwarze, L. Maron, A. Stasch, C. Jones, *J. Am. Chem. Soc.* **2015**, *137*, 8944.

(3) K. Jonas, R. Mynott, C. Krüger, J. C. Sekutowski, Y-H. Tsay, *Angew. Chem. Int. Ed.* **1976**, *15*, 767.

(4) a) W. Rösch, T. Allspach, U. Bergsträßer, M. Regitz in W. A. Herrmann (ed.), *Synthetic Methods of Organometallic and Inorganic Chemistry*, volume 3, Thieme: Stuttgart, **1996**; b) G. Becker, G. Gresser, W. Uhl, *Z. Naturforsch. B* **1981**, *36*, 16–19.

(5) P. Büschelberger, C. Rödl, R. Wolf in P. P. Power (ed.), *Inorganic Syntheses, volume 37,* chapter 4.8, 76-84.

(6) a) G. M. Sheldrick, SADABS, Bruker AXS, Madison, USA, **2007**; b) CrysAlisPro, Scale3 Abspack, Rigaku Oxford Diffraction, **2019**; c) R. C. Clark, J. S. Reid, *Acta Crystallogr. A* **1995**, *51*, 887–897.

(7) O. V. Dolomanov, L. J. Bourhis, R. J. Gildea, J. A. K. Howard, H. Puschmann, *J. Appl. Crystallogr*. **2009**, *42*, 339–341.

(8) G. M. Sheldrick, *Acta Crystallogr. A* **2015**, *71*, 3–8.

(9) G. M. Sheldrick, *Acta Crystallogr. C* **2015**, *71*, 3–8

(10) G. M. Sheldrick, *Acta Crystallogr. A* **2008**, *64*, 112–122.

(11) A. Jerschow, N. Müller, *J. Magn. Reson.* **1997**, 125, *2*, 372–375.

(12) (a) F. Neese, *WIREs Comput. Mol. Sci.* **2012**, *2*, 73–78; F. Neese, *WIREs Comput Mol Sci*. **2018**, *8*, e1327; (b) S. Grimme, J. Antony, S. Ehrlich, H. Krieg, *H-Pu. J. Chem. Phys.* **2010**, 132, 154104; (c) S. Grimme, S. Ehrlich, L. Goerigk., *J. Comput. Chem.* **2011**, *32*, 1456–1465; (d) J. Tao, J. P. Perdew, V. N. Staroverov, G. E. Scuseria, *Phys. Rev. Lett.* **2003**, *91*, 146401; F. Weigend, R. Ahlrichs, *Phys. Chem. Chem. Phys.* **2005**, *7*, 3297–3305.

(13) J. L. Whitten, *J. Chem. Phys.* **1973**, *58*, 4496–4501.

(14) Frisch, M. J.; Trucks, G. W.; Schlegel, H. B.; Scuseria, G. E.; Robb, M. A.; Cheeseman, J. R.; Scalmani, G.; Barone, V.; Petersson, G. A.; Nakatsuji, H.; Li, X.; Caricato, M.; Marenich, A.; Bloino, J.; Janesko, B. G.; Gomperts, R.; Mennucci, B.; Hratchian, H. P.; Oritz, J. V.; Izmaylov, A. F.; Sonnenberg, J. L.; Williams-Young, D.; Ding, F.; Lipparini, F.; Egidi, F.; Goings, J.; Peng, B.; Petrone, A.; Henderson, T.; Ranasinghe, D.; Zakrzewski, V. G.; Gao, J.; Rega, N.; Zheng, G.; Liang, W.; Hada, M.; Ehara, M.; Toyota, K.; Fukuda, R.; Hasegawa, J.; Ishida, M.; Nakajima, T.; Honda, Y.; Kitao, O.; Nakai, H.; Vreven, T.; Throssell, K.; Montgomery, J. A., Jr.; Peralta, J. E.; Ogliaro, F.; Bearpark, M.; Heyd, J. J.; Brothers, E.; Kudin, K. N.; Staroverov, V. N.; Keith, T.; Kobayashi, R.; Normand, J.; Raghavachari, K.; Rendell, A.; Burant, J. C.; Iyengar, S. S.; Tomasi, J.; Cossi, M.; Millam, J. M.; Klene, M.; Adamo, C.; Cammi, R.; Ochterski, J. W.; Martin, R. L.; Morokuma, K.; Farkas, O.; Foresman, J. B.; Fox, D. J.; Gaussian09 program package (Revision E.01); Gaussian Inc.; Wallingford CT, **2016**.

(15) (a) T. Lu, F. Chen, *J. Comput. Chem.* **2012**, *33*, 580-592; (b) T. Lu, F.Chen, *J. Mol. Graph. Model.* **2012**, *38*, 314-323.